A field study of event based, seasonally affected, depression focused recharge in glaciated terrain

by

Paul Gary Menkveld

A thesis

presented to the University of Waterloo

in fulfillment of the

thesis requirement for the degree of

Master of Science

in

Earth Sciences

Waterloo, Ontario, Canada, 2019

©Paul Gary Menkveld 2019

Author's Declaration

I hereby declare that I am the sole author of this thesis. This is a true copy of the thesis, including any required final revisions, as accepted by my examiners.

I understand that my thesis may be made electronically available to the public.

Abstract

To observe the dynamics of depression focused recharge (DFR) and the effects of seasonality related to transient surface water features, a field scale experiment was designed and conducted within glacial terrain in southern Ontario. The site selected for this case study is located in Mannheim, Ontario, on a property adjacent to a public supply well and a perennial stream known as Alder Creek. The site is characterized by hummocky topography and localized closed depression features. During hydrologic events, surface runoff collects in one of the closed depressions located near Alder Creek and the public supply well forming a transient surface water feature and causing DFR. Detailed subsurface characterization was completed to support the hydrogeologic conceptual model and three vertical instrument clusters were installed to observe groundwater recharge. Vertical instrument clusters include arrays of monitoring wells, surface water pressure transducers, neutron probe access tubes, arrays of time domain reflectometry sensors, and arrays of temperature sensors, which were installed along a transect perpendicular to Alder Creek through the closed depression. The clusters were positioned adjacent to the stream, in the center of the closed depression and in agricultural land up hill of the closed depression area in order to observe recharge processes and groundwater surface water interaction in these different settings. As part of the experiment, the site was instrumented with a meteorology station, water quality samples were collected, and direct soil samples were retrieved during hydrologic events.

Two major meteorological events were selected in the scope of this study: November snow melt and rainfall event in 2014 (the November Event including 80 mm of precipitation), and the spring melt and rainfall event in 2015 (the Spring Melt Event including 110 mm of precipitation). Both events were caused by a similar magnitude of combined snow melt and rainfall. The two events provide the opportunity to contrast unfrozen soil conditions during the November Event with the presence of frost (35 cm) in the shallow soils during the Spring Melt Event. The two events also contrast in intensity; the November Event lasted 1.8 days and the Spring Melt Event took place over 35 days.

Observations of recharge dynamics and their implications were made during the two events. During the November Event, DFR and recharge from Alder Creek occurred rapidly, causing the water table to rise to the ground surface. During this time period, surface water was observed to infiltrate rapidly, and depending on the microbial composition of the surface waters, the recharge could potentially be carrying pathogens into the shallow aquifer. This provides a case study of the potential risk of contamination by a transient surface water feature resulting in DFR, adjacent to a public supply well. During the Spring Melt Event, seasonality affected the recharge dynamics in several ways including the temporary formation of a thin layer of ice in the surficial sediments immediately below the closed depression in frozen soils, the complex thawing of this ice layer, and a significant temporal lag between recharge related to high water levels in Alder Creek and recharge related to the closed depression feature. At the start of the Spring Melt Event, the transient ice layer reduced infiltration beneath the topographic depression such that surface water remained in the closed depression for weeks as air and ground temperatures slowly increased. During this time period, there was evidence of groundwater recharge near the stream and beneath the depression that is interpreted to be related to enhanced infiltration from Alder Creek during the spring freshet. As the shallow soil zone warmed, it thawed in small bursts allowing cold water to infiltrate, then the ice layer refroze, stopping the flow of water. The ice layer then finally thawed permitting significant infiltration and the surface water drained from the closed depression for the first time since the start of the Spring Melt Event. The ice layer had the effect of delaying recharge from the closed depression. The continuous monitoring of the subsurface instrumentation clusters along the transect permitted the identification of discrete recharge phenomena related to changes in the stream stage and infiltration of surface water within the closed depression during both of these major hydrologic events. In addition, by combining the subsurface hydrogeologic information with transient soil water data, vertical soil temperature profiles and hydraulic head data, quantitative estimates of event-based groundwater recharge were completed. During the November Event, Alder Creek contributed 0.27 m of recharge and the closed depression contributed 0.31 m of recharge, however this is an overestimate. The effect of the two simultaneous sources of recharge is that the groundwater head increases are superimposed on each other in the groundwater hydrographs and therefore the WTF method would potentially overestimate the recharge during this event and would be of limited value. During the Spring Melt Event, Alder Creek contributed 0.18 m of

recharge and the closed depression contributed 0.20 m of recharge. The results indicate that significant rates of recharge can occur beneath localized features such as closed depressions and perennial streams in response to major hydrologic events such as periods of intense precipitation and spring melt. If the infiltrating water is carrying potential contaminants such as pathogens, these infiltration events may represent a short-lived, yet significant, threat to groundwater quality. This would be of highest concern at locations where this type of infiltration event occurs close to a supply well, as is the case for this study site.

Acknowledgments

There are a lot of people who deserve credit for their contributions to this study. The first thanks should go to my excellent and patient supervisor, Dr. David Rudolph. Thank you for your patience, insight, and investment in my career. Thank you for the right amount of guidance and lots of opportunity to try out ideas and learn from my mistakes.

The group surrounding Dr. Rudolph's research were an invaluable resource in the completion of this work. Thank you, Andrew Wiebe, for your many practical insights into field studies and the hours we spent sketching and arguing on your white board. Thank you to Paul Johnson and Bob Ingleton for your help, a friendly face in the shop, and for your sage advice in the implementation of this labour intensive study.

Thank you to the coop students who assisted with the study. Thank you, Jeff Stevens, Niki Long, Elton Huang, Elliot Pai, Ian Mercer, Kristen Blowes, Emily Mesec, and Elliot Pai, for your hard work.

Thank you also to Cristina Missori, Gabriele Perotti, Ehsan Pasha, and Cailin Hillier for the help and the background your studies provided to this one.

Thank you to the sponsors of this research: the Regional Municipality of Waterloo (RMOW) and the Southern Ontario Water Consortium (SOWC). The RMOW a helpful partner with insights into recharge processes, financial support, and background data. The SOWC provided funding and useful equipment for field studies.

Dedication

I dedicate this to my lovely and gracious wife and best friend, Alison. Thank you for your exceptional patience and for sharing me with my research for the last few years.

Table of Contents

List of Figures

List of Tables

1. Introduction

Groundwater is a critical resource for water supply and is of ever-increasing value as climate change and population growth increase the frequency and severity of water stress. Groundwater makes up a large portion of the world's supply of fresh water and is broadly available, even in areas where surface water is not. Groundwater contaminants tend to have long residence times in the subsurface compared to that of surface water, which allows more time for the filtration and degradation (Appelo and Postma, 2005). However, the interaction between surface water and groundwater is complex and transient in nature. Of particular importance are the processes by which groundwater recharge occurs, which can influence the vulnerability of drinking water supplies and the long term management of aquifer systems (Scanlon et al. 2002). Many of the key recharge phenomena are related to climatic seasonality.

A potent example of the potential risk to drinking water supplies by seasonal recharge processes occurred in the year 2000, when an intense rain event caused surface water to form on a farmer's field near Walkerton, Ontario (O'Connor, 2002). This overland flow transported bacterial contamination close to a supply well head, where it rapidly infiltrated and contaminated the drinking water supply in Walkerton. This caused 7 deaths and more than 2300 illnesses were reported. Following this tragedy researchers and regulators in Ontario and elsewhere recognised the need to more effectively protect groundwater supplies and began to study the vulnerability of public water wells to contaminated surface water, spilled contaminants, and natural health hazards (Province of Ontario, 2004). The vulnerability of wells to the presence of transient surface water conditions is the first area of focus of this research program.

The second major implication of recharge dynamics is the management of aquifer systems. In areas, such as the Region of Waterloo, where surface water is inadequate to supply the full requirements of the urban centres, groundwater is heavily relied upon as an alternate source. Groundwater management practices are used to ensure the long-term viability of aquifers. Christian-Smith, et. al (2015), reviewed a case of failed aquifer management in light of significant variability in climatic conditions. In California, a severe drought led to water stress in many industries. Water users reacted to declining reservoir volumes and falling water allotments

from the state water infrastructure by exploiting the groundwater resources of California. Many new deeper wells were drilled during the drought to sustain water-intensive practices, such as agriculture. This has led to the rapid depletion of groundwater resources and land subsidence and serves as an example of the need for thoughtful aquifer management policy. In order to manage an aquifer, understanding the distribution of recharge in time and space is crucial. Physical processes affect the quantity, rate, distribution, and quality of groundwater recharge. Groundwater resources can be better managed by a more comprehensive understanding of processes affecting groundwater recharge, particularly as influenced by variable climatic conditions related to seasonality. This is a second focus of this study.

1.1. Research Objectives

The objective of this study is to advance the understanding of seasonal recharge processes, provide a detailed case study of recharge quantifications, and evaluate the implications of recharge dynamics for groundwater resources by observing recharge phenomena in detail on a site scale. A high level of field monitoring detail would be required to allow for recharge to be measured discretely in both time and space, and inform conceptual models about the processes by which recharge occurs. The duration of the study allowed for the observation of seasonality on recharge dynamics including the influence of the winter season. Most notably, this study focusses on near surface processes associated with event-based, depression focused recharge (DFR) in hummocky glacial terrain.

The field site selected for this recharge is located within the Waterloo Moraine in southern Ontario near the town of Mannheim. The site is situated near a large public supply well and adjacent a perennial stream where a surface topographic depression results in the transient collection of surface runoff during the course of the year. It is hypothesized that during the course of the annual seasonal cycle, groundwater recharge associated with both the topographic depression and variations in stream stage may be significant in magnitude and will vary considerably significantly in both time and space and that this type of recharge phenomena may represent a threat to groundwater quality within the local public supply well.

The goals of the research are to develop and implement a monitoring strategy to quantify site-specific recharge in time and extent during transient climatic events and seasonal influences. The integrated data sets would then be assessed to quantify groundwater recharge and provide insight into the nature of seasonal groundwater recharge in this type of glaciated terrain. Finally, the overall results will be evaluated relative to the potential impact that this type of seasonal recharge may have on the vulnerability of adjacent public supply wells and how these types of transient recharge processes should be considered in regional groundwater assessments. The events considered within this study include an early winter melt event in November (referred to as the November Event) and the spring melt in 2015 (referred to as the Spring Melt Event).

1.2. Thesis Organization

This thesis contains a review of scientific studies focussed on recharge in glacial terrain (in Chapter 2) and the background information gathered at the research site (in Chapter 3), to provide context for further study and analysis. Methods employed to characterize, observe hydrologic events, and analyze the data are contained in Chapter 4. Chapter 5 summarizes the result of the study; the site characterization, observations of recharge dynamics, and analysis of recharge processes. Finally, Chapter 6 summarizes the conclusions of the study and provides recommendations further work to better the understanding of recharge processes and their implications.

2. Scientific Background

Recharge processes are a critical part of the hydrologic cycle and, in particular, the flow and quality of groundwater. Recharge studies are driven by two needs: aquifer scale management and aquifer vulnerability to contamination (Scanlon, 2002). The literature available on the topic of recharge has generally grown to support these applications of recharge information. This review of scientific literature includes the areas of research which directly apply to the current research program.

Aquifer replenishment is a significant area of interest for this research because the study scenario and physical setting are related to a region where groundwater is used extensively as a water supply, something that is common throughout southern Ontario. The study site is located within a region of thick glacial overburden sediments characterized by intermingled aquifer and aquitard units and hummocky surface topography (Bajc et al. 2014). The geomorphology causing the presence of hummocks and closed depressions (and potentially DFR) is the result of complex glacial depositional processes (Bajc et al. 2014). Because these processes were active throughout much of southern Ontario, the hummocky landscape and associated DFR conditions are widespread and are a typical phenomenon of this region and other glacial landscapes (Bajc et al. 2014). Literature related to this area of study includes: recharge flow processes, implications for regional numerical modelling, DFR, and recharge quantification techniques.

The second area of practice around which literature has developed is the vulnerability of aquifers and water supplies to contamination and the influence of recharge processes on these issues. Studies of aquifer contamination are typically focussed on either local scale processes occurring on an individual site, which could influence the transport of contaminants to an aquifer or on a more regional scale involving non-point source contaminants related to agricultural activities for example (Scanlon et al. 2002). Areas of study supporting the vulnerability of aquifers, relevant to the current study include vadose zone flow processes, well vulnerability, frozen soil hydrogeology, seasonality in recharge processes and numerical modelling.

2.1. Recharge Terminology and Physical Processes

Recharge is one of the most fundamental processes in hydrogeology and the driving force behind flow in surficial aquifers. Recharge is defined as "the downward flow of water reaching the water table, [and] adding to groundwater storage" (Healy, 2010). The typical downward flow path begins when precipitation or surface water infiltrates, flows through the unsaturated zone, through the capillary fringe, and crosses the water table contributing recharge to the aquifer. The term infiltration refers to water crossing the interface between the surface and the subsurface. The unsaturated zone is the space between the land surface and the capillary fringe where some pores are saturated and others are air filled (Healy, 2010). In the unsaturated zone, the moisture content is less than the porosity of the material. The capillary fringe is defined as the zone immediately above the water table (phreatic surface) where the soil is completely saturated, with a negative pore water pressure (Fetter, 2001). A related term is the vadose zone, which is defined as the zone between the ground surface and the water table, and therefore includes the unsaturated zone and the capillary fringe (Healy, 2010). Processes such as overland flow into a closed depression can influence the distribution of infiltration, and therefore recharge. When these processes lead to increased infiltration and subsequent recharge, this is known as focused recharge. Focused recharge can be caused by surface water bodies (ex. streams) or by the collection of surface water in closed depressions (DFR). Figure 2.1. shows a typical schematic of processes of infiltration, unsaturated zone flow, and recharge.

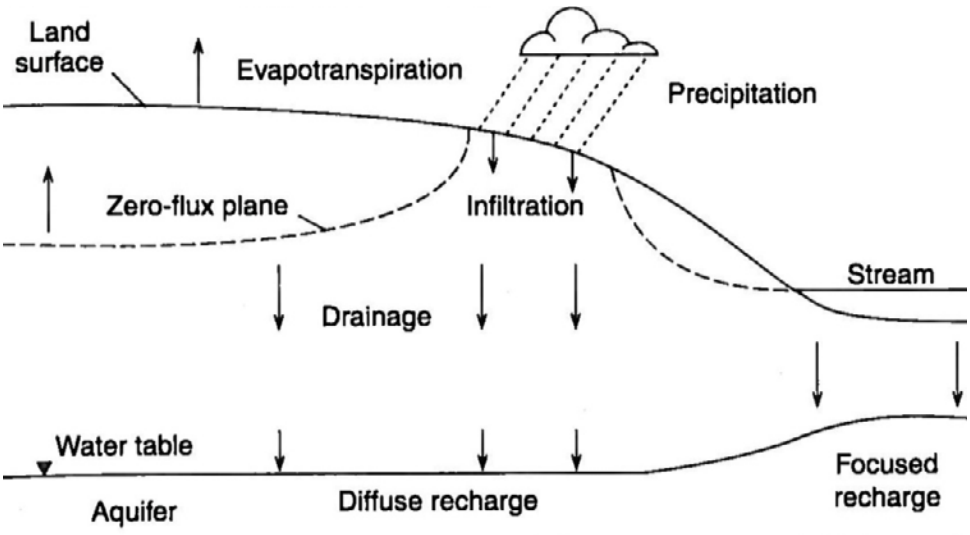

Figure 2.1. Vertical cross section through typical groundwater flow system including recharge processes (Healy, 2010).

Flow in the unsaturated zone is dependent on the unsaturated hydraulic conductivity and the head gradient in the unsaturated zone (described as "Drainage" in Figure 2.1.). The equation describing the vertical flow of water in the unsaturated zone is known as Richards' Equation. Eqn. 1 is known as Richards' Equation for unsaturated flow in the vertical direction (Richards, 1931).

$$\frac{\partial \theta}{\partial t} = \frac{\partial}{\partial z}\left[K(\theta)\left(\frac{\partial \Psi}{\partial z} + 1\right)\right] \qquad \text{(Richards, 1931) (1)}$$

Where θ is the volumetric water content, t is time, z is a vertical axis, K(θ) is the unsaturated hydraulic conductivity as a function of the volumetric water content, and Ψ is the soil water tension. This expression states that the flow of soil water with respect to time is proportional to the spatial gradient of head and the hydraulic conductivity. This expression includes Darcy's law (Eqn. 2), with provision made for flow continuity in both the saturated and unsaturated zones by Buckingham (1907).

$$q_{sat,x} = k_{sat} \frac{dh}{dx}$$ (Buckingham, 1907) (2)

Where $q_{sat, x}$ is the saturated Darcy's flux in the x direction, k_{sat} is the saturated hydraulic conductivity, and dh/dx is the hydraulic head gradient in the x direction.

The zero flux plane (ZFP) (as depicted in Figure 2.1.) is a position in the unsaturated zone at which the hydraulic head gradient is zero (Scanlon et al. 2002). At the ZFP no flow takes place. Above this depth flow is upward, due to evapotranspiration, and below downward drainage toward the water table takes place. In some situations, it is possible for no ZFP to exist or for multiple ZFPs to exist.

Additional complexity exists in Richards' Equation as the result of the relationship between the hydraulic conductivity and the soil water content, or soil water tension. The relationship between the soil water tension and soil water content is governed by capillary forces. The fundamental equation of capillarity relates the fluid properties and the pore size to calculate the maximum height above the phreatic surface (Eqn. 3).

$$h_c = \frac{2\sigma\cos(\phi)}{pgR}$$ (Fetter, 2001) (3)

Where h_c is the maximum height of at which a pore with radius, R, will remain saturated, σ is the surface tension of the fluid, ϕ is the contact angle of the fluid's meniscus with the soil, ρ is the density of the fluid, and g is the acceleration due to gravity. Because capillary forces are stronger in smaller pore spaces (because of a much smaller radius), smaller pores can remain saturated greater distances above the water table, while larger pores remain saturated only at small heights above the water table. A typical relationship of the reduction in moisture content as pores drain in response to increasing tension head, is shown on Figure 2.2.

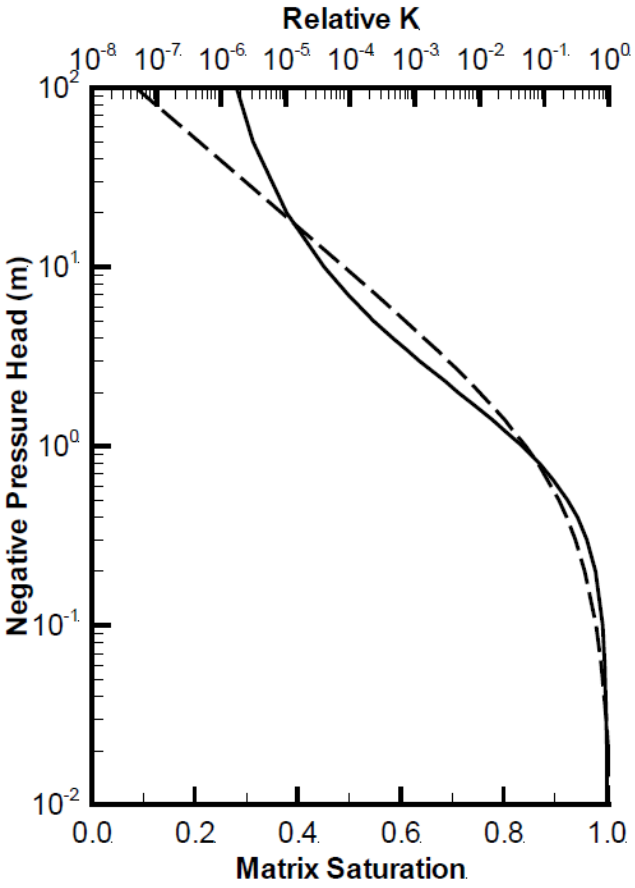

Figure 2.2. Typical soil moisture (solid line) and hydraulic conductivity (dashed line) for a range of soil water tension (Cey, 2007).

The flow of water through the unsaturated zone depends on hydraulic conductivity, as suggested by Richards' Equation. In the saturated case, hydraulic conductivity is treated as a constant but in the unsaturated case hydraulic conductivity is reduced by air filled voids in the soil which do not transmit water (Figure 2.2.) (Fetter, 2001). This relationship becomes even more complex when the repeated wetting and drying processes are considered. Figure 2.3. shows a typical hysteretic relationship between soil water tension and water content during a wetting and drying cycle in the soil.

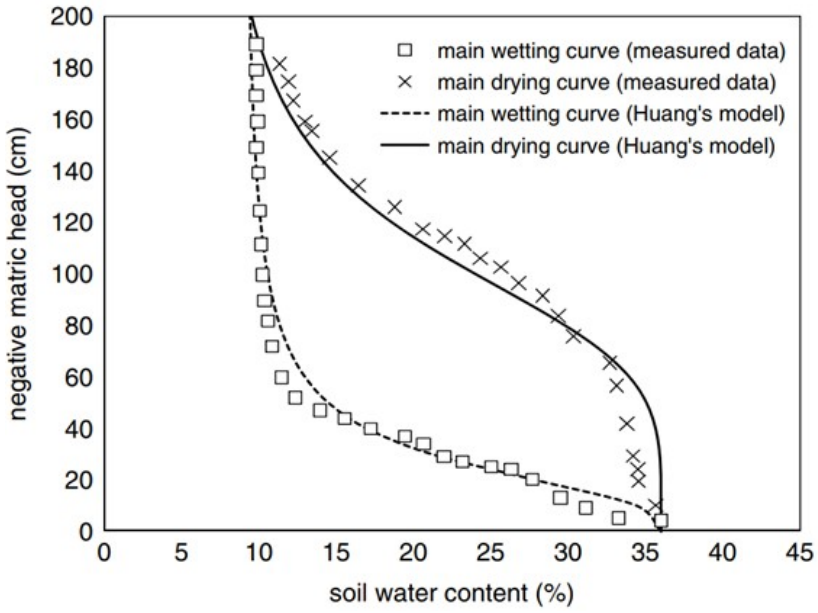

Figure 2.3. Typical hysteresis in water content with respect to soil water tension (Ma, Tan, & Chen, 2011) (Where Huang's model is a fitted curve to the observed data).

Figure 2.3. shows that soil water content depends not only on the soil water tension, but also on the draining-wetting path. Dependence on previous conditions between two parameters is known as hysteresis. Since the hydraulic conductivity of a material is dependent on the soil water tension (as shown in Figure 2.2.), the hysteretic relationship between the moisture content and the soil water tension means that the hydraulic conductivity of an unsaturated soil is also a hysteretic parameter. These relationships complicate the solution to Richards' equation.

The complexity of unsaturated hydraulic conductivity, hysteresis, and capillarity often lead to unpredictable infiltration fronts when observed in field studies. Even subtle heterogeneities can cause irregular or unstable infiltration fronts (Figure 2.4.).

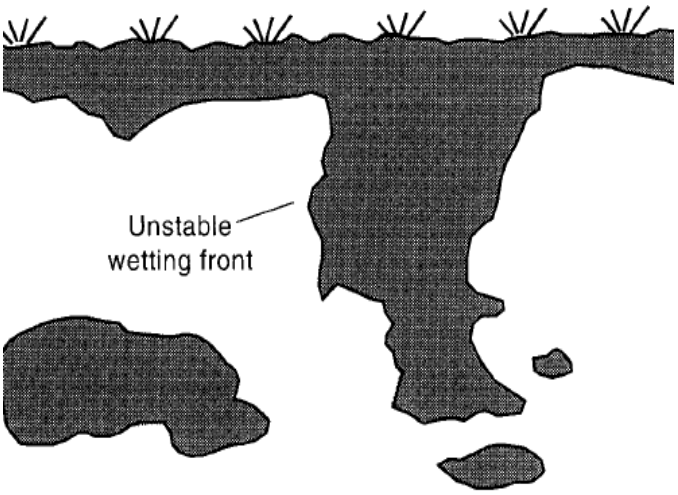

Figure 2.4. Conceptual diagram of typical irregular infiltration front (Scanlon et al. 2002)

One effort to resolve complexity in the hysteretic relationships between moisture content, soil water tension, and unsaturated hydraulic conductivity, is contained in the publications of van Genuchten (1980). The van Genuchten approach is based on empirical curve fitting of wetting and drainage curves to simplify the hysteretic relationship to a single solution. Moisture content and hydraulic conductivity can be related to head using equations 4, 5, and 6.

$$\theta(h) = (\theta_s - \theta_r)(1 + (\alpha h)^n)^{-m} + \theta_r \qquad \text{(van Genuchten, 1980) (4)}$$

$$K_r(h) = \frac{\{1 - (\alpha h)^{n-1}[1 + (\alpha h)^n]^{-m}\}^2}{[1 + (\alpha h)^n]^{m/2}} \qquad \text{(van Genuchten, 1980) (5)}$$

$$m = 1 - {}^1/_n \qquad \text{(van Genuchten, 1980) (6)}$$

Where θ(h) is the moisture content as a function of head, θ_s is the saturated moisture content, θ_r is the residual moisture, h is the tension head, K_r is the unsaturated hydraulic conductivity, and α, n, and m, are empirical fitting parameters. For applications of van Genuchten's equations without expensive site specific data, it is necessary to estimate the required parameters. Estimates are often based on a summary by soil type based on thousands of experimentally

derived van Genuchten parameters (Carsel and Parrish, 1988). The experimental results were used as the basis a software (known as Rosetta) was developed to improve estimates of unsaturated zone properties (Schaap and Leij, 2000; Schaap et al. 2001). These equations with typical parameters have been applied widely to solve vadose zone flow problems. In order to include hysteresis in numerical solutions to the flow and transport of moisture, the alpha parameter can be modified depending on the wetting and drying sequence of the soils (Huang et al., 2011).

2.2. Regional Scale Numerical Modelling

One of the chief needs discussed above is the understanding of an aquifer's recharge. A common approach for quantifying the water supply potential of an aquifer system is the use of large scale numerical models (often with a catchment or sub-catchment domain). This allows users to analyze the potential effects of additional water takings, drought conditions, or other scenarios on the aquifer system. Although this technique is a powerful tool to analyze aquifer systems and answer the questions of water managers, it depends on numerous parameters to physically represent the aquifer system (Sousa et al., 2013). In particular, models require information about the hydraulic properties of the aquifer materials, aquifer discharge, and aquifer recharge to describe the physical flow system. The flow system is driven by recharge, which influences regional hydraulic head distributions and groundwater discharge. Recharge is difficult to measure and highly variable both spatially and temporally. In fact, Risser et al. go so far as to say, it is "nearly impossible to measure recharge directly" (2008). By the use of piezometers, the distribution of hydraulic head in the aquifer system can be fairly well understood. Discharge is generally more localized than recharge, at natural features such as a stream or lake, or at anthropogenic features such as a water supply well (Sousa et al., 2013). The hydraulic properties of the aquifer include the hydraulic conductivity, porosity, and storage properties. Because of intense heterogeneity and spatial variability, none of these parameters are easy to characterize over large regional scales. Hydraulic conductivity is a highly variable parameter, so it is one of the most difficult to parameterize accurately (Sousa et al., 2013).

Porosity and storage properties are related properties. Because of the relatively small range in porosity values (between 0 and 1), it is a fairly well constrained property, by comparison to hydraulic conductivity. Two of the most significant and most difficult to measure aquifer parameters are recharge and hydraulic conductivity. The observed hydraulic head distribution within a groundwater flow system is primarily a function of the ratio between recharge and hydraulic conductivity (Scanlon et al. 2002). Figure 2.5. illustrates the relationship between recharge and hydraulic conductivity and their impact on the results of modeling groundwater head and flow systems. If the transmissivity of the aquifer was increased while the rate of recharge remained the same, a steady state would result in lower head values in the recharge area and equal discharge from the aquifer. However, if both the head and the recharge increase proportionally, no change would take place to the head distribution and discharge from the aquifer would increase.

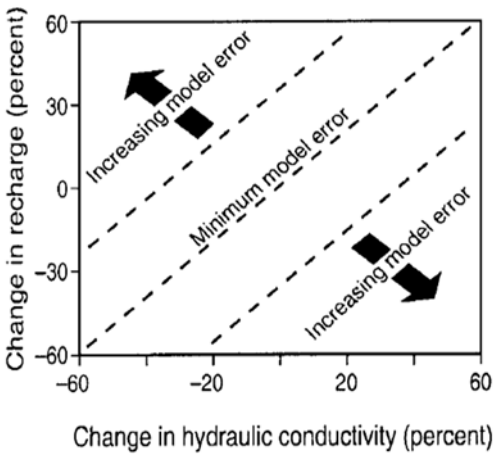

Figure 2.5. Relationship between recharge and hydraulic conductivity in groundwater flow models (Scanlon et al. 2002).

Because the solution to a groundwater flow model is governed by the ratio of hydraulic conductivity and recharge, a solution with an unknown (or poorly known) recharge and hydraulic conductivity is not unique. In order to find a unique solution to a modelled groundwater flow system, characterizing hydraulic conductivity and/or recharge is necessary. Sousa et al. (2013)

suggest that direct measurements of both recharge and hydraulic conductivity are advisable to reduce uncertainty in model results. To provide recharge estimates to support the parameterization of models and reduce uncertainty, various techniques have been applied, commonly including empirical water balance models, information about surficial lithology, and baseflow separation.

2.3. Depression Focused Recharge

Depression focused recharge (DFR) is the process by which surface water flows along a local topographic low or into a closed depression where it is accumulates as a standing surface water pond and subsequently infiltrates causing locally increased recharge, compared to up gradient locations. Closed depressions can collect surface water from drainage areas varying from square centimeters to square kilometers in scale (Hayashi et al. 2003). In the Canadian environment, DFR often occurs after a spring melt where large amounts of precipitation stored as snow, melts quickly and flows over the ground surface and after large or intense rainfall events. During the winter, sub-zero average air temperatures, cause soils to freeze from the top down. The portion of the soil profile below zero is referred to as the frost zone. Figure 2.6. shows a typical conceptual model of DFR during a spring melt event illustrating the influence of the frost zone and its gradual thawing in the spring.

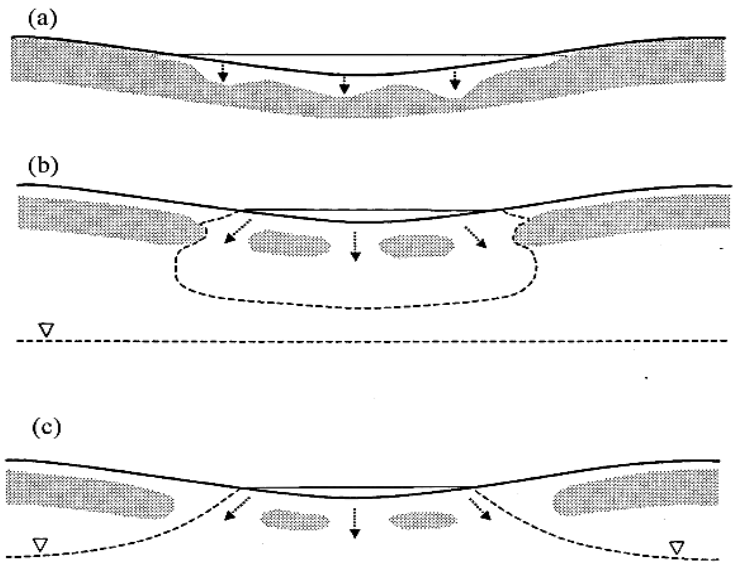

Figure 2.6. Conceptual model of depression focused recharge during a spring melt. (shaded areas indicate soils within the frost zone) (Hayashi et al. 2003) a) DFR process during the start of the melt event b) DFR process during the middle of the melt event c) DFR process during the late stages of the melt event.

The conceptual model of the DFR process with a frozen soil begins with the formation of surface water originating from snow melt in a closed depression on a frozen soil (Figure 2.6.(a)). Because of the relatively low permeability frequently associated with frozen soil, little infiltration may occurs initially. The frost zone then thaws in the presence of warmer melt water and fast flow occurs through the gaps in the frost zone (Figure 2.6.(b)). Finally, the infiltration front reaches the water table causing a rise in water levels and groundwater recharge (Figure 2.6.(c). DFR is typically more rapid without the presence of a frost zone impleading flow.

Depression focused recharge has a significant influence in many areas of the world, with implications for groundwater hydrology, surface water dynamics, and for ecology. The transient formation of ponds in closed depressions contributes significantly to groundwater recharge (Hayashi et al. 2003). In some areas such as the Prairie Potholes, there is "little or no measurable" recharge apart from DFR (Van Dijk, 2005). Replenished groundwater levels, as the result of DFR, are needed for water supply, ecological services, and baseflow in streams (Scanlon et al. 2002). There are also ecosystems that directly depend on the presence of

ephemeral ponds (Hayashi et al. 2003). Because DFR is such a significant process, extensive research programs have been conducted to characterize the processes and effects of DFR. For purposes of this research project a subset of the most recent and relevant papers were reviewed to assess the current state of literature on the topic of DFR. Although there is a significant body of literature on the topic of DFR, there has been very little published since 2005. To review the available literature, observations have been addressed as subtopics including lithological effects, freeze-thaw, spatial variability, temporal variability, physical flow processes, and surface water estimation techniques.

2.3.1. Lithological and Surface Water Distribution Affects on Depression Focused Recharge

Critical considerations to estimating DFR are the lithology between the ground surface and the aquifer and the distribution of surface water above the ground surface. As discussed in Section 2.2., many hydrologic models use information about surficial lithology to help inform recharge distribution. In recent years DFR studies have occurred in a number of different settings and demonstrated the effect of lithology on the recharge process. Table 2.1. summarizes research on the role of lithology in controlling DFR since the year 2000.

Table 2.1. Summary of Depression Focused Recharge Studies by Surficial Lithology		
Author	Year	Surficial Lithology, Geomorphology
Daniel and Staricka	2000	Clay rich glacial till, "Prairie pothole region"
Hayashi and Van Der Kamp	2000	Clay rich glacial till, "Prairie pothole region"
Hayashi et al.	2003	Clay rich glacial till, "Prairie pothole region"
Berthold et al.	2004	Clay rich glacial till, "Prairie pothole region"
Van Dijk	2005	Clay rich glacial till, "Prairie pothole region"
Minke et al.	2010	Clay rich glacial till, "Prairie pothole region"
Hayashi and Farrow	2014	Clay rich glacial till, "Prairie pothole region"
Delin et al.	2000	Coarse interbedded sand, Minnesota, glacial outwash
Bekeris	2007	Coarse sand, Woodstock, ON
Brook	2012	Clay to coarse sand, Woodstock, ON
Pasha	2017	Clay to coarse sand, Woodstock, ON
Wiebe and Rudolph	In progress	Various soils, Alder Creek Subwatershed, ON

Surficial lithology is defined as the soil material exposed at the ground surface, which can have a significant impact on recharge. The recent studies on the topic of depression focused recharge are centered on glaciated terrain in Woodstock, Ontario, where ephemeral surface water features on sandy soils create rapid dynamic recharge (Brook, 2012, and Pasha, 2017) and the Prairie pothole region, typified by the clay-rich glacial tills, small surface water filled closed depressions, low hydraulic conductivity, and low annual recharge rates (Hayashi and Farrow, 2014).

Studies of recharge in Woodstock, Ontario, observed the presence of ground surface infiltration and focused infiltration beneath an ephemeral stream channel. Surficial soils on the site range from silty clay to coarse sand. First, Bekeris observed the effect of lithostratigraphy at this field site on recharge processes (2007). During the study, vertical profiles of equipment were installed to observe recharge, based on the assumption that recharge is predominantly a vertical flow process. In some near vertical instrument arrays, a discontinuous clay layer was observed in the shallow subsurface. The low hydraulic conductivity of the clay layer slowed the

progress of infiltrating water in the unsaturated zone and caused infiltrating water to flow laterally. Bekeris also noted the occasional formation of an ephemeral stream during hydrologic event. Brook followed up on Bekeris' study by installing detailed instrumentation in the clayey silt soil adjacent to the ephemeral stream channel to observe dynamics and quantify recharge during the Spring Melt of 2012 (2012). The study used water level, moisture content, and temperature data to observe rapid recharge, calibrate a numerical model, and quantify recharge. Brook (2012) observed 0.15 m of recharge at the monitoring location and further noted that the ephemeral stream in the area posed a risk to the nearby public supply wells (Christie et al., 2009). The study also noted that the presence of seasonal frost slowed groundwater recharge. Finally, Pasha instrumented the ephemeral stream channel to observe water level, moisture content, and temperature during the Spring Melt in 2015 (2017). The study observed 0.73 m of recharge beneath the ephemeral stream, highlighted the spatial variability of recharge, and observed that the presence of partially frozen conditions in the subsurface led to delayed groundwater recharge. The methods and findings of the studies at the Woodstock site provide the most relevant background for this study in Mannheim, Ontario.

Studies of DFR in the prairie potholes region show little or no recharge happens apart from event based DFR (Hayashi and Van Der Kamp, 2000), (Berthold et al. 2004), and (Van Dijk, 2005). This means that the prairie pothole region is very sensitive to DFR for water supply and irrigation needs, which has driven extensive research in this area. Studies have also taken place in sandy soils (Delin et al., 2000, Bekeris, 2007, Brook, 2012, and Pasha, 2017). These studies showed that surficial lithology has a significant influence on the infiltration rate, potential recharge in a DFR area, and seasonality's affect on recharge dynamics. During the formation of surface water in a depression, near surface storage is filled rapidly, and then infiltration primarily depends on the underlying hydraulic conductivity with evaporative losses playing a smaller role (Hayashi et al. 2003).

Shallow lithology, the soils immediately below the ground surface, can also influence the process by which DFR occurs. Studies have shown the influence of soil texture, lithostratigraphy, capillary affinity contrasts, and macropores. Soil texture's influence on DFR was observed during an extensive research project undertaken by Delin et al. (2000), which took place in agricultural corn fields in Minnesota. The study observed two groundwater recharge

sites, one in an upland area, and the other in a depression focused area. The results of the study found that the depression focused recharge area received more (30% to 80%) than the compared upland area. However, when the sites were selected, it was thought that the lithologies were nearly identical to facilitate the comparison of the two locations. After performing more detailed characterization during the experiment, it was found that the upland site contained interbedding, which significantly influenced the progression of the wetting front and the infiltration capacity. This small texture difference in the shallow lithology led to the significant differences in the two sites and increased uncertainty in the study (Delin et al. 2000). A capillary barrier effect was observed by Van Dijk (2005). In that study, water infiltrated in closed depressions in the surficial soil, a fine clay, flowed vertically downward where it reached the interface between the fine shallow soils and the underlying unsaturated gravel aquifer. At the interface, flow was impeded by a capillary barrier, the affect of the greater capillary affinity of the clay materials than the coarser underlying sediments. Macroporosity has also been observed to affect DFR. Macroporosity can be the result of bioturbation (Cey, et al. 2009) or of freeze-thaw dynamics (Daniel and Staricka, 2000). Berthold et al. (2004) instrumented a site in the low permeability prairie pothole region. They observed that the shallow subsurface had significant macroporosity due to the presence of worm holes and root holes in the soil. When surface water formed during the spring melt, the depression rapidly filled the shallow storage (dominated by bioturbation) then infiltrated slowly as controlled by the intact hydraulic conductivity of the clay rich till (not bioturbated).

The findings of these studies are used for background information for this study. The most relevant studies are Brook (2012) and Pasha (2017), which observed dynamic recharge in similar soils. Typically, the responses to hydrologic events are rapid, because of the high conductivity of sands. The numerous studies in the prairie potholes are not an ideal comparison for this study, however the observations drawn from these studies provide insight into the influence of near surface lithology and surface water distribution on DFR processes.

2.3.2. Freeze-Thaw Affects on Depression Focused Recharge

In northern climates, recharge is strongly influenced by seasonality. During winter months, soils and pore water freeze from the ground surface downward. When pore water freezes it expands by 10% typically (Daniel and Staricka, 2000). This frozen portion of the subsurface is referred to as the frost zone. Literature about the potential effects of the frost zone on depression focused recharge includes: multiphase flow, frozen soil hydraulic conductivity, impervious ice layers, rate limiting processes, thermal energy flux modeling, and events with sequential infiltration rates.

Flow in the frost zone is a more complex process because of the addition of an ice phase to the flow and storage equations. The simplest groundwater flow problem is the saturated case with two (2) phases, soil and water. A more complicated case is flow in the unsaturated zone with three (3) phases, soil, air, and water (as discussed in Section 2.). As freezing and thawing take place a fourth phase is introduced, ice. This flow problem now includes the influence of these four (4) distinct phases within the porous medium, several of which are interrelated through soil water flow, temperature, and energy flux (Daniel and Staricka, 2000). Additionally, the hydraulic properties of the soil are related to the ice/water/air content in the pore spaces. As pore water freezes into ice, hydraulic conductivity is reduced. In the case where pore spaces are entirely filled with ice, the hydraulic conductivity is zero (0). When the soil reaches a frozen state all of the soil water freezes and the liquid water content is zero. Depending on soil saturation during the freezing process, the ice content can range from the residual moisture content, or even the wilting point, to the soil's saturated water content. A soil that freezes with low moisture content will still have a greater than zero permeability and storage. As a result, when water is released during a melt event from the snow pack the water can infiltrate and flow through the frost zone as a function of the hydraulic conductivity of the soils in the frost zone. In general, the soil water content is relatively high within the frost zone, especially at the freezing front (Daniel and Staricka, 2000).

Daniel and Staricka, (2000) reviewed the literature on the effects of frost on the hydraulic conductivity of soils. They summarized 3 primary effects of frost on hydraulic conductivity.

First, the presence of ice forms a physical impediment to flow by occupying pore space. Water preferentially freezes the smallest pore spaces, since they are the most likely to be saturated by capillary forces. The effect on hydraulic conductivity is proportional to the ice content in the pore spaces and which pores are filled by ice. Second, the hydraulic conductivity can be increased by the presence of ice macropore structures. During the freezing process, ice increases in volume from its liquid state. If the soil structure does not have the adequate pore space to accommodate the increased volume this can create fractures and macropore structures in the frost zone. Another source of macroporosity in the frost zone is the partial melting of ice in the frost zone during the thawing process, which can leave preferential flow paths through the frost zone. These structures often only exist temporarily. During thawing macropore features and preferential pathways often collapse during thawing, are filled by silt, or refreeze and the soil returns to a value close to the original hydraulic conductivity (Daniel and Staricka, 2000). The presence of macropores in the shallow soils and frost zone temporarily increases hydraulic conductivity radically in some cases. Some DFR studies have observed "rapid" infiltration through frozen soils at the beginning of an infiltration event, which could be attributed to the presence of frost zone macroporosity and preferential pathways (Bekeris, 2007) (Daniel and Staricka, 2000). There is a wide variety of processes observed in frozen soils, which can both increase and decrease the permeability of the soils. Detailed observation is called for in order to characterize the hydraulic behavior of frozen soils.

A number of field studies of DFR occurring in frozen soils have contributed to conceptual models of DFR including: Daniel and Staricka (2000), Hayashi et al. (2003), Delin et al. (2000), (Bekeris, 2007), Van Dijk, (2005), Brook (2012), and Pasha (2017). Because many of the processes in the frost zone occur on a small scale, many researchers comment on the bulk behavior of the soil instead of considering the physical processes occurring on the pore scale. The notable field scale study contributions to the conceptual models of the influence of the frost zone on DFR are summarized below.

Hayashi et al. (2003) made detailed observations of a DFR site in the Prairie potholes region of western Canada and developed the "rate limiting process" model for the rate of DFR. Similar to other studies Hayashi et al. (2003) noted distinct variation in infiltration rates, and were able to develop and apply a conceptual model for the rate changes. Two rates were

observed during an infiltration event. First, a slow rate was observed under a standing body of surface water. Then a sudden increase of infiltration was observed days after the formation of surface water. This is explained using the "rate limiting process" principle (Hayashi et al. 2003). At an early time the slow infiltration was controlled by ice content in the frost zone. After cold melt water infiltrated into sub-zero frost zone melt, water refroze and formed an "impervious" layer (Hayashi et al. 2003). This layer migrated downward, as energy from the surface caused the layer to melt, flow downward, and again refreeze in the sub-zero frost zone. This process limited infiltration to the storage capacity above the impervious ice layer. The impervious ice layer progressed downward until the ice layer reached the bottom of the frost zone. After the thawing of the frost zone the infiltration rate was limited by the hydraulic properties of the underlying soil. This model was validated with the application of an innovative energy flux model, used to predict the downward movement of the ice layer. The flux of energy from the warm surface water conducted through the soil and stagnant pore water to slowly melt the ice layer. This approach closely matched results from the field study. The second rate of infiltration was limited by the hydraulic properties of the soils as shown by comparison to the rate of infiltration during intense summer rain events.

In addition to making observations about the rate limiting process during spring infiltration, Hayashi et al. (2003) also noted the effect of thermal energy fluxes to the frost zone on the flow pattern during infiltration. It was observed that under snow covered ground surrounding the closed depression the frost zone received fairly little thermal energy flux and thawed slowly. In the low area of the closed depression, surface water formed, and melted the snow. The sun heated the water, and a greater thermal flux caused thawing of the frost zone. This was described using an energy flux model. The greater thermal mass of the water around the accelerated the thawing of frost zone under the DFR area, as opposed to the thermal mass of the air thawing areas outside of the closed depression. Surrounding soils were still frozen when the infiltration rate increased in the DFR area. This meant that the permeability of the surrounding soils was reduced compared to those under the DFR area. The contrast in hydraulic conductivity caused flow to be more vertical in response to infiltration compared to a summer event when all the soils are unaffected by frost. This is effectively transient anisotropy in the permeability of the soils.

Another detailed study of a DFR feature affected by frozen soils was completed by Daniel and Staricka (2000). That study observed a similar variation of infiltration rate. They described the infiltration rate in three distinct steps. For a short time period after the start of the event, very rapid infiltration occurred, believed to be the result of frost related macroporosity. Second, a slow infiltration rate was observed, likely due to a partial melting and refreezing process in the frost zone. Finally, the infiltration rate increased suddenly as a result of the frost zone's complete thawing. The progression of the infiltration rates was similar to that of Hayashi et al. (2003). The notable difference was that the initially rapid infiltration was not observed by Hayashi et al. (2003), which Daniel and Staricka (2000) attributed to frost created macropore structures. The study also included detailed monitoring of the water table beneath the DFR. This showed some recharge was taking place during the phase of slow infiltration. This could be explained by melting ice on the bottom of the frost zone or by incomplete formation of the ice layer allowing the small amounts of flow through the frost zone.

DFR is studied most often in cold northern climates, where frozen soils affect the dynamics of recharge. Extensive studies in this area have shown the complex effects of frost on soils and their hydraulic properties. There have also been field studies which observed impervious ice layers, rate limiting processes, thermal energy flux to the frost zone, and variable infiltration rates. The literature in this important area of study provides a starting place for this study, but also highlights the need for more field observations of these complex phenomena.

2.3.3. Spatial Variability of Depression Focused Recharge

Depression focused recharge causes spatial variability in the distribution of recharge at the water table. Significant research has been done examining the spatial variability of DFR including studies by Delin et al. (2000), Van Dijk (2005), Daniel and Staricka (2000), Brook (2012), Pasha (2017), and Scanlon (2002). These studies have served to highlight the variable influence of DFR, the spatial occurrence of DFR, the need for detailed information in interpretation of DFR, and the uncertainty surrounding the distribution of recharge.

Delin et al. (2000), Van Dijk (2005), Brook (2012), and Pasha (2017) performed studies on sites with different surficial lithologies and topography, then observed different spatial distributions of recharge as a result. Delin et al. (2000) studied DFR on a sandy corn field with the primary objective of assessing the spatial difference in recharge. They found that depression focused areas received 30% more recharge in that case, as compared to sites on an adjacent plane at a higher elevation. In 2005, Van Dijk studied spatial variability in the prairie potholes region. Here he observed "little or no" recharge in uplands areas by comparison to the DFR areas (Van Dijk, 2005). In these two studies a contrast of 30% occurs in a sandy soil, and ~100% in a clay rich till. DFR can have a wide range of impacts on recharge distribution from a fairly small influence to a dominant process.

Most DFR studies are sited where it is obvious that surface water is concentrated in a depression. Interestingly, Delin et al. (2000) observed that DFR occurred in a sandy aquifer without evidence of large scale overland flow. In this study, the site at a lower elevation typically received 40% more recharge than the station at a higher elevation. This highlights the difficulty of identifying where DFR can occur, since it may be a significant process even on sites without obvious visual evidence of DFR taking place.

Daniel and Staricka (2000) observed recharge at the water table and the frost zone, using piezometers to estimate groundwater storage increases and temperature probes. During recharge events piezometers in the closed depression and at background locations were monitored to estimate recharge using the water table fluctuation method. At to DFR areas, groundwater hydrographs showed a rise shortly after the infiltration event. Without additional data, this would lead to the interpretation that recharge had taken place from the closed depression. However, temperature and head data under the surface water in the closed depression, showed that: first the frost zone thawed, then groundwater levels rose under the closed depressions, and finally, groundwater levels rose in the piezometers surrounding the depression. The authors concluded that the initial rise in groundwater levels in piezometers adjacent to the closed depression was a result of lateral flow from the ground water mound under the DFR area. This study shows the need for ground water levels to be interpreted in context of other recharge processes around it (Daniel and Staricka, 2000).

Finally, Bekeris (2007) and Scanlon et al. (2002) point out that in many cases the subtle influences of lithology and unsaturated flow processes increase uncertainty in recharge distribution estimates. Both studies used extensive field data sets and noted that various processes affected the distribution of recharge at the water table in unpredictable ways. As in many hydrogeology applications, subtle heterogeneities can have substantial influences and complicate the analysis of hydrologic phenomena in these natural systems.

2.3.4. Temporal Occurrence of Depression Focused Recharge

Depression focused recharge should generally be considered as a time discrete recharge event. The specific temporal occurrence of the recharge is often caused by meteorological influences. Researchers have observed the temporal occurrence of recharge during spring melt and intense rain events. Hayashi et al. summarized the observations on DFR occurrence as typical during snow melt events and only during "exceptional" rain events (2003).

In northern climates DFR occurs during spring melts as a result of reduced infiltration capacity and large amounts of water available at surface. As discussed in Section 2.3.2, the hydraulic conductivity and storage capacity of soils are typically reduced by the presence of a frost zone. During winter months, a snow pack generally accumulates and densifies. During the spring, temperatures rise and the snow pack melts, releasing months of stored precipitation. The exact air temperature, precipitation, evaporation, wind, solar radiation, and albedo coefficient control the melting of the snow pack and warming of the frost zone (Van Dijk, 2005). How fast and energetic a melt event is, strongly relates to whether the snow melt happens rapidly enough to exceed infiltration capacity, flow as surface water, and contribute to DFR. The occurrence and magnitude of DFR are sensitive to the meteorological conditions during snow melt (Van Dijk, 2005). During the Van Dijk (2005) research program, surface water generally formed in significant quantities in response to snow melting. On one occasion snow melt was particularly slow, no surface water formed, and DFR did not occur. It is thought that the slower melt allowed the frost zone to partially thaw, increasing the infiltration capacity of the soils, and that more

evaporation took place over the longer melt period. This example highlights the sensitivity of snow melt to meteorology conditions.

The second common occurrence of DFR is during intense rainfall events. Studies have also shown that this process is sensitive to specific meteorological conditions (Berthold et al. 2004) and antecedent soil moisture (Hayashi et al. 2003). Berthold et al. (2004) noted that a certain magnitude and intensity of precipitation caused the formation of surface water and DFR. This is believed to be related to the infiltration capacity of the soils. When the infiltration capacity was exceeded, runoff and DFR would take place. This means that the frequency of precipitation at certain intensities and magnitudes is related to the frequency of DFR. Hayashi et al. (2003) observed that the temporal occurrence of DFR depended on the antecedent moisture content in the shallow subsurface. Where a recent infiltration event occurred (such as a rain event) and soils near the surface had little available storage such that surface water runoff occurred and caused DFR.

Previous studies have shown that the occurrence of DFR, both in response to rain and snow melt events, is sensitive to meteorological conditions. Many studies have shown that climate change is taking place throughout the world. The magnitude and frequency of DFR could be altered significantly by climate change (Hayashi and Farrow, 2014). This would have significant implications for aquifers and ecosystems dependent on DFR.

2.3.5. Flow Processes Associated with Depression Focused Recharge

Compared to most hydrogeologic flow systems, depression focused recharge is a very rapid event leading to uncommon flow dynamics. Studies have observed a number of phenomena including large volumes of entrapped air, macropore dominated flow, transient groundwater mounding, and capillary barriers.

In 2000, Daniel and Staricka observed that DFR can entrap large amounts of air in the shallow subsurface. Typically, air is assumed to be infinitely mobile in groundwater flow systems, but the sudden introduction of positive head at the ground surface did not allow the air

beneath it to be displaced. For a significant amount of time, groundwater heads observed were well above surrounding heads, and then sharply declined. This was explained as entrapped air venting suddenly.

During the same study Daniel and Staricka (2000) noted that macropores were not subject to the refreezing of melt water, the way the bulk material was (see Section 2.3.2. for details). Cey et al. (2009) noted the transport potential of macroporosity. Because of the larger aperture of macropores, they are able to transport small particles, such as colloids including pathogens, which could not move through the bulk material. In the context of DFR this represents an increased risk to water supply vulnerability.

A phenomenon observed during DFR is groundwater mounding under the infiltration area. Many studies observed the increase in groundwater temporarily stored under a DFR area (Daniel and Staricka, 2000; Hayashi et al. 2003; Berthold et al. 2004 and Van Dijk, 2005). This storage increase phenomenon is the basis of the Water Table Fluctuation Method (WTF) (Healy, 2010) (See Section 2.4.1. for details). Daniel and Staricka (2000) observed the formation and disappearance of groundwater mounds. They noted two processes that are active to dissipate groundwater mounds. First, higher head in the mound than the surrounding aquifer material causes lateral flow. Groundwater mounds can also be reduced by upward flow through the vadose zone driven by evapotranspiration (ET) at the ground surface. This is more likely to happen in soils with hydraulic properties that do not allow groundwater mounds to redistribute readily within the subsurface.

The final flow process observed by researchers in the unsaturated zone that can influence DFR is the effect of a capillary barrier. Van Dijk (2005) monitored infiltration and unsaturated zone flow in a depression in the prairie potholes. The water table was located in a gravel aquifer underlying the clayey till topsoil. When melt water from the DFR area reached the interface between the clay till and the gravel aquifer, the capillary affinity of the much smaller pores in the till prevented downward flow from continuing into the gravel aquifer.

The breadth of possible flow processes that can take place under a DFR area considerably complicates the conceptualization of how aquifer recharge takes place. More field studies

making detailed observations are needed to understand flow processes and make predictions about the behavior of DFR areas.

2.4. Recharge Quantification Methods

Recharge is a critical parameter to groundwater flow and transport problems that is "nearly impossible" to observe directly (Risser et al. 2009). There are a number of reasons why recharge is so difficult to measure reliably. One of the reasons is that recharge occurs at the water table surface, a specific 2D plane, which is dynamic in time and space (Healy and Cook, 2002). As discussed in Section 2.3.5., unsaturated flow is the mechanism by which recharge occurs and is difficult to parameterize and solve. Temperature fluxes, evapotranspiration, and hysteresis also complicate the recharge process. Complexity in the physical processes surrounding recharge has led to the design of various approaches to quantify recharge. These vary widely in scale of observation, level of detail, cost, assumptions, and conceptual approach. Quantifying event based recharge on a site scale is one of the key objectives of this study. This section reviews literature methods of recharge to quantify recharge and assesses the applicability of the method to this study's application. These methods are generally based on data from surface water, ground surface, unsaturated zone, and saturated zone.

Surface water methods to quantify groundwater recharge include stream flow regression methods, large scale water budgets, and site scale water budgets. These methods have the benefit of using the readily available surface water data to estimate recharge.

Stream flow regression methods use observations at stream gauging locations where stage and discharge are measured. The stream hydrographs contain both baseflow and higher flow stages based on hydrologic events. Some recharge estimation techniques use the premise that the baseflow of the stream is driven by aquifer discharge, which in the long term is equal to recharge (this assuming no change in long term aquifer storage) (Risser et al. 2009). Any recharge estimate based on a stream hydrograph is representative of broad areal recharge of the upstream catchment from that point. Examples of this technique include software packages such

as, PART and HYSEP. They perform baseflow regression using some empirical and "somewhat arbitrary" criteria (Risser et al. 2009). The other usage of surface water data to estimate recharge is by creating a model of the aquifer, applying a recharge pulse to it, calculating groundwater discharge to surface water (using the equations known as the Rorabaugh equations), and calibrating the resulting hydrograph to the observed hydrograph. RORA and PULSE are software applications designed to implement this conceptual approach to quantifying recharge (Risser et al. 2009). The large averaging area of stream flow regression methods based techniques makes it unsuitable for this site scale study.

The second surface water recharge quantification considered is estimating DFR on a larger scale using a water balance technique. This method was developed to estimate recharge in the prairie potholes region (discussed in Section 2.3.1.) use readily available ground surface elevation data and easily collected water depth information in DFR areas to estimate surface water volumes in each depression using equations. The method includes equations to estimate volume in irregularly shaped depressions given a water level (Minke et al. 2010 and Hayashi and Van Der Kamp, 2000). By estimating the volume of water in the closed depressions and measuring potential evapotranspiration, the residual, infiltration, can be calculated. Because of the availability of the data, surface water budget methods have potential to provide recharge estimates on a large scale, however this method is not suitable for this study due to large area of application and relatively low precision.

The third surface water method for quantifying groundwater recharge is a detailed site scale water balance. The water balance is calculated on the premise that after precipitation falls, it will either evaporate, be caught in vegetation, runoff, change in soil storage, or immediately contributes to recharge, as shown in equation 4.

$$P_i = Ea_i + I_i + R_i + B_i + \Delta S_i \qquad \text{(Finch, 1998) (4)}$$

Where Pi is precipitation (in mm), Eai is evaporation (mm), Ii is precipitation caught in the canopy (mm), Ri is runoff (mm), Bi is the immediate contribution to recharge (mm), and Si is

change in soil water (mm) (Finch, 1998). In order to use a water balance to estimate groundwater recharge using a water balance, all the other parameters in the equation must be measured directly or estimated. In practice these parameters can typically be measured at point observations or estimated for a larger area (Finch, 1998). A sensitivity analysis showed that soil parameters and rooting depth have the largest influence on the groundwater recharge, estimated using a water balance approach and caused significant uncertainty in groundwater recharge estimates (Finch, 1998). A water balance to quantify groundwater recharge can be accomplished by estimating all terms of the water balance and calculating the groundwater recharge as the residual. However, the residual includes the cumulative errors of each term in the water balance, leading to significant uncertainty in the residual term (Wiebe et al. 2015). Due to the level of uncertainty and the difficulty quantifying overland flow over irregular surfaces on the study site, a water balance would be difficult to apply on this site.

The second category of recharge quantification methods are those applied at the ground surface. Broadly, these methods include monolith lysimeters and surface water budgets. Monolith lysimeters are an expensive and complex field method used to directly quantify infiltration at the ground surface by collecting and measuring water flowing through the unsaturated zone. Any recharge estimate from a lysimeter is a potential recharge value. Lysimeters have also been shown to be sensitive to the construction methodology (Risser et al. 2009). Water budgets make use of readily available data such as meteorology, surficial elevation, land use type (and associated vegetation properties), and surficial lithology to estimate the recharge over large areas (Risser et al. 2009). When a water balance is applied, the balance can be closed by measuring all terms or one term can be estimated by the residual in the water balance equation. A frequently used model based on this technique is HELP3, which estimates recharge as the residual in a water balance equation. Wiebe et al. studied the effect of cumulative error in a water balance which estimates a parameter as the residual (2015). It was found that the residual errors and uncertainties from other terms can introduce error on the magnitude of the residual term. While the water budget method can be helpful on a large scale, it is not suitable for the site scale recharge estimates required for this study.

A third approach to quantify recharge makes use of data collected in the unsaturated zone. These approaches are based on the physical flow processes in the unsaturated zone and

require data (measured or assumed) to describe these flow processes. Darcy's law describes the flow of water through porous material in response to an applied head. It can be applied in the unsaturated zone. The difficulty in this method is in estimating the hydraulic conductivity of the unsaturated soil, because this is a function of the moisture content (Scanlon et al. 2002). A second approach requiring considerably more data is the zero flux plane (ZFP) method described by Scanlon et al. (2002). The ZFP method measures soil water tension at an array of depths to calculate the hydraulic head distribution after an infiltration event. The point at which the head gradient is zero is said to be the ZFP. Water above the ZFP will be drawn upward by evapotranspiration and water below it will contribute to recharge. Finally, calibrated numerical models (such as HYDRUS) can be used to describe flow of water in unsaturated soils. This method has the least assumptions, because a numerical model spatially explicitly represents the flow of water (Bekeris, 2007) (Scanlon et al. 2002). All of these approaches use spatially specific parameters, so they yield point estimates of recharge. Of methods that make use of unsaturated zone data, the use of a numerical model is feasible for this study.

The final conceptual approach to estimating recharge is by using saturated zone data. This is a particularly appealing concept, because of the abundance of head observation and the comparative simplicity of its observation. By using direct head observations recharge can be estimated using the water table fluctuation (WTF) method (Healy and Cook, 2002) (Risser et al. 2009). Another method using saturated observations is to use a tracer to observe recharge rates. The tracer is introduced at the ground surface and observed by repeatedly sampling in the saturated zone for the presence of the tracer (Scanlon et al. 2002) (Bekeris, 2007) (Cey, et al. 2009). Both of the saturated zone methods for recharge quantification could be applied on a site scale, making both methods feasible for application in this study.

Of the methods discussed above, the WTF method, the tracer method, and the use of a numerical model are reasonable for application on this site scale DFR study. The available literature on these topics is reviewed in the remainder of this section.

2.4.1. Recharge Quantification Using the Water Table Fluctuation Method

The water table fluctuation method makes use of observations of the piezometric surface to estimate recharge. Healy and Cook described the WTF method in detail and its potential applications (2002). In order to apply the WTF method there must be a sharp rise in the well hydrograph, as is shown in Figure 2.7.

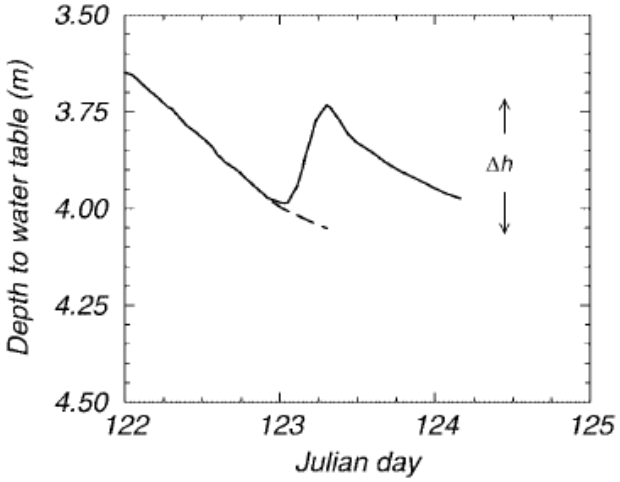

Figure 2.7. Typical rise in water table rise in response to recharge (predicted water table recession shown in dashed line) (Healy and Cook, 2002)

In order to quantify recharge, the WTF method assumes that recharge occurs in a near instant pulse so that the recharging water contributes to storage and does not flow away from the point of recharge. The storage filled is equal to the specific yield of the soils filled by the water table rise. The observed height of water level change, Δh, is the head increase observed in a piezometer compared to the predicted water level at the peak of the well hydrograph. The estimation of the predicted water level is often achieved using an extrapolation (generally linear, but other extrapolation techniques have also been applied) of the well hydrograph from the days prior to the recharge event. Equation 5 describes the WTF method's approximation of the recharge rate at the point of observation.

$$R = S_y \frac{\Delta h}{\Delta t}$$ (Healy and Cook, 2002) (5)

Where R is the recharge rate, S_y is the specific yield, and Δh is the rise in hydraulic head observed over the time interval Δt, in which the recharge occurs.

The WTF method is simple enough to be implemented with readily available hydraulic head data and has other significant benefits. It is broadly applicable wherever an unconfined aquifer is observed. Analysis of the well hydrograph using the above equation can be done easily using a spreadsheet program (Healy and Cook, 2002). Another major advantage of the WTF method over many recharge estimation methods is the fact that it directly observes recharge near the water table, while most other methods either yield a "potential recharge" or a residual in a water balance (Risser et al. 2009).

Risser et al. used a detailed field study of recharge to compare recharge quantification techniques, including the WTF method (2009). They found that the WTF method proved the least variable method applied to the collected data sets. The reliability of the results is attributed to the more direct observation of recharge near the water table, as opposed to other techniques discussed in Section 2.4. It is also noted that in cases where methods with significant assumptions are being made, multiple techniques should be applied to assess the range of possible recharge rates and the reliability of the assumptions supporting each method (Risser et al. 2009) (Healy and Cook, 2002).

Assumptions made by this recharge quantification method include:

(1) the aquifer is unconfined,

(2) a rise in water levels is associated with a recharge event,

(3) recharge is near instant,

(4) the selected wells are representative of head in the aquifer of interest, and

(5) specific yield is constant.

The first two assumptions are dictated by the conceptual model. Water is transported through the vadose zone in an unconfined aquifer and arrives at the water table causing a rise in

the water table and an increase in storage (Healy and Cook, 2002). The assumption that recharge happens in a near instant pulse is made to simplify the groundwater flow problem. If the pulse of recharge arrives quickly, it can be estimated that all recharge contributes to increased storage and that any flow away from the point of recharge is slow by comparison. This method therefore excludes any vertical or horizontal flow during the sharp rise in groundwater levels. In order to make generalizations about the quantity of recharge supplied to an aquifer unit, representative piezometers must be selected to accurately assess the increase in storage throughout the aquifer. Finally, the WTF method assumes that the specific yield is constant.

The applicability and accuracy of the WTF method is limited by its assumptions. One of the most significant problems with the WTF method is that it fails to recognise more gradual recharge. If a large recharge event took place with slow recharge afterward, the WTF method would estimate the recharge of the initial pulse, but would not estimate any recharge during the slow recession of the piezometric surface (Healy and Cook, 2002). To generalize the recharge rate calculated by the WTF method, wells representative of the aquifer should be selected for analysis (Healy and Cook, 2002). The siting and depth of these representative wells can be problematic when trying to estimate recharge on an aquifer scale (Scanlon et al. 2002). The WTF method in the absence of other data could lead to mistakenly estimating lateral flow in an aquifer as recharge. This shows the need for water table measurements to have context to show the simultaneous arrival of recharge through the vadose zone (Daniel and Staricka, 2000). The equation used to calculate the recharge rate by the WTF method assumes that specific yield is a constant. This often proves to be a poor assumption due to changes in entrapped air, affecting moisture content changes (Scanlon et al. 2002). Because the air entrapment is a function of hysteretic changes in soil moisture tension and soil moisture content (as discussed in Section 2.1.), specific yield is also a hysteretic variable (Scanlon et al. 2002). Furthermore, the specific yield of a fractured rock aquifer system can be very difficult to estimate, with estimates routinely varying by an order of magnitude (Risser et al. 2009) (Healy and Cook, 2002). Spatial variability and measurement error also contribute to error in the WTF method (Healy and Cook, 2002). The WTF method assumption of rapid recharge, neglects vertical flow taking place during the event.

2.4.2. Recharge Quantification Using an Observed Tracer

The use of a tracer can provide a simple and powerful technique to estimate groundwater recharge (Scanlon et al. 2002). The fundamental concept of tracer studies is that infiltrating water can carry tracers into the subsurface. The distribution of the tracer can be observed at later times to make inferences about the movement of infiltrating water. There are 3 conceptual models for evaluating recharge using tracers: profile method, mass balance, and peak displacement (Scanlon, 2010). The profile method requires a known time and rate of application of a tracer and spatially dense observation of concentration at a later time. The peak concentration or the centre of mass is observed in the profile to measure the displacement of the tracer over a known time. The second method to analyze tracer data is the mass balance method. The mass balance method requires a known time and application rate. It measures the mass flux into and out of the unsaturated zone to approximate recharge (Scanlon, 2010). This study took place where complex surface water processes made it difficult to apply a tracer at a known time and application rate, to a known area. Because both the profile method and the mass balance method require a known application rate and timing, they could not be applied in this study. The final analytical approach does not depend on a known initial concentration. It is the peak displacement method, which measures the concentration profile, with spatial density, at two times to observe the displacement of the peak concentration over time (Scanlon, 2010). This method is the most suitable, so it was applied during this study. The velocity of flow in the unsaturated zone is calculated by comparing the displacement between the peak concentrations at two times (Eqn. 6).

$$v = \frac{\Delta z_t}{\Delta t} \qquad \text{(Scanlon, 2010) (6)}$$

Where v is the tracer velocity, Δz_t is the displacement of the peak concentration, and Δt is the time between observations. The recharge rate is calculated by multiplying the velocity of flow in the unsaturated zone by the moisture content to account for the fact that not all the pores are saturated and contributing to flow (Eqn. 7).

$$R = v\theta$$ (Scanlon, 2010) (7)

Where R is the recharge rate observed using the peak displacement tracer method, v is the tracer velocity, and θ is the water content.

Theoretically, anything that can be transported by water could be used as a tracer. In practice, there are often complicating factors associated with the use of tracers, such as absorption, reactions, preferential flow, natural occurrence, and measurement error (Scanlon, 2010). Tracers can be classified in 3 categories: applied, natural, and historical. Applied tracers are selected and dispersed on the ground surface. Common tracers selected include Cl, Br, and dyes (Scanlon et al. 2002). These tracer types are generally suitable with either the profile method or the peak displacement method. Natural tracers are those which occur naturally with sufficient contrast to be observed as a tracer in the groundwater flow system. Natural tracers include isotopic tracers (^{36}Cl, ^{3}H, ^{18}O, ^{2}H) and heat (Scanlon, 2010). Isotopic tracers are the result of processes which create isotopic fractionation. Of particular interest is the fractionation of ^{18}O and ^{2}H by evaporation and precipitation. On a site scale each precipitation event will have a distinct isotopic signature. When this water infiltrates it can be used as a tracer in the groundwater system. Scanlon notes that though ^{18}O and ^{2}H measurements can yield valuable qualitative information, there has been little success using them to quantify recharge (2010). This is thought to be due to low contrast in ^{18}O and ^{2}H values and diffusion in the vadose zone. Another natural tracer is heat. Because of the interaction of heat with the matrix, analysis of temperature as a tracer is more complex. To analyze temperature fluxes associated with infiltration and groundwater flow, programs such as VS2HD are commonly applied (Scanlon, 2010). Finally, historical tracers are those introduced by events with a known composition at a known time on a very large scale. These tracers are usually introduced through the atmosphere and are therefore widespread. Historical tracers include ^{129}I, ^{36}Cl, ^{3}H, and potentially chlorofluorocarbons (Scanlon, 2010).

Tracers are a valuable tool, which can help to inform recharge estimates. They provide direct physical evidence of the recharge process and can provide context to other techniques used to quantify recharge. Tracers have the drawback of significant costs associated with sampling and analyzing water samples and the possibility of dilution making tracer based recharge rate estimates unreliable (Scanlon, 2010).

2.4.3. Recharge Quantification Using a Numerical Model

Recharge is governed by complex partial differential equations with high variable parameters in space and time. This often requires a spatially explicit numerical model to represent the physical processes surrounding recharge. A wide variety of numerical models exist to quantify recharge, ranging in scale, level of detail, and model premise (Healy, 2010). Healy classified models into 4 categories: watershed scale models, unsaturated zone water balance models, groundwater flow models, and Richards' equation based models (2010). Watershed scale models and unsaturated zone water balance models depend on large averaging areas or empiricism to approximate the behavior of large natural systems (as discussed in Section 2.2.) (Scanlon et al. 2002). These methods are inappropriate for the scale of this study. Groundwater flow models can be used to estimate recharge by creating a recharge distribution to match observed water levels. This is called a "model-generated estimate of recharge" estimate (Healy, 2010). Scanlon et al. point out that this method requires detailed information to constrain recharge or hydraulic conductivity to resolve an equivalence problem in the model results (as discussed in Section 2.2) (2002). This method can yield physically unrealistic recharge rates, because it is not constrained by available water at the ground surface (Scanlon et al. 2002). Richards' equation (discussed in Section 2.1.) is the basis of the most physically based models (Healy, 2010). This allows models to explicitly represent and quantify recharge processes (Healy, 2010). In particular, models based on Richards' equation are valuable in situations with multiple simultaneous processes affecting recharge (Scanlon et al. 2002). The drawback to using physical models is the need to parameterize them with detailed site specific data including: soil water tension, moisture content, van Genuchten parameters, porosity, hydraulic conductivity, specific storage, root uptake, and meteorology data (Healy, 2010). In a field study, Delin et al. demonstrated the need for extensive data to model unsaturated zone flow, including performing detailed lab experiments to determine the van Genuchten parameters of the soils (2000). In order to make predictions about recharge, numerical models must be calibrated to observed data to validate the model results (Healy, 2010). Similarly, studies in Woodstock, collected detailed field observations and used numerical models to quantify recharge (Brook, 2012, and Pasha,

2017). This is accomplished by calibrating the model to observed head, moisture content profiles, and temperature profiles during hydrologic events. This is a useful method for quantifying recharge on a site scale using detailed datasets.

2.5. Contribution to Literature

In the context of the literature reviewed in this chapter, this study will contribute a unique detailed field scale study of DFR in a permeable agricultural setting, the risk of transient DFR features to water supplies, and provide an example of seasonal affects on DFR dynamics. Few studies have observed DFR in an agricultural setting and with a sandy surficial soil. Examples of detailed studies of seasonally affected DFR in agricultural settings include Delin et al. (2000), Bekeris (2007), Brook (2012), and Pasha (2017). This study provides a unique study due to its detailed observation of seasonal dynamics, proximity to a water supply well, and multiple recharge sources. Firstly, the detailed observation of the effects of seasonality showed the dynamics of DFR in the presence of a frost zone. Secondly, this study provides an example of focused recharge of water containing microbial indicator species from a transient surface water feature adjacent to a water supply well. The observations of this site scale study are useful to demonstrate the potential vulnerability of supply wells to transient surface water features. Finally, this study presents an atypical challenge because of the complexity of multiple simultaneous recharge sources in close proximity to one another. On the current field site, depression focused recharge and infiltration related to the adjacent Alder Creek, contribute to recharge and highlights the analytical methods needed to attribute recharge to a specific source. Generally, both recharge processes occur in response to a single meteorological event (rain or snow melt), so the recharge processes are often simultaneous. Using complimentary datasets, the sources of groundwater recharge can be assessed. The research conducted on this topic will advance understanding of recharge in the available scientific literature and provide an example to support the conceptual model for further studies.

3. Study Background

As is the case with most studies in natural sciences, this study is influenced by many of the specifics of the location. Important context for this study includes: location, position in the aquifer system, site history, climate, topography, surface water flow patterns, lithology, hydrogeologic characterization, aqueous geochemistry, and previous research. These background areas will serve to inform and give context to the results of this study.

3.1. Location

The location of this study is in Mannheim, Ontario, shown in Figure 3.1. This small community is located west of Kitchener. The area around Mannheim is dominated by an agricultural landscape.

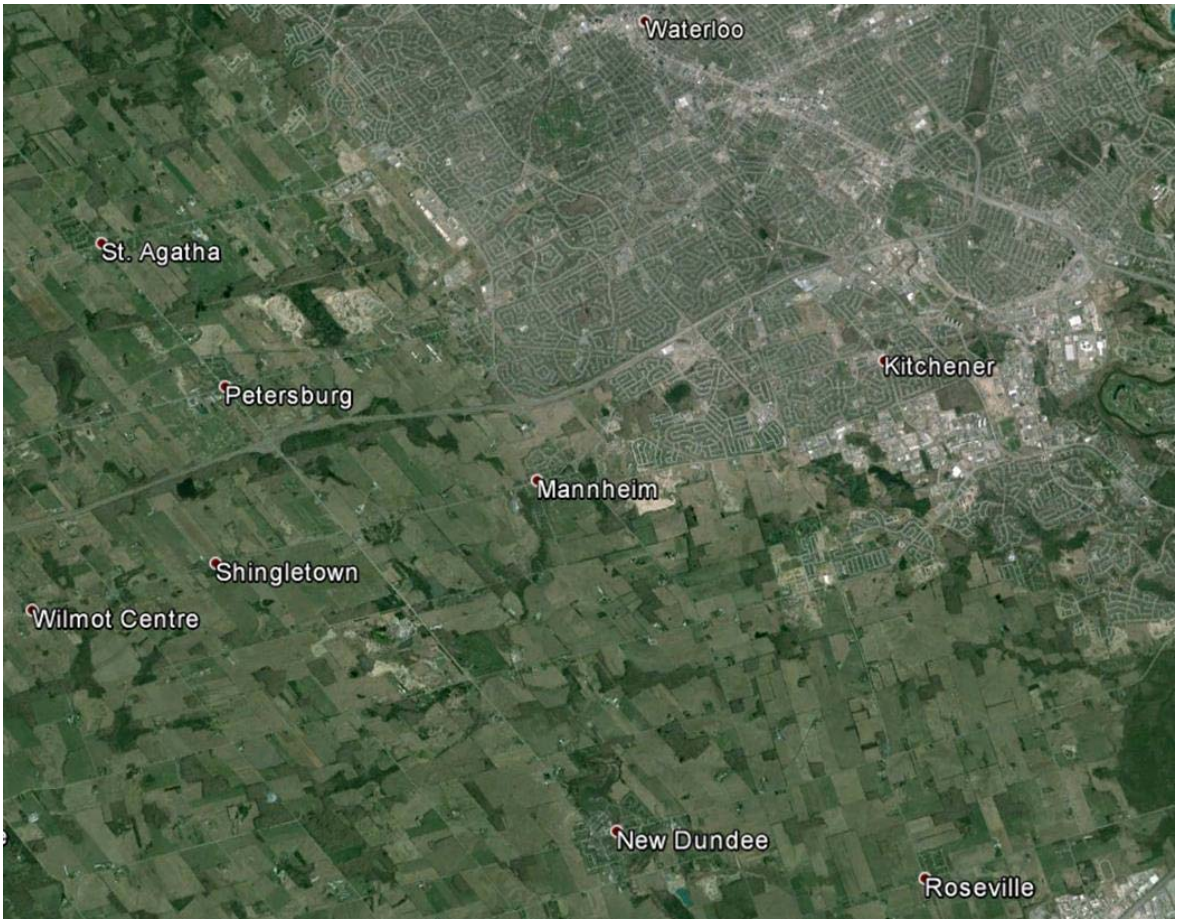

Figure 3.1. Location plan (September 27, 2013) (Image © 2016 DigitalGlobe).

In the town of Mannheim one of the largest businesses is Colour Paradise Greenhouses, located south of Bleams Road and West of Alder Creek. The research site is located on the low lying agricultural field managed by Colour Paradise Greenhouses on the west side of Alder Creek (Figure 3.2.).

Figure 3.2. Site plan of Colour Paradise Research Site (September 27, 2013) (Background Image © 2016 DigitalGlobe).

Significant features on the site include Alder Creek, the Colour Paradise Greenhouses facility, a large parking lot, a storm water pond, agricultural land adjacent to Alder Creek, Bleams road, the Bleams Road drainage ditch, and a public supply well. Alder Creek flows from north to south in its cobbly bed. The greenhouses cover an area of 929 m^2. The greenhouse was

constructed in 2004 and currently portions of it are used for plant growing and retail space. To accommodate customers a large parking lot was built on the west side of the greenhouses with storm water drains. The property owned by Colour Paradise Greenhouses also includes a few acres of agricultural fields between the greenhouses and Alder Creek. Bleams Road and its drainage structure run along the north end of the site. This fairly busy road contributes runoff and road salt to the site (which is further discussed in Section 3.5). A significant feature on the site is the Regional Municipality of Waterloo's (RMOW) public supply well. The well is located south of Bleams Road and East of Alder creek. This well is currently not used for water supply needs for geochemical and vulnerability reasons but could be returned to use in the future. The features on the site make it a unique location to investigate transient groundwater recharge phenomena and, in particular, the presence of a public supply well close to a transient closed depression highlights the potential vulnerability of water supplies to transient surface water features.

In 2013 a 60-day pumping test was conducted on a test well drilled adjacent to the public supply well in the shallow sand aquifer to analyze aquifer properties and assess the vulnerability of the test well (Hillier, 2015). The results of the test showed that shallow groundwater on both sides of Alder Creek responded rapidly to pumping and to within hours to precipitation. The supply well was found to be vulnerable to surface contaminants at the ground surface (Hillier, 2015).

3.2. Waterloo Moraine Aquifer System

Unlike many Canadian cities, the cities of Waterloo and Kitchener have limited access to surface water. To meet the water supply needs of residents and industries the RMOW makes extensive use of groundwater resources in the Waterloo Moraine aquifer system. The Waterloo Moraine is a significant aquifer system to the Region of Waterloo and as a result has been studied extensively by government agencies, academia, and private companies (Bajc, et al., 2014). Bajc, et al. synthesized all of the various types of work done to characterize the Waterloo

Moraine aquifer system in 2014. This paper was used as background to inform this research and to give context to the significance of the location of the Colour Paradise Research Site.

The area in which the Colour Paradise Research Site is located is lies in an area with sandy soils exposed at the surface. Mapping in Figure 3.3 shows that there is direct exposure of the aquifer at the ground surface. Recharge in such an area would contribute directly to aquifer resupply and therefore recharge features in this area are significant.

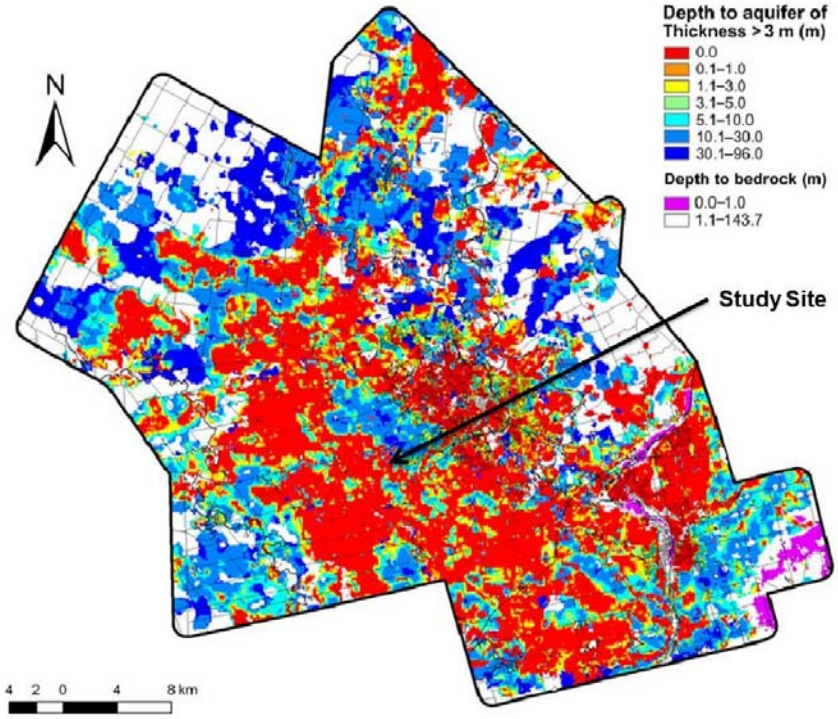

Figure 3.3. Study location relative and aquifer exposure map (Bajc, et al., 2014).

The aquifer exposed in this area is connected to a regionally significant aquifer often used for public water supply. Bajc et al. conceptualized the aquifer system in the region as depicted in Figure 3.4. (2014).

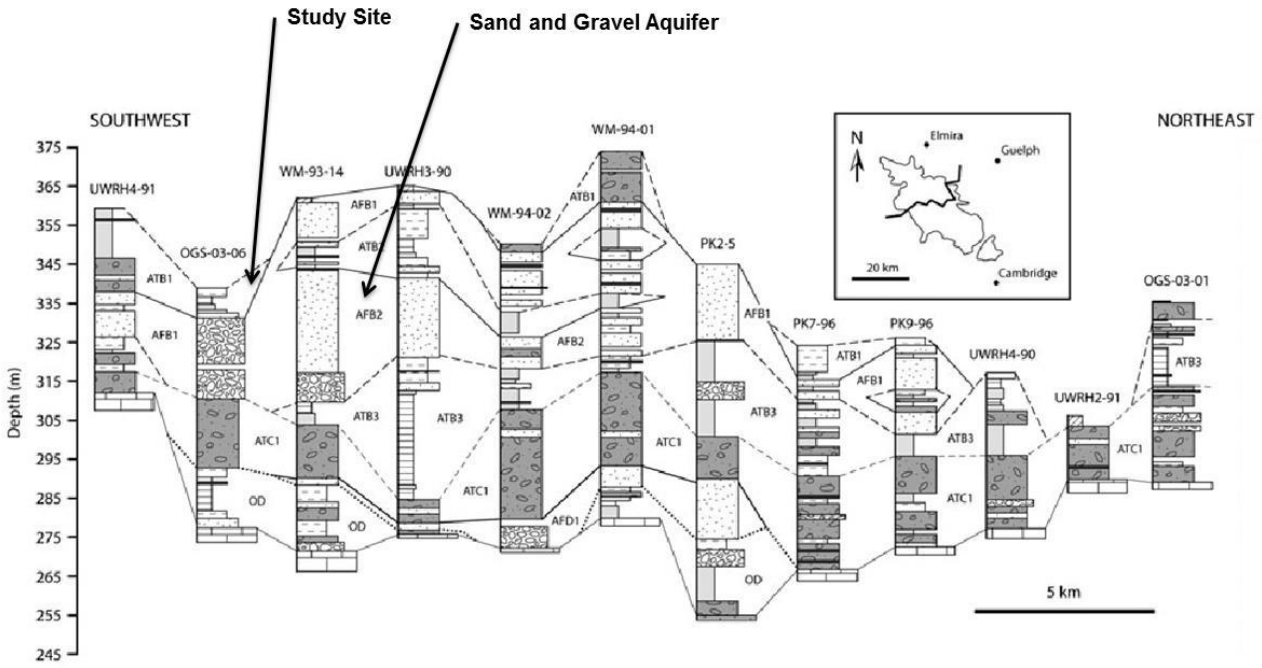

Figure 3.4. Study location in the Waterloo Moraine aquifer system cross section view (annotated from Bajc, et al., 2014).

The sand and gravel aquifer referred to as AFB2 is used for part of the RMOW's drinking water supply. Much of its recharge is from areas of aquifer exposure at surface, including this research site. The significance of the location in the Waterloo Moraine aquifer system makes this an ideal site to demonstrate the significance of recharge dynamics to groundwater supplies.

3.3. Site History

The Colour Paradise Research site is located in the town of Mannheim slightly to the west of Kitchener. This site has experienced a history typical of many areas in Southern Ontario and across the world. Originally, the area was settled and developed for agricultural purposes. As population grew in the city of Kitchener and surrounding areas, the site has been increasingly affected by urbanization. Development of this area is documented by a series of eleven air

photos contained in Appendix A, from 1946 to present. In 1946 the area was in use for agricultural activity (Figure A.1). The farm house, Bleams Road, and the bridge over Alder Creek were constructed prior to this point. By 1955, the RMOW had installed a pumping station across Alder Creek to increase available water supplies (Figure A.2). Urbanization surrounding Kitchener continued from 1955 to 1985, with the construction of homes along Bleams Road (Figure A.4). The farm on the site also developed with the construction of a chicken barn and a second farm house. A suburb to the east of the site was constructed between 1990 and 2000 (Figure A.7). The most significant development on the research site occurred in 2004 when the land was bought by Colour Paradise Greenhouses (Figure A.8). The hill slope was significantly regraded and a 929 m^2 greenhouse was constructed. A storm water pond and storm water catchment systems changed the behavior of surface water on the site considerably (see Section 3.5.). Figure A.8 shows the impact of the developments on the surface water. Prior to 2006 little or no evidence is seen of overland flow, but following the development on the site surface water is evident from storm water drainage structures. Because the developments of 2004 had little or no effect on the Bleams Road drainage ditch, it is likely the some overland flow has occurred throughout the recorded history of the site. Improved resolution and frequency of images may contribute to the post 2006 observation of surface water patterns on the site. In 2013 air photos first observed overland flow from the storm water pond flowing into the closed depression (Figure A.10). An air photo in the summer of 2015 shows the irrigated row crop pattern on the field and the equipment used in this study on the east side of the field (Figure A.11).

The site was used as an agricultural field, until 2004 when the land was bought by Colour Paradise Greenhouses. Prior to 2004 exact crops are unknown, but it is believed that typical crops and agricultural practices were applied. What is known is that the land was used regularly by local farmers, tilled, tiled, and harvested. The land tilling process contributed to the mixing of organic matter through the upper 10 to 20 cms. Clay tiles were installed on the field to improve drainage of the soils, but there is now little evidence of their persistence other than occasional clay fragments in the field. It is believed, as is typical of aged clay tiles, they have collapsed over time or been filled with soil material. It is possible that construction and agricultural processes contributed to the crushing of the clay tiles. Now the only evidence of their presence is the shards of tile that can be found occasionally in the field. An attempt was made to explore any exposed pieces of tile with a video snake, but it was found that the tiles had collapsed after

short distances. It is unlikely that the tiles still have any significant impact on drainage. Since 2004, the land has been infrequently used for crop development. Because the operators of Colour Paradise Greenhouses were chiefly concerned with the greenhouses, natural plants were allowed to grow most years for up to 2 months at a time then tilled down into the soil to maintain the appearance of the property. This contributed to an organic rich upper layer of the soil. In the spring of 2016 the operating practise of the fields changed considerably. During this growing season strawberries were planted on irrigated, fertilized, tarped rows. Because this falls outside of the time scope of this study it did not significantly affect the findings of this work.

3.4. Climate

In southern Ontario seasonality has a significant impact on natural hydrologic systems. The annual average temperature is 7 °C. Annual precipitation averages about 900 mm/year, with monthly averages between 60 mm/month in the winter and 90 mm/month in the summer. Summers are warm and humid with average daily temperatures around 18 °C, with annual maximum temperatures reaching 36 °C. During the winter daily average temperatures are -6 °C, with extreme cold temperatures reaching -32 °C (Environment Canada, 2016).

Notable hydrologic events include midwinter melt events, spring freshets, and major rain events. Mid-winter melt events happen occasionally in Southern Ontario. These events occur on thin to non-existent frost zones during the winter. They can lead to partial or complete melting of snow packs and can be accompanied by rain. Spring freshets happen regularly each spring. These events typically begin gradually as temperatures rise above zero and the snow pack ripens and melts onto soils with a mature frost zone. The final types of hydrologically significant events are intense rainfalls.

3.5. Surface Water Flow Patterns

This research site has a complex set of surface water conditions which influence the formation and distribution of surface water and infiltration on this site. The significant surface water features on the site include, Alder Creek, the storm water pond, the storm water pond catchment, Bleams Road's drainage ditch, and the bridge on Bleams Road. These surface water features and their functional connections are shown in Figure 3.5.

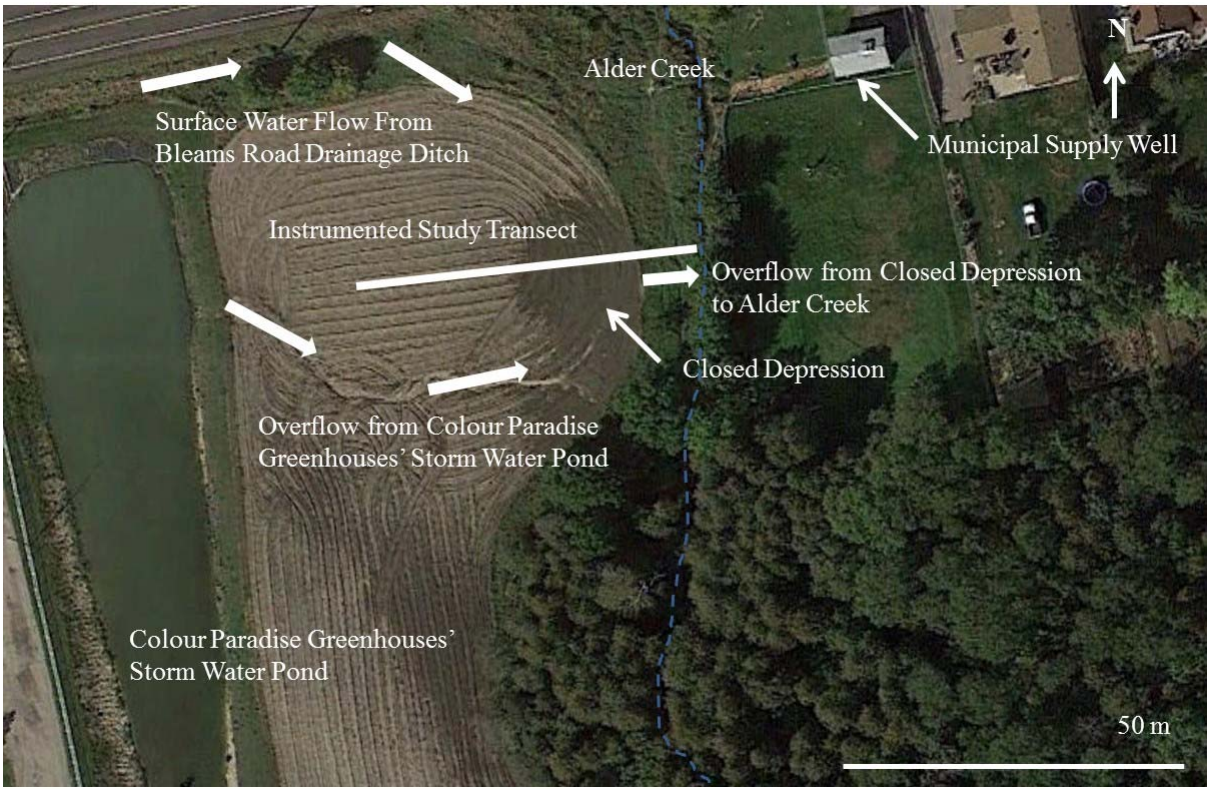

Figure 3.5. Surface water flow map on Colour Paradise Research Site (September 27, 2013) (Background Image © 2016 DigitalGlobe).

Alder Creek is a fairly small creek flowing from North to South. Alder Creek is contained within the Grand River watershed draining into the Nith River approximately 10 kms

from the study site. On this site, Alder Creek is affected by anthropogenic activities. The construction of the bridge on Bleams Road constrained the stream course and affected the stream gradient upstream and downstream of the bridge. This in turn has affected the flow speed of the water and the sediment type in the creek bed. South of the bridge Alder Creek flows fairly quickly in a hard cobbly bed.

The storm water pond was created in compliance with storm water regulations in Ontario at the time of the greenhouse's construction in 2004. The storm water pond receives water caught on the roof of the 100,000 ft^2 greenhouse and from the storm water drains in the parking lot. Steep relief in the hummocky terrain causes storm water to move quickly through the system. Water enters the pond through a stilling well at the south end of the pond. The pond is lined with a geotextile and a clay layer to limit infiltration. Throughout most of the year the inflows are balanced by gradual evaporation and infiltration. During large hydrologic events the pond's storage capacity is unable to accommodate the water and it overflows a gravel weir near the north end of the pond. The overflow from the pond flows across the field, following the natural lows of the terrain.

The other major surface water feature on the site is the drainage of Bleams Road. As is typical of rural roads Bleams Road has unlined ditches on each side of the road. These catch runoff from the impervious road surface during rain events and store snow removed from the road surface during snow events. Snow stored on the road embankment and ditch contains road salt. During a spring melt event the water and salt stored in the ditch are released. The gradient of Bleams Road sloping eastward to Alder Creek is approximately 4% so run-off in the drainage ditch flows quickly down to Alder Creek. The embankment on the west side of the bridge on Bleams Road obstructs flow in the drainage ditch and no attempt was made to redirect the flow. The result is that run-off in the drainage ditch flows east down the hill beside Bleams road until it reaches the bridge embankment, then it flows south onto the agricultural field. Once on the field, surface water flows across an irregular tilled surface to a low enclosed area on the east side of the field.

A low area of the agricultural field has been enclosed by decades of tilling processes, which have caused a slight berm (about 20 cm) around the edge of the field. Surface water from the Bleams Road drainage ditch and overflow of the Colour Paradise Greenhouses storm water

pond both drain into this low area on the field. The closed depression stores water until the minimum height of the berm is reached. The surface water then flows over the irregular grassy surface for 9 m to Alder Creek. For purposes of this study this area is referred to as the closed depression. The surface water sources on the site contribute to water from a catchment considerably larger than the surrounding field being transported to the closed depression quickly during significant hydrologic events. Compared to the volume of water supplied during hydrologic events, the storage of this depression is small, so it fills rapidly. Once filled the inflows are equal to evaporation, infiltration, and outflows discharging to Alder Creek. This surface water system functions similarly to a constant head tank applied to the top of the soils in the closed depression.

This surface water system is complex and affected by anthropogenic activities. This kind of complexity is typical of the Alder Creek subwatershed where large parts of the subwatershed are urbanized and parts that are un-urbanized are dominantly used in intense agricultural activities. This study site is an illustrative example of the affects of anthropogenic activity on surface water processes and their subsequent affect on infiltration and groundwater recharge.

4. Methodology

This section describes the methods used to characterize the field site, on site (Section 4.1.1.) and in the lab (Section 4.2.), as well as methods used to observe hydrologic events (Section 4.1.2. to Section 4.1.12.).

4.1. Field Methods

For purposes of this study, the collection of comprehensive field measurements will provide the basis for the quantification of recharge and the observation of the mechanisms by which it occurs. This section details the methods applied during this study to characterize the site and observe the recharge events. Site characterization included retrieving soil cores and in situ hydraulic conductivity testing. To observe hydrologic events and subsequent DFR, the site was then instrumented with monitoring equipment to measure hydraulic head, soil water content, subsurface temperature and meteorological parameters.

In order to observe the vertical flow of water infiltrating and contributing to recharge, the equipment was generally deployed in vertically dense clusters and evenly spaced between the surface and the average annual water table depth. Equipment clusters were installed in 3 locations for purposes of this study: the background area (intended to represent an area unaffected by preferential recharge), in the DFR area, and adjacent to Alder Creek, as shown in Figure 4.1., Figure 4.2. Table 4.1. provides a summary of instruments installed at the Site.

Figure 4.1. Colour Paradise Research Site instrument cluster photo.

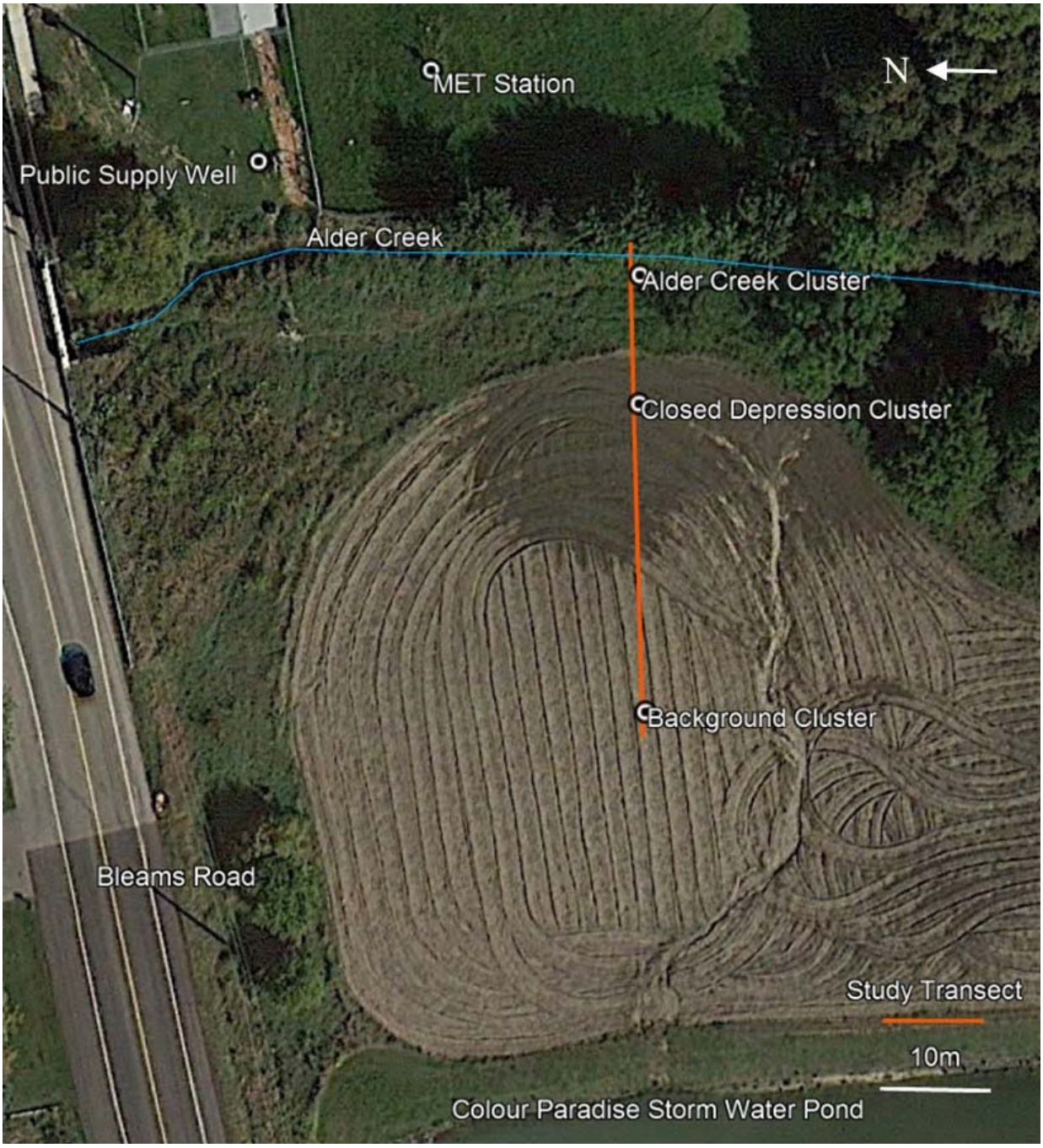

Figure 4.2. Colour Paradise Research Site plan (Refer to Table 4.1.) (Background Image © 2016 DigitalGlobe).

Table 4.1. Summary of instrumentation at the Site

Instrument Cluster	Instrument Type	Instrument Name	Bottom Depth (mbgs)	Measurement Interval (m)
Adjacent to Alder Creek	Surface Water Pressure Transducer	Alder Creek Head		
	Piezometer	CPP1	4.18	0.3
		CPP7	2.6	0.3
		DP3	1.7	0.1
		DP4	2.089	0.1
		DP5	3.058	0.1
	TDR Probe	TDR A	0.3	0.3
		TDR B	0.61	0.3
	Neutron Access Tube	CPAT1	2.67	2.67
Closed Depression	Surface Water Pressure Transducer	Closed Depression Head		
	Piezometer	CPP2	4.13	0.3
		CPP3	2.6	0.3
		CPP4	2.1	0.3
		CPP5	1.6	0.3
		CPP8	2.6	0.3
		CPB1	2.1	0.05
	TDR Probe	TDR C	0.3	0.3
		TDR D	0.61	0.3
		TDR E	1.5	0.3
		TDR F	0.3	0.3
		TDR G	0.6	0.3
		TDR H	0.91	0.3
	Neutron Access Tube	CPAT2	2.71	2.71
	Surface Water Temperature Logger	ST1 to ST13		
	String of Thermisters	Temp1	2.8	2.7
Background Location	Piezometer	CPP6	4.13	0.3
		CPP9	2.6	0.3
		CPP10	2.1	0.3
		CPP11	1.6	0.3
		CPP12	2.6	0.3
	Neutron Access Tube	CPAT3	2.71	2.71
	String of Thermisters	Temp2	2.8	2.7
Bleams Road Drainage Ditch	Surface Water Pressure Transducer	Bleams Road Head		
CP Storm Water Pond	Surface Water Pressure Transducer	GH Pond Head		

4.1.1. Soil Characterization Methods

The soil characteristics are an important consideration for the estimation of recharge quantity and the observation of recharge processes. Soils on this site were characterized by the collection of 51 mm intact continuous soil cores along the study transect using a Geoprobe 7822 DT drill rig, at the locations shown on Figure 4.3. in order to develop a lithostratigraphic model of the shallow soils at the site. Boreholes were drilled on November 7, 2014, and on October 2, 2015. A test pit was excavated in June, 2015, to a depth of 1.8 m below ground surface to observe the undisturbed soil textures (Figure 4.3.). Additionally, surficial soils were mapped using a 6 mm soil probe to observe the top 305 mm of the soil profile. The same soil probe was used during the Spring Melt Event to observe shallow soil structure (the results are discussed in Section 5.2.6.).

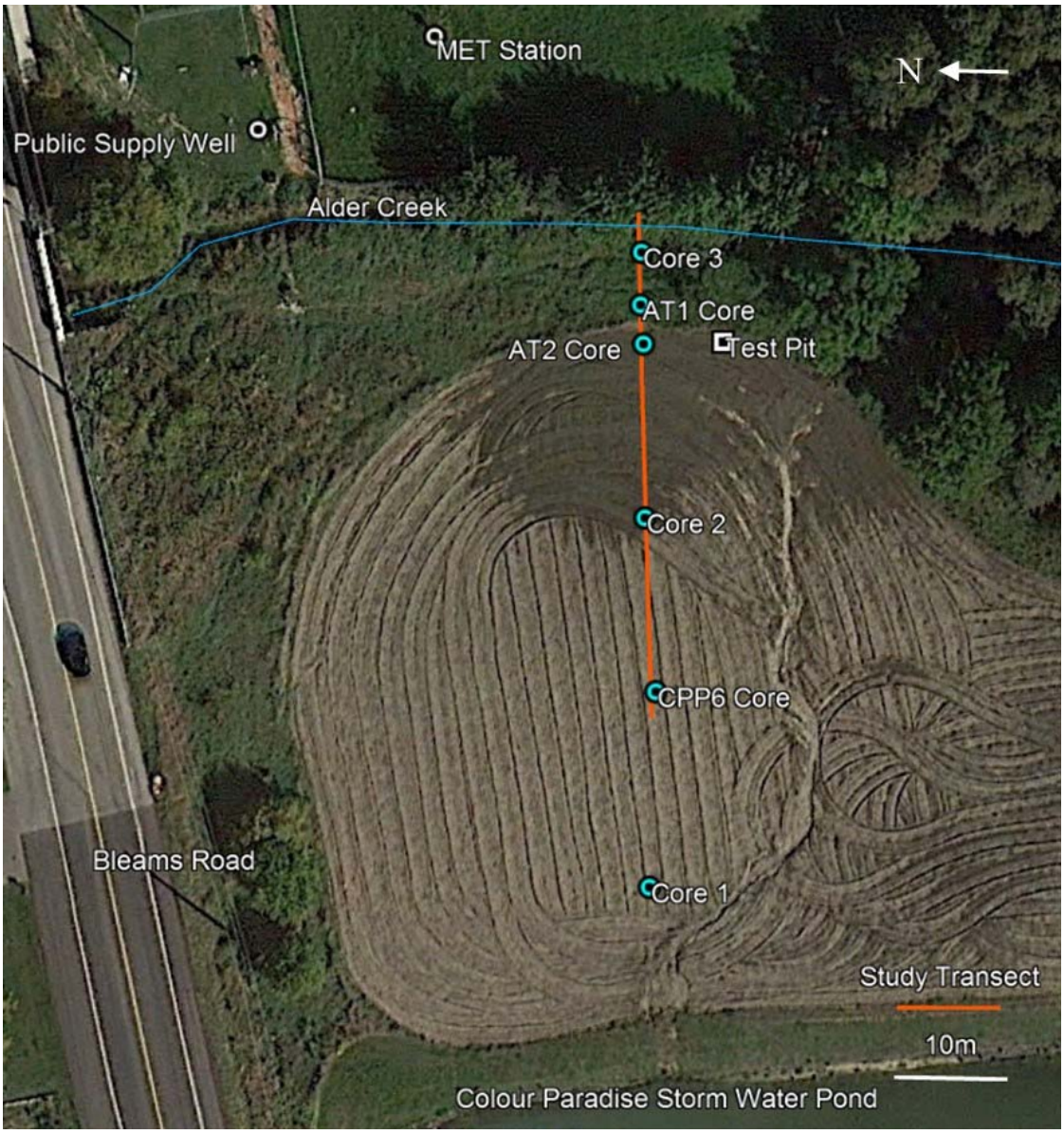

Figure 4.3. Borehole and test pit locations used to characterize the Site (Background Image © 2018 DigitalGlobe).

4.1.1.1. Piezometer Installation Methods

Piezometers were installed to observe groundwater head, electrical conductivity, temperature, and provide access for groundwater sampling. Typically, direct push methods were

used to create an open hole to the desired depth. Piezometers were installed in open holes. Typical piezometers were constructed using 51 mm schedule 40 PVC well pipe and a 0.91 m screen backfilled with No. 3 filter sand to the top of the screen, where native materials did not collapse around the screen. A 0.61 m layer of bentonite pellets were placed on top of the sand pack to provide a seal along the well annulus to vertical flow. Native materials were used to fill the rest of the annulus by filling and tamped at 0.15 m lifts to compact the soil to near native conditions. Following the completion of the monitoring wells, they were developed by removing a minimum of five well volumes, until purge water became clear, up to a maximum of 15 well volumes.

Typically, piezometers were designed to provide observations immediately below and across the water table, to provide the best possible observation of recharge. Some piezometers were designed as part of a vertical array, including piezometers screened at elevations typically in the vadose zone. Piezometer details are summarized in Table 4.1.

To supplement the vertical array of piezometers in the closed depression, a single piezometer bundle was installed across the upper 2.1 m of the subsurface. The bundle was constructed with six small diameter tubes, cut to different lengths with short screens (~2 cm) to observe the vertical groundwater head distribution. The bundle was installed in an open hole and backfilled with native material as described above.

4.1.2. Water Level and Hydraulic Head Observation Methods

Following the installation and development of piezometers they were instrumented with data loggers to monitor pressure, temperature, and in some piezometers, electrical conductivity. Where unvented transducers were used, they were corrected to barometric pressure as observed at weather station placed onsite. Occasional manual water level measurements were taken to confirm the pressures observed data loggers readings. In multilevel piezometers where the internal diameter of the casing did not allow for the insertion of a data logger, manual measurements were taken at a higher frequency to monitor groundwater head.

4.1.3. Surface Water Monitoring Methods

The research program included the observation of surface water in the closed depression, from the drainage ditch along Bleams Road, the overflow from the greenhouse pond, and Alder Creek. One of the objectives of the monitoring network was to observe which of the surface water sources were contributing to the water in the closed depression. The closed depression is instrumented to observe head, temperature, and conductivity. The parameters observed in Alder Creek included stage, temperature, and conductivity. Alder Creek was monitored using a transducer installed in a protective housing on the creek bed. The transducer remained under the ice during the winter. The water level and temperature of the Colour Paradise Greenhouse storm water pond was monitored continuously during the study period. The drainage ditch along Bleams Road was instrumented to observe pressure, temperature, and conductivity.

4.1.4. Neutron Probe Soil Moisture Methods

Neutron probe access tubes were installed in vertically dense instrument clusters in the closed depression, adjacent to Alder Creek, and at background location, to make vertically discrete profiles of soil moisture content. Neutron probe access tubes were installed by taking a soil core and installing water tight schedule 40, 2" PVC tube into the hole. Soil moisture measurements were made at 20 cm intervals starting 10 cm below ground surface. The access tubes were designed to extend 50 to 100 cm below the minimum water table surface during a typical seasonal cycle.

4.1.5. Time Domain Reflectometry Methods

Time domain reflectometry devices (TDR) were installed to make frequent measurements of water content and conductivity in the unsaturated zone at specific depths. The wave guides of each TDR probe are 30 cm long, over which it measures soil moisture content. For purposes of study, the moisture content values were assumed to be measured at the center point of the TDR wave guides. TDR probes were installed by hand auguring to the design depth, then installing the probe vertically into the undisturbed native soil. After installation, the hole was backfilled with native materials and tamped to a typical soil density. They were installed as part of vertically dense instrument clusters spanning the top 0.6 m to 1.5 m of the subsurface.

4.1.6. Temperature Observation Methods

In addition to groundwater temperature monitoring methods discussed in Section 4.1.2. and surface water temperature monitoring methods described in Section 4.1.3., temperature was observed in the air and soil during the hydrologic events included in the study. Air temperature was observed at the meteorology station on site as well as monitored using temperature loggers above the ground surface in the closed depression and at the background array. Soil temperature was observed at the background location and in the closed depression, using soil temperature arrays. Each array was constructed using solid stem PVC rods, instrumented with temperature loggers placed at 10 cm intervals above the ground surface to 60 cm below the ground surface, then at 20 cm intervals thereafter. Soil temperature arrays were installed in open holes of the same size. The rods allowed for direct observation of vertical temperature profiles throughout the study period.

4.1.7. Water Sampling Methods

Groundwater and surface water were sampled during the study period. Samples were taken from piezometers by purging three well volumes using a peristaltic pump or Watera tubing, then collecting a sample. Surface water samples were collected by filling bottles directly from marked locations. Water samples were analyzed for ionic solutes and stable isotopes to use as tracers of recharge. Water quality and isotopes were analyzed by the water quality laboratory at the University of Waterloo. Specifically, the analytes include: sodium, ammonia, potassium, magnesium, calcium, chloride, nitrate, nitrite, sulphate, phosphate, $\delta^{18}O$, and $\delta^{2}H$. Although these data were not specifically used in the course of the overall scope of the research work, due to the limited nature of the spatial and temporal coverage of the data sets, the collection activity and data are mentioned and included in Appendix G for the sake of completeness. These data may be of use in subsequent studies.

Additional surface water samples were collected from the closed depression on April 2, 2015, the storm water pond and Alder Creek, during the Spring Melt Event, were analyzed for microbial indicator species by Maxxam Analytics Ltd.

4.1.8. Guelph Permeameter Methods

The Guelph Permeameter was applied on the site using the typical constant head configuration and analyzed using the analytical equations described by Reynolds and Elrick (1986). The Guelph Permeameter is an instrument used to determine intact field saturated hydraulic conductivity for near surface unsaturated soils. It is based on the application of a multiple known heads to a borehole unsaturated soil. Water is then allowed to flow out of the reservoir at a variable rate to maintain a constant head in the test hole. Flow continues into the soil until a steady state is reached. At that point, the soil is said to be “field saturated”, and the hydraulic conductivity can be estimated based on the flow rates and known heads induced in the

surficial soil, as described by Reynolds and Elrick (1986). One of the limitations of this method is that the Guelph Permeameter is limited to the ground surface and shallow depths where soils can be exposed using a soil auger. As a result, field saturated hydraulic conductivity data was only collected for the surficial layer. Testing was applied at three locations in and near the closed depression, as shown in Figure 4.4. (Missori, 2015).

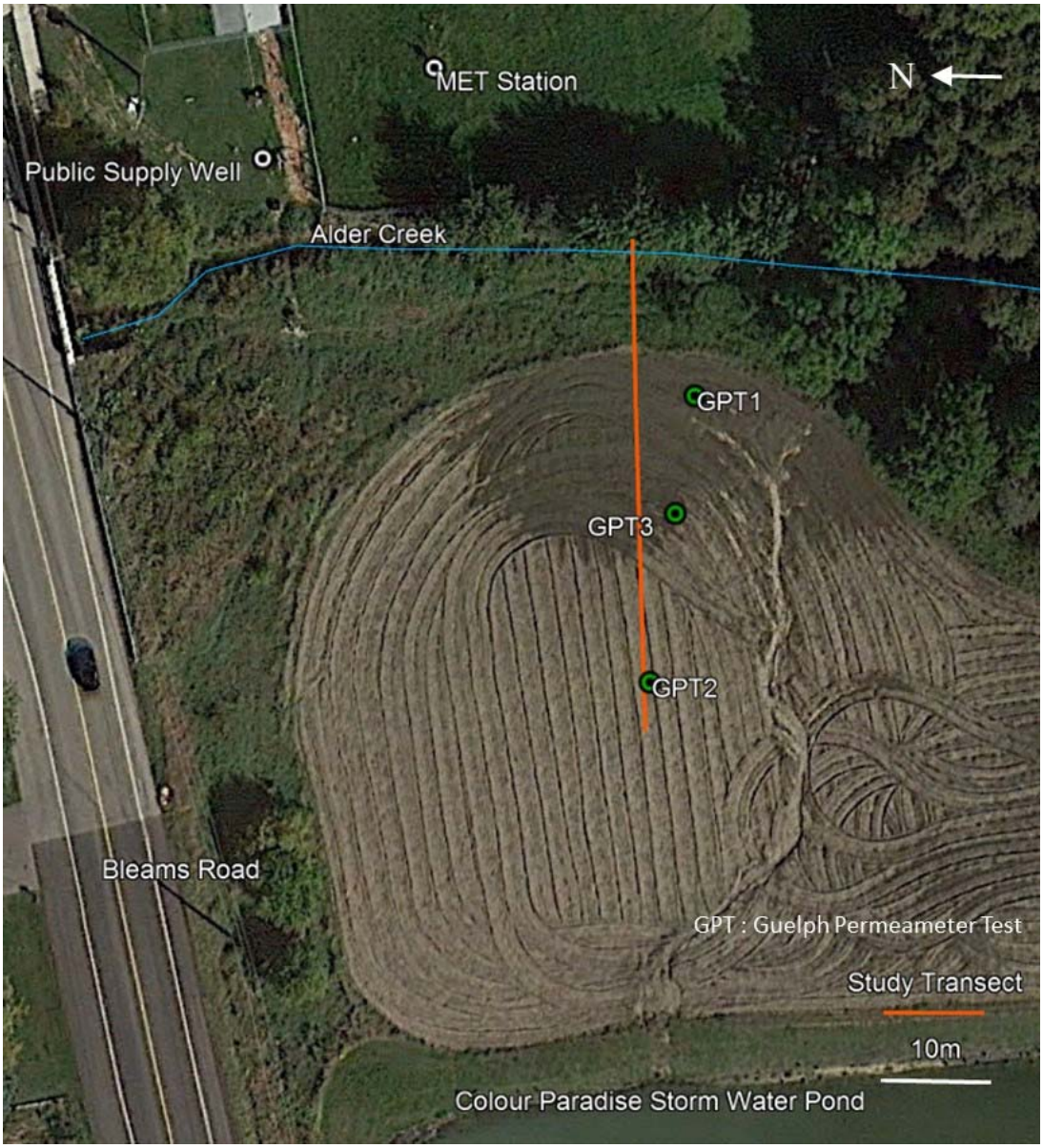

Figure 4.4. Guelph Permeameter testing locations at the Site.

4.1.9. Specific Yield and Porosity Measurement

In the calculation of recharge into a shallow aquifer the storage properties of the soil are crucial for estimating the total recharge amount. Frequently, literature values or lab experiments are used to estimate porosity and specific yield in vadose zone flow studies. This field site offers the opportunity to collect general estimate in situ of specific yield by using complementary data obtained using the neutron probe, which measured the water content across the depth of the typical vadose zone. Opportunistic measurements of the soil's moisture content were collected at field saturation, during hydrologic events, and at a field dry condition using the neutron probe, during dry portions of the year. Field saturated measurements were collected during the November Event, the groundwater head below the closed depression rose to nearly the level of the ground surface and the soils reached field saturation (as discussed further in Section 5.1.3.2.). The porosity was estimated using the maximum observed moisture content at each observation depth throughout the soil profile. Similarly, the specific yield was estimated using the difference between the field saturated moisture content and the field dry moisture content.

4.1.10. Rising and Falling Head Test Methods

Rising and falling head tests (commonly known as slug tests) were conducted to measure in situ hydraulic conductivity around the well screen. The technique involves the sudden displacement (positive or negative) of the static water level in the well and the monitoring of the recovery of equilibrium water level. A more permeable material will return to equilibrium more quickly than a less permeable material. In order to monitor the recovery of the head in the wells, a pressure transducer was deployed above the well screen to monitor head at five second intervals. A number of techniques were used to cause sudden displacements to the water level in the well. Both positive and negative head displacement techniques were used when possible. For wells with standing column of water one meter or more above the well screen a slug of known volume was introduced to increase the head in the well. After full recovery was

observed, the slug was removed to induce a negative head displacement recovery test. Some wells included in the testing program, had short water columns so a solid slug was an unsuitable technique. These wells were tested by suddenly introducing a known volume of water to increase the head in the well and monitoring recovery. One of the limitations of typical slug test analysis methods is that it can only be applied to saturated well screens. This is due to the fact that the method assumes that the change in the storage around the well screen to be zero. Some of the piezometers installed for this experiment are intentionally placed near the water table and at heights above the water table. These wells could not be tested under typical water table conditions using this method.

To characterize the soils a series of 25 slug tests were performed on five wells, which meet the assumptions of the slug testing method (Missori, 2015). Analysis of the slug tests included the application of the Hvorslev Method (Hvorslev, 1951) and the Bouwer and Rice Method (Bouwer and Rice, 1976). As the assumptions of both methods are similar, both methods are equally applicable to the slug tests conducted on wells at the Site, so each analytical method was applied to each test.

4.1.11. Photographic Monitoring Methods

During hydrologic events selected for the inclusion in the study, photos were taken near daily from 13 of perspectives to capture the melting of snow, presence of surface water, surface water flow patterns, extents of surface water in the closed depression, and the extents of Alder Creek. To capture consistent photos, photos were taken from consistent locations, at consistent zoom factors, and framed using visual landmarks.

4.1.12. Meteorological Observation Methods

An SOWC meteorology station (referred to as the MET Station) is deployed onsite, east of Alder Creek and south of the public supply well (as shown in Figure 4.2.). It measures precipitation using a rain gauge, temperature, solar radiation, relative humidity, wind direction, wind speed, and snow depth. Snow depth was measured using an ultrasonic range sensor mounted on an arm above the ground where snow would accumulate typically. To confirm accuracy, meteorological observations were compared to nearby meteorology stations.

In order to associate the snow depth with a snow water equivalent (SWE), snow depth was estimated to linearly relate to the average SWE of snow samples collected at nine locations prior to the start of a melt event. The nine SWE sample locations were located throughout the agricultural field within the catchment of the closed depression. SWE was calculated by collecting a snow sample of known volume and weighing it before and after evaporating off all the water in the sample.

4.1.13. Surveying Methods

In order to characterize the site topography and the locations of equipment, surveys were completed. A detailed elevation survey was completed of the study transect geometry and the creek thalweg along the defined study transect using an automatic transit level. Elevations were determined by back sighting known elevations. Additionally, a GPS survey device was used to survey latitude, longitude, and elevation of all the instrumentation on site. The GPS device was also used to collect a detailed survey of the topography of the closed depression, as shown in Section 5.1.1. The topographic data was linearly interpolated to produce an estimated ground surface elevation map.

4.2. Lab Methods

To better characterize the site, lab methods were used to compliment field methods. Lab methods generally provide the benefit of a controlled environment to control variables and make detailed observations. However, most lab methods have the disadvantage of using disturbed samples. Lab methods detailed in this section include grain size analysis and hydraulic permeameter testing. Buchner funnel tests were also performed as described in Appendix E. Soil samples were retrieved during coring (as described in Section 4.1.1) and selected to represent each lithostratigraphic unit. The samples were selected to be representative of the hydrostratigraphic units and their relative size, heterogeneity, and suitability for this type of analysis. More samples were taken from larger units to better characterize units which comprise a great portion of the system. Units with greater observed heterogeneity were sampled more densely to capture a more representative sample of the unit and its variability.

4.2.1. Grain Size Analysis Methods

A grain size analysis is a lab bench experiment where a dried, disturbed soil sample is separated by grain sizes using a series of sieves. Each sieve is weighed and plots of cumulative weight distribution by grain size are created. Various empirical experiments performed on disturbed soil samples have attempted to use soil particle size distribution to estimate the hydraulic conductivity. Instead of selecting and applying only one empirical formula to estimate the hydraulic conductivity of a grain size sample, HydrogeoSieveXL was used. HydrogeoSieveXL applies 15 empirical formulas, as applicable, as described by Devlin (2015). Each formula provides an empirical estimate of hydraulic conductivity, then HydrogeoSieveXL calculates a geometric mean of the estimated hydraulic conductivity. Fourteen soil samples were selected from the cores retrieved at the site, as described by Missori (2015).

For each sample analyzed the grain distribution is plotted as shown in Figure 4.5. A) and the soil is named by its grain size distribution. Each of the grain size distributions were then analyzed using a range of empirical formulas to estimate hydraulic conductivity (Figure 4.5. B). A representative hydraulic conductivity of the sample is estimated by calculating the geometric mean of the applicable empirical hydraulic conductivity models. A complete record of the hydraulic conductivity calculations in Appendix D (Devlin, 2015).

A) B)

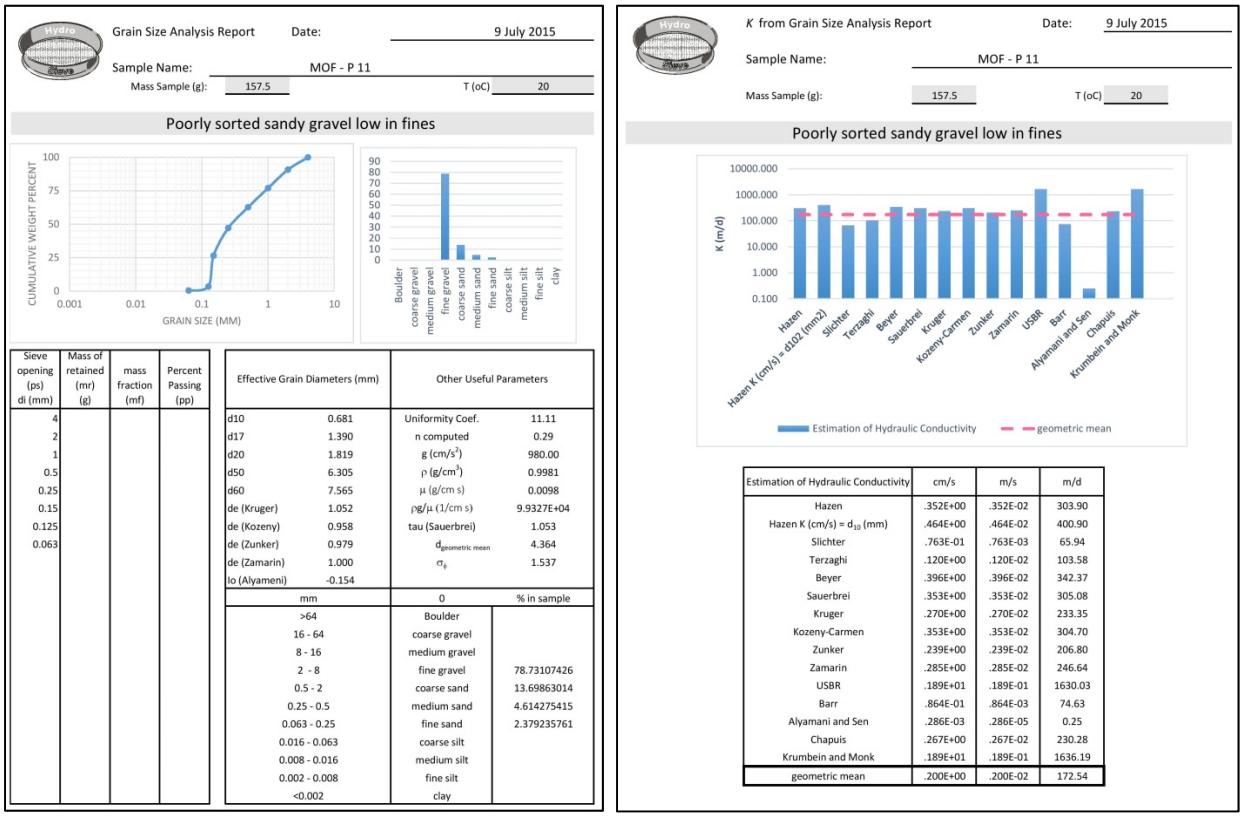

Figure 4.5. Sample grainsize analysis results A) Sieving results B) Hydraulic conductivity estimate based on grainsize analysis (Devlin, 2015) (Missori, 2015).

4.2.2. Hydraulic Permeameter Methods

Permeameter testing is based on the application of a known constant or falling head to a soil in a lab bench experiment. The flow rate or the time at which the applied head has fallen to a known level. The falling head permeameter method was extensively applied to help characterize the Site. The sections of the soil cores retrieved were homogenized, packed, and tested using an in lab permeameter (Missori, 2015). Permeameter tests were performed on fourteen soil samples retrieved from locations shown on Figure 4.3.

5. Results and Discussion

The results of the field program yielded a characterized site and detailed data sets suitable for making observations about the quantity and distribution of groundwater recharge, the physical processes affecting recharge, and the affects of seasonality on recharge dynamics.

In order to observe and document the physical processes which affect recharge, two seasonal events were monitored in detail at the field site. The site instrumentation is detailed in Figure 4.2., and Section 4.1. The first event occurred in November of 2014 (the November Event) and the second in the spring of 2015 (the Spring Melt Event).

5.1. Site Characterization

Prior to the observation of hydrologic events and groundwater recharge, the site was characterized by surveying the site, collecting soil cores, and testing the hydraulic properties of the soils.

5.1.1. Ground Surface Elevation

The ground surface at the site significantly influences how DFR takes place. A microtopographic survey was performed of the closed depression to map its extent and depth on September 27, 2014 (Figure 5.1.). These efforts were complicated by the irregular surface created by tilling of the field.

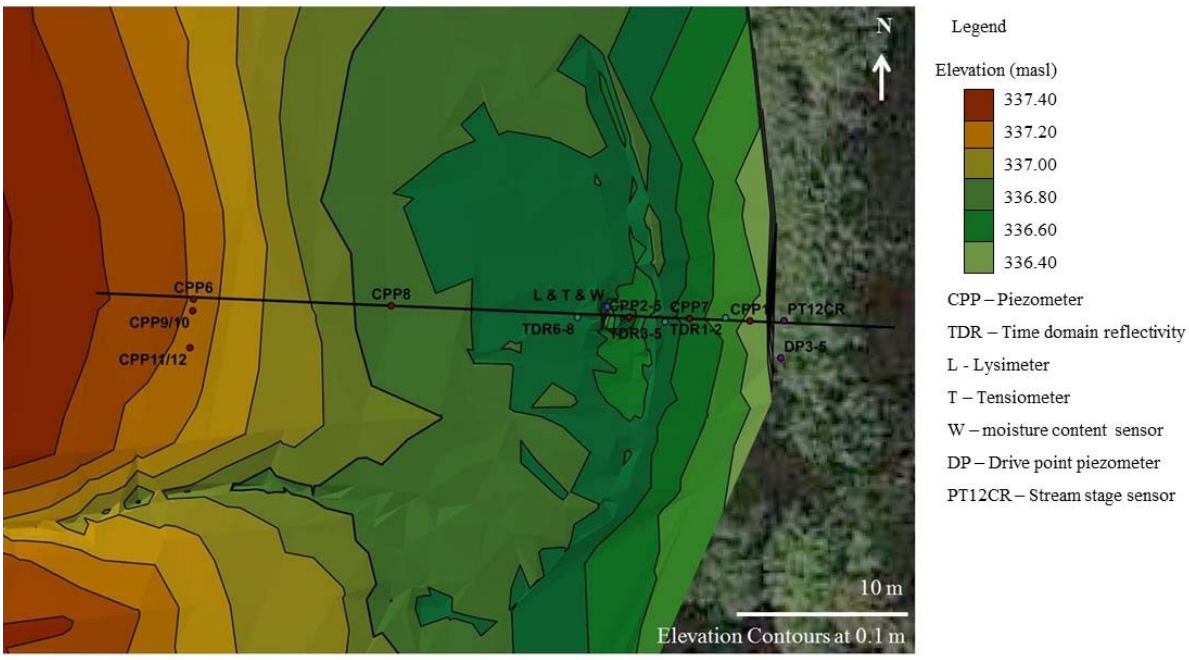

Figure 5.1. Microtopographic survey of the closed depression and equipment locations (Background Image © 2018 DigitalGlobe).

5.1.2. Lithostratigraphy

The collection of undisturbed samples allows for a precise log of the depth of interfaces between soil layers, observation of soil textures, and the collection of samples for lab analysis. Borehole logs are included in Appendix B. Boreholes ranged from 2 m to 6 m in depth. Six cores were collected along the 62 m study transect, as shown in Figure 4.3.

Generally, soil cores had high rates of retrieval, with the exception of some low recovery rates around a hard cobbly layer. The level of retrieval from this layer was inconsistent as well since the head of the drill would occasionally be obstructed by large cobble. Finally, the information obtained from the collection of soil cores was supplemented with information from the test pit and the shallow soil probe as described in Section 4.1.1. Selected photos of the test pit were included in Appendix C.

Following extraction of soil cores they were logged and spatially interpreted to describe the lithostratigraphy of the site. The cross section interpretation of the lithostratigraphy is shown in Figure 5.2.

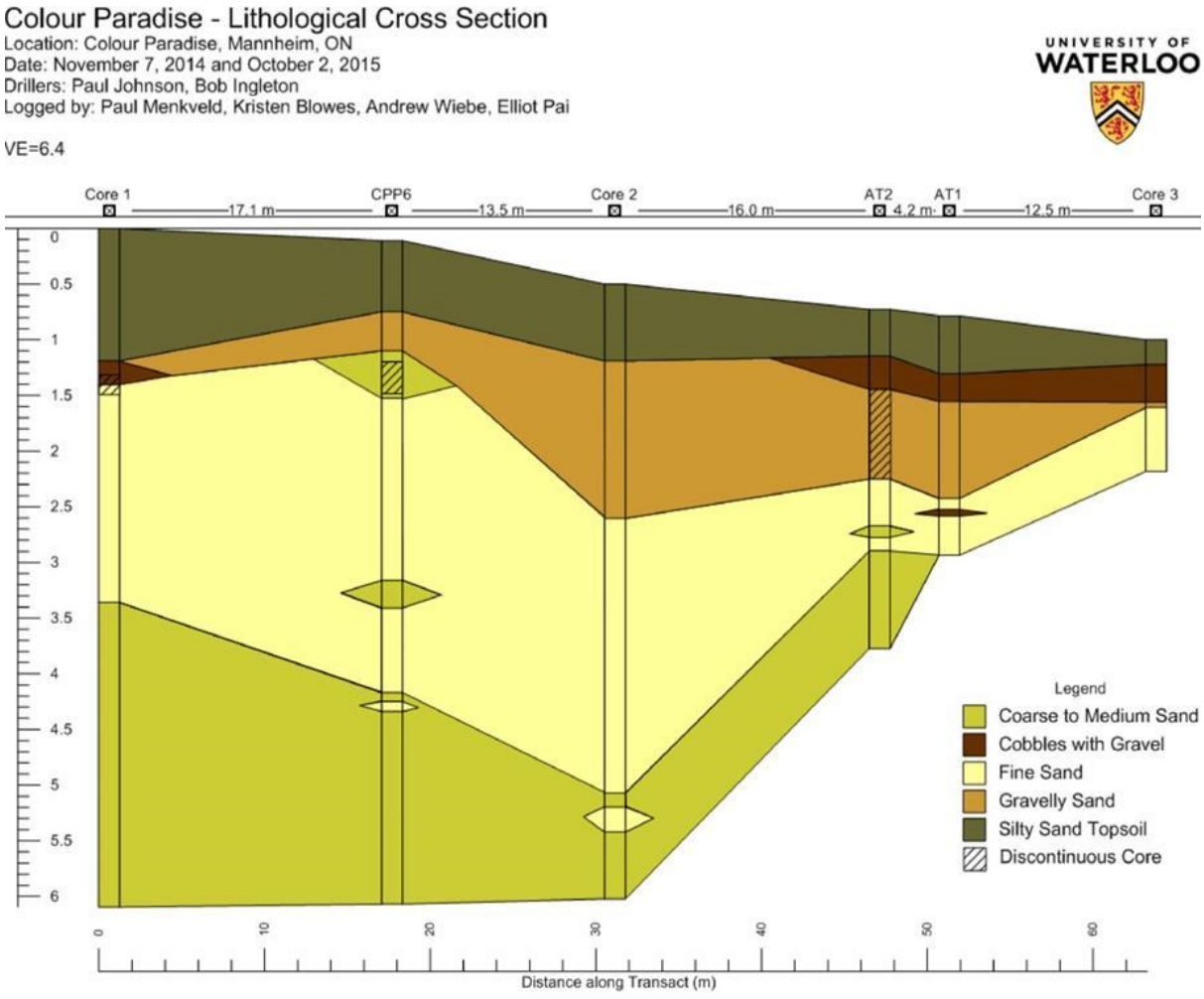

Figure 5.2. Interpreted Site lithostratigraphic cross section.

The typical sequence of soils on the site includes a thin top layer of silty sand topsoil, rich in organic material. This layer varies in thickness across the length of the transect. The second layer observed is a discontinuous cobble, gravel, and sand layer. This layer is a recently buried stream bed. During the excavation of the test pit this layer was intercepted and a number of river

mollusc shells were uncovered, suggesting strongly that this sediment is a former stream bed of Alder Creek. The other significant finding upon excavating this was a shard of glass. This suggests that the Alder Creek's course has changed and the upper meter of sediments have been deposited since the arrival of glass products in the area. The third layer logged in the soils cores is a gravelly coarse sand layer. This layer has a sharp interface with the underlying fine sand layer. The fourth layer observed in the soil sequence is fine sand with silt. Lenses of gravel and silt were also observed within the layer. The final layer in the cross section is a uniform layer of coarse sand with little gravel.

5.1.3. Hydrostratigraphy

A critical part of accurately constructing a hydrostratigraphic model is parameterizing it with the hydraulic properties. In order to do this, the best available hydraulic properties are assigned to the stratigraphic model units. The primary investigation of soil stratigraphy is detailed in Section 5.1.2. Hydrostratigraphic units are assigned to the lithological units in Figure 5.3. This chapter will describe the results of various techniques applied to study the physical and hydraulic properties of the soils at the Site and synthesize them into a hydrostratigraphic model. While lithostratigraphic units are not perfectly homogenous, attributing hydraulic properties to hydrostratigraphic layers provides the best possible interpretation of the hydraulic properties of the soil sequence. The soil stratigraphic analysis resulted in the assignment of five lithological units which will be treated as five hydrostratigraphic units, as shown in Figure 5.2.

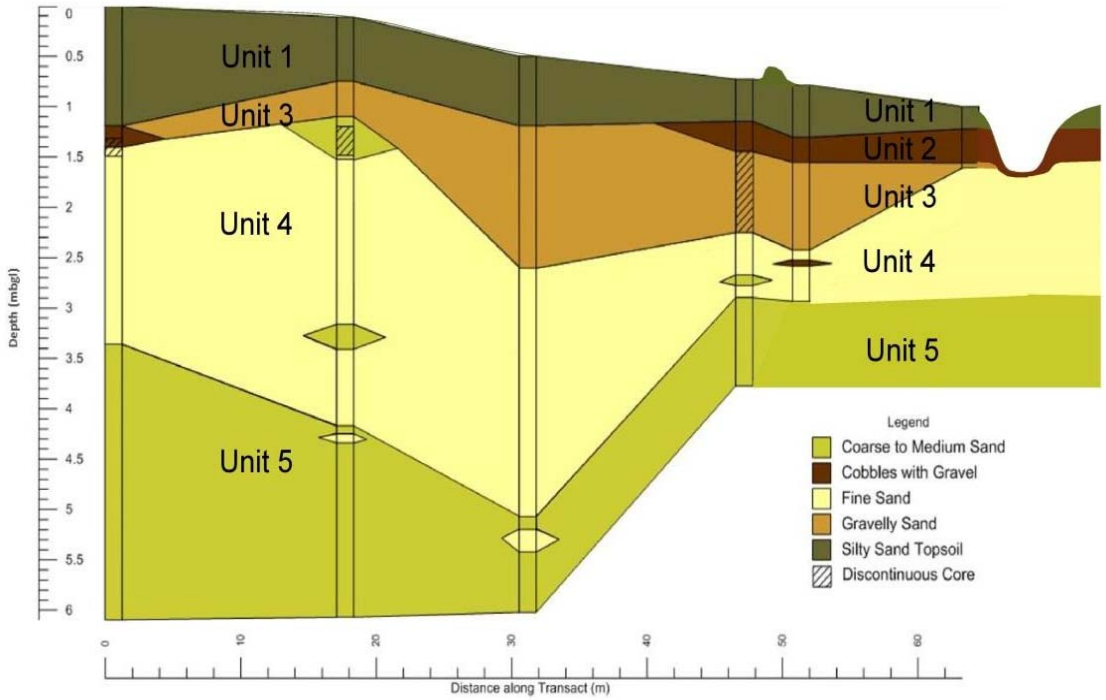

Figure 5.3. Hydrostratigraphic unit conceptualization of the Site.

5.1.3.1. Hydraulic Conductivity Measurements

The hydraulic conductivity of the soils at the Site are an important parameter to support the quantification of recharge. Multiple techniques were used in different situations to achieve the best possible estimates of hydraulic conductivity for each unit. Techniques applied include the use of grain size analysis based hydraulic conductivity estimates, hydraulic permeameter testing, rising and falling head testing, and Guelph Permeameter testing.

5.1.3.1.1. Hydraulic Conductivity Based on Grain Size Analysis

Empirical equations were applied to the grain size distributions to estimate hydraulic conductivity, as described in Section 4.2.1. The results of the analyses are plotted on the lithostratigraphic cross-section in Figure 5.4. and summarized by unit in Table 5.1. A complete record of the hydraulic conductivity calculations included in Appendix D.

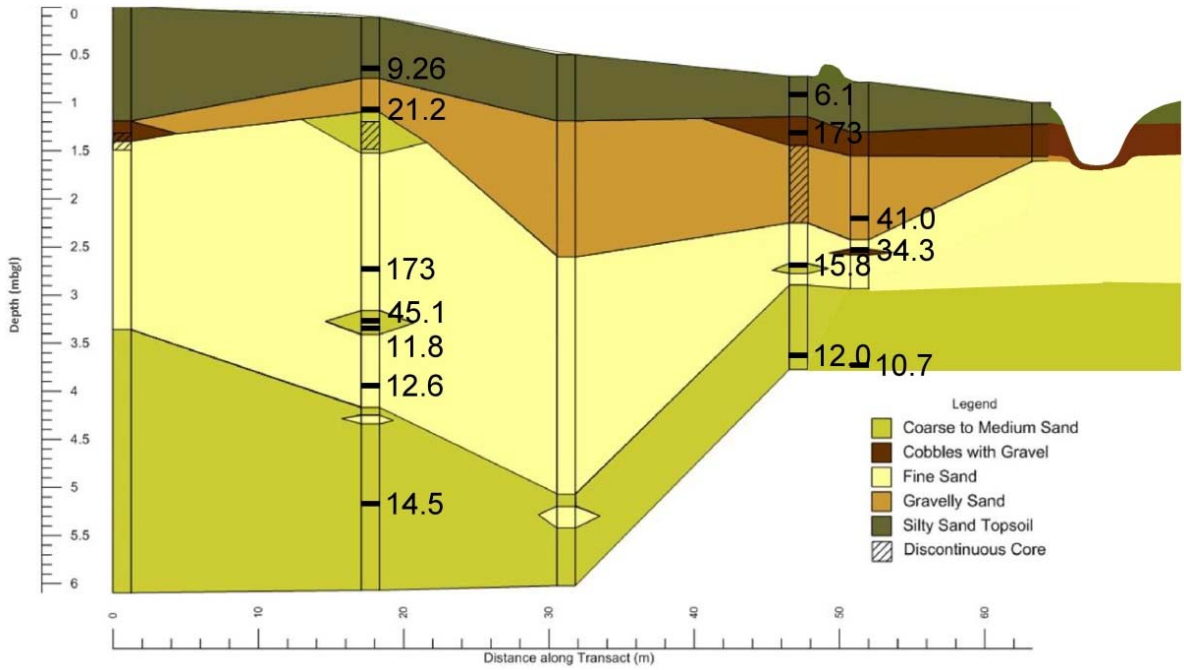

Figure 5.4. Site hydraulic conductivity estimates based on grain size distribution (m/d).

Table 5.1. Grainsize analysis estimated hydraulic conductivity

Unit Number	n	Mean k (m/d)	Standard deviation k (m/d)
1	2	8E+00	2E+00
2	1	2E+02	n/a
3	2	3E+01	1E+01
4	5	5E+01	6E+01
5	3	1E+01	2E+00

The mean hydraulic conductivity for each unit is given in Table 5.1. It is within the expected range of values of the sediments observed on this field site (Fetter, 2001). The relative ranking of the units by hydraulic conductivity also conforms to the expected results. The coarsest units with the fewest fines were assigned the highest hydraulic conductivity values (Unit 2), while the units with finer matrix materials and higher amounts of fines had lower estimates of hydraulic conductivity (Unit 1). Core logs reflect that the most variable layer in sequence is the fine sand (Unit 4) with lenses of gravel, coarse sand, and silt interbedded within the layer. The analyses reflect this complexity; Unit 4 has the highest standard deviation of the units analyzed despite a larger number of samples being analyzed.

5.1.3.1.2. Hydraulic Conductivity Based on Rising and Falling Head Tests

Wells selected for slug testing are screened in Units 4 and 5, as described in Section 4.1.10 and Section 5.1.2 and shown in Figure 5.5. The results of those tests and analysis are contained in Table 5.2. The results are then summarized by layer in Table 5.3. The slug test results (as per the Hvorslev Method) are plotted spatially in Figure 5.5.

Table 5.2. Rising and falling head test hydraulic conductivity by piezometer

Well Name	Unit Number	Hvorslev estimated k (m/d)			B&R estimated k (m/d)	
		n (tests)	Mean	Standard dev.	Mean	Standard dev.
CPP1	5	6	3E-01	2E-01	3E-01	3E-01
CPP4	4	7	2E+00	3E-01	1E+00	1E-01
CPP6	5	1	4E+00	-	7E+00	-
CPP7	4	9	3E-01	1E-01	3E-01	2E-01
CPP10	4	2	3E+00	3E+00	6E+00	8E-01

Table 5.3. Rising and falling head test hydraulic conductivity by unit					
Unit Number		Hvorslev estimated k (m/d)		B&R estimated k (m/d)	
	n (wells)	Mean	Standard dev.	Mean	Standard dev.
4	2	3E+00	7E-01	4E+00	2E+00
5	3	2E+00	2E+00	2E+00	3E+00

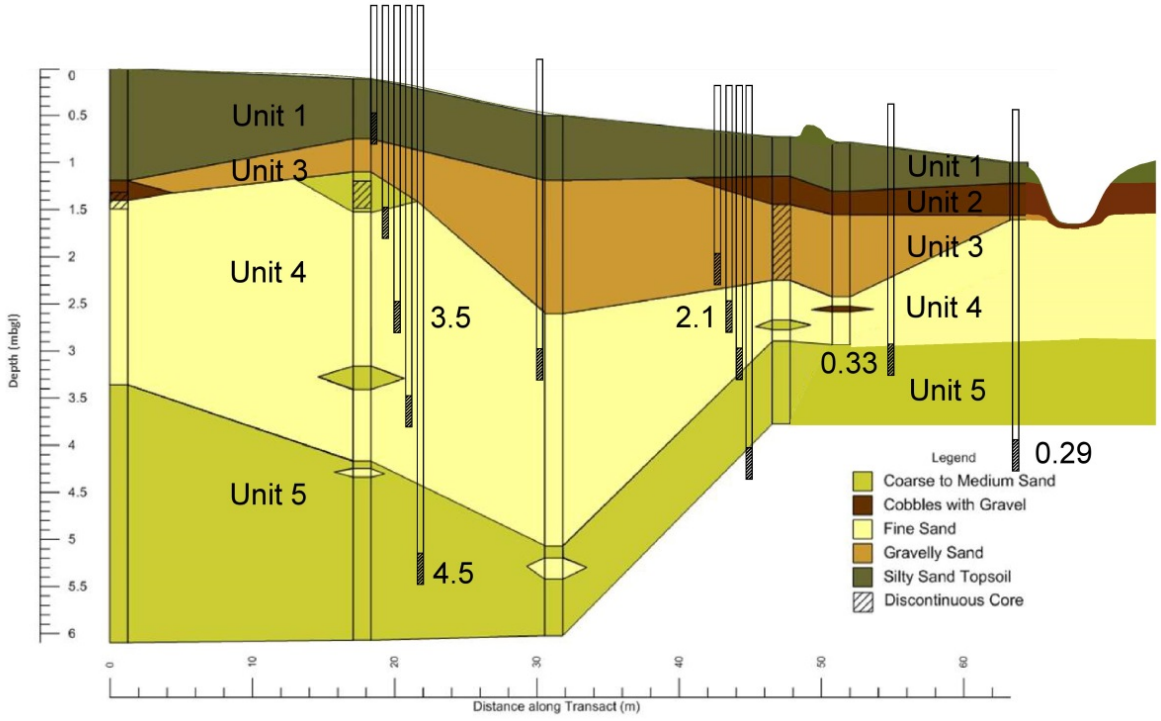

Figure 5.5. Cross section of hydraulic conductivity resulting from rising and falling head tests (m/d).

Slug testing yielded valuable estimates of hydraulic conductivity of the lower units where monitoring wells are screened in saturated soils. The low level of standard deviation around the mean of each individual well's analyses indicates that tests were reliable and repeatable in each monitoring well. In general, the wells analyzed in the fine sand (Unit 5) showed a hydraulic conductivity approximately 0.3 m/day, with the exception of the deeper and longer screened well located further from Alder Creek (CPP6). This is lower than the coarse sand (Unit 4) which

showed approximately 3 m/d. These tests conform to typical values for these sediment types and to the expected relative permeability of the sediments.

5.1.3.1.3. Hydraulic Conductivity Based on Permeameter Testing

Falling head permeameter tests were applied to the soil samples selected to represent the hydrostratigraphic units, as described in Section 4.2.2. The soil sample locations are shown on Figure 5.4. (the same soil samples were tested with a permeameter and used for sieve analysis). The results of the permeameter testing is summarized in Table 5.4. by layer (Missori, 2015).

Table 5.4. Permeameter test estimated hydraulic conductivity

Unit Number	n	Mean k (m/d)	Standard deviation k (m/d)
1	6	1E+00	4E-01
2	3	3E+01	1E+00
3	6	1E+01	3E+00
4	18	5E+00	3E+00
5	9	3E+01	4E+01

5.1.3.1.4. Hydraulic Conductivity Based on Guelph Permeameter Testing

The Guelph Permeameter method was applied at the Site by Missori (2015) to the surficial soils in the study area, as described in Section 4.1.8. and shown in Figure 4.4. The results of the Guelph Permeameter testing are summarized in Table 5.5. The results were very consistent showing less than 1% variation among the three sites tested. This indicates that fresh surficial soils tested by the Guelph Permeameter were fairly homogenous.

Table 5.5. Guelph permeameter results		
Test Location	Unit Number	k (m/d)
1	1	5E-01
2	1	5E-01
3	1	5E-01

5.1.3.1.5. Hydraulic Conductivity Summary

In this section, hydraulic conductivity values determined by the various analyses are summarized, compared, representative values are selected. This section contained hydraulic conductivity estimates based on grain size distributions, slug tests, permeameter tests, and Guelph permeameter tests. To select the most appropriate values of hydraulic conductivity it is necessary to compare the strengths and weaknesses of the methodologies.

Grain size distributions are useful to estimate hydraulic conductivity because of the easily applied empirical method. The grain size test distribution itself measures a physical property of the soil, simply and reliably. After this a variety of empirical formulas, can be applied to estimate the hydraulic conductivity based on grain size distribution. Because this method involves the use of a disturbed sample and empirical relationships, it does not reliably produce hydraulic conductivity values. In this case, grain size distribution based estimates of hydraulic conductivity produced results generally within 1 order of magnitude of the other methods.

Permeameter testing is another method in which a sample can be analyzed in the lab to estimate hydraulic conductivity. An advantage of this approach, is that it can be applied to any soil sample. It can also be repeated to improve the accuracy of the results. A significant limitation of this method is its use of a small disturbed sample to represent field conditions. Additionally, it can be problematic to test highly permeable materials or low impermeable materials, since the test relies on duration observations (inaccurate with the former case) and negligible leakage and evaporation (not true in the latter case).

The Guelph Permeameter compares favorably to lab methods because it uses in field medium scale tests of relatively undisturbed soil to estimate hydraulic conductivity. The limitations of this method are the accessibility of layers lower in the soil column for testing and the partial saturation of the tested soils. In this study, the Guelph Permeameter was well suited to test the surficial soils.

Finally, the slug test was applied to test the in situ soils around the saturated well screens. For the interpretation of slug test results two commonly applied zero storage models were applied: the Hvorslev method (Hvorslev, 1951) and the Bouwer and Rice Model (Bouwer and Rice, 1976). The assumptions of the models are generally applicable to the site so both methods were evaluated. There was little difference between the methods, so the Hvorslev method was selected for simplicity of analysis. The slug tests, test the largest volume of aquifer material, most reliably, with the least level of disturbance to the soil, so it is the preferred testing method where testing was possible.

The number of tests conducted, standard deviation of those tests, and the accepted reliability of those methods were all considered in the selection of representative hydraulic conductivity values for each layer in the hydrostratigraphic model. The results of the site characterization, testing, analysis, and selected values (highlighted in grey) are shown in Table 5.6.

Table 5.6. Hydraulic Conductivity Analysis Summary Table

Analytical Method		Grain Size	Permeameter	Guelph Permeameter	Slug Test - Hvorslev	Slug Test - B&R	Selected k
Unit 1	k_{av} (m/d)	8E+00	1E+00	5E-01	-	-	5E-01
	n	2E+00	6E+00	3E+00	-	-	
	k_{stdev} (m/d)	2E+00	4E-01	1E-03	-	-	
Unit 2	k_{av} (m/d)	2E+02	3E+01	-	-	-	3E+01
	n	1E+00	3E+00	-	-	-	
	k_{stdev} (m/d)	-	1E+00	-	-	-	
Unit 3	k_{av} (m/d)	3E+01	1E+01	-	-	-	1E+01
	n	2E+00	6E+00	-	-	-	
	k_{stdev} (m/d)	1E+01	3E+00	-	-	-	
Unit 4	k_{av} (m/d)	5E+01	5E+00	-	3E+00	4E+00	3E+00
	n	5E+00	2E+01	-	2E+01	2E+01	
	k_{stdev} (m/d)	6E+01	3E+00	-	7E-01	2E+00	
Unit 5	k_{av} (m/d)	1E+01	3E+01	-	2E+00	2E+00	2E+00
	n	3E+00	9E+00	-	7E+00	7E+00	
	k_{stdev} (m/d)	2E+00	4E+01	-	2E+00	3E+00	

Notes: All k values are expressed in m/d.
Sources of selected k values are shaded.

5.1.3.2. Specific Yield and Porosity Measurements

Specific yield and porosity were observed in situ beneath the closed depression, as described in Section 4.1.9. by using the field dry and field saturated observations with the neutron probe. The results of the porosity analysis showed that the average porosity of the soils beneath the closed depression is 0.32. The results showed that the average specific yield of the typically unsaturated zone beneath the closed depression is 0.10. The values for porosity and specific yield were then compared to literature values to check the results of the field

experiments. The porosity is within the expected range, albeit near the high end of range of typical values (0.20 to 0.35, Fetter, 2001), which is reasonable considering that the soils are young and believed to fluvial in origin. The specific yield is also within the typically expected range, near the low end of the range of expected values (0.10 to 0.28, Fetter, 2001). The results of these field based assessments are used in the calculation of recharge quantities in Section 5.4.

In assessing the porosity and specific yield using this method, there is variability due to measurement error and variability of entrapped air. Firstly, this method relies on the accuracy of the neutron probe data, which of course is limited. Further, the neutron probe measures only a limited volume of the in situ sediments, and is assumed to be representative when calculating recharge in Section 5.4. Secondly, when the water table rises, air may be entrapped unpredictably in pore spaces. This will result in variation of the observed moisture contents and specific yield. In this case, specific yield had little variation with time, presumed to be due to air entrapment.

5.2. Observations

The field techniques used to characterize the field site, monitor climatic conditions and measure groundwater hydraulic head, surface water levels, water and soil temperatures, and soil moisture data are described in Section 4.1. The following section contains summaries and observations of the data collected during the two hydrologic events that were monitored during the course of the study.

5.2.1. Climatic Data

Climatic data were collected during the course of the experiment at a meteorology station (MET Station) located approximately 40 m NE of the instrumented field site (Figure 4.2.).

Although the meteorological conditions vary even on small scales, observations from this location were taken to be representative of the field site for purposes of this study. This MET Station is operated by the Southern Ontario Water Consortium (SOWC) at the University of Waterloo. Additional data were also obtained from an Environment Canada MET Station in Roseville and from several other SOWC meteorology stations located near the field site over the observation period (Environment Canada, 2017).

5.2.1.1. Climatic Data During the November Event

Between November 17th and November 21st, 2014, (referred to as the November Event) a snow pack of approximately 15 cm accumulated at the site (Figure 5.6). Snow depth and snow water equivalent (SWE) were measured at the MET station (as described in Section 4.1.12.). On November 22nd, temperatures exceeded zero degrees and 12 mm of rain fell. These factors caused the entire snow pack to melt on November 22nd. On November 24th, an additional 50 mm of rain fell on the field site in a short and intense rainstorm. The combined impact of these climatic events was the accumulation of surface water in the depression area and significant increase in water level and flow in Alder Creek. This kind of early winter melt event is typical of southern Ontario, so its inclusion in the study provides a valuable example of the recharge processes in the area.

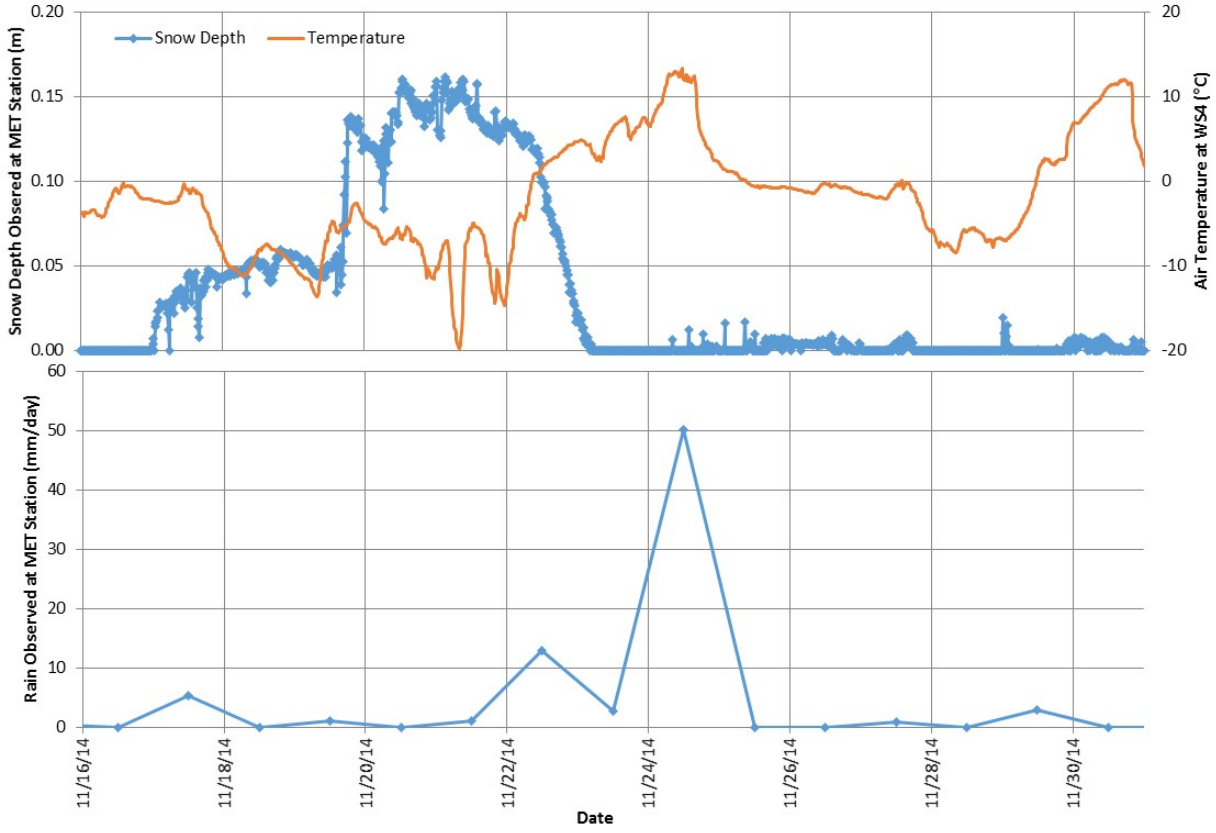

Figure 5.6. Snow depth, air temperature, and precipitation observed at the MET Station during the November Event.

Snow melt and rainfall combined to contribute a total of ~80 mm of water to the ground surface over the November 22nd to 24th time period (1.8 days), as shown in Figure 5.7.

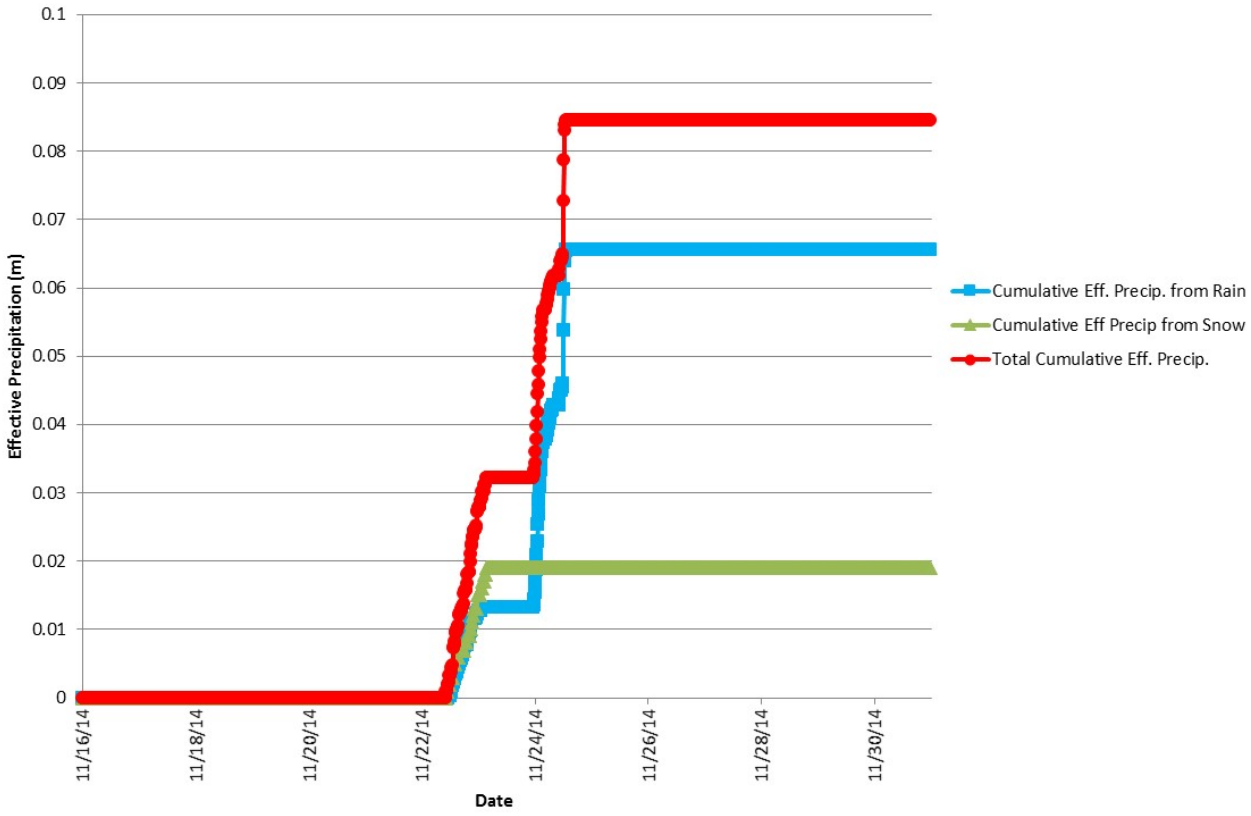

Figure 5.7. Cumulative water from precipitation and snow melt (cumulative effective precipitation calculated by summing cumulative rainfall and snow melt) observed at the MET Station during the November Event.

The climatic data also included air temperature measurements. Temperatures throughout the first weeks of November in 2014 were above zero in Mannheim (Figure 5.6.). Snowfall began as the temperatures fell on November 17th. As a result, the snow accumulated on unfrozen soils. The absence of subsurface frost was confirmed with direct soil probe observations of shallow soils.

Following the snow melt and rainfall on November 22 to 24, temperatures dropped below zero and remained below zero for several days. Only trace precipitation was observed in the subsequent days.

5.2.1.2. Climatic Data during the Spring Melt Event

During the winter of 2014 to 2015, a slightly below average amount of snowfall accumulated during the winter months (116.5 cm, at the Roseville EC Station) (Environment Canada, 2017), as compared to the previous 20 years (134.4 cm average, at the Roseville EC Station) (Environment Canada, 2017). The temperature of the 2014-2015 winter was below historical averages (Environment Canada, 2017). During the winter months, some extreme cold temperatures were observed, including a record low temperature of -32˚C (Environment Canada, 2017). By the end of the winter, before the beginning of the spring melt (referred to as the Spring Melt Event), a 40 cm deep snow pack with a snow water equivalent of 84 mm had accumulated around the MET station noted above. As discussed in Section 4.1.12., snow water equivalent is calculated by averaging the water equivalent of nine snow samples located on the agricultural field in the catchment of the closed depression. For simplicity of calculating cumulative water from snow storage, snow water equivalent was assumed to be linearly correlated with snow depth observed at the MET Station.

Temperatures remained below zero and snow accumulated throughout the winter with one exception. On December 24th, 2014, a partial melt and rainfall caused the surface water to flow across the agricultural field and into the closed depression. The surface water refroze in the depression forming a 10 cm layer of ice above the ground surface when temperatures dropped again hours later.

The Spring Melt Event began on March 7, 2015, when daytime high temperatures began to consistently reach positive values (Figure 5.8.). This caused gradual snowmelt over the first 22 days of the melt event. Rainfall increased the rate of snowmelt and snow pack compaction, as shown in Figure 5.8. During the Spring Melt, a combined total of 110 mm of water were released from the snow pack and fell as rain on the ground surface (84 mm in snow melt and 25 mm in rainfall), as measured at the MET station by the method described in Section 4.1.12. (Figure 5.9.).

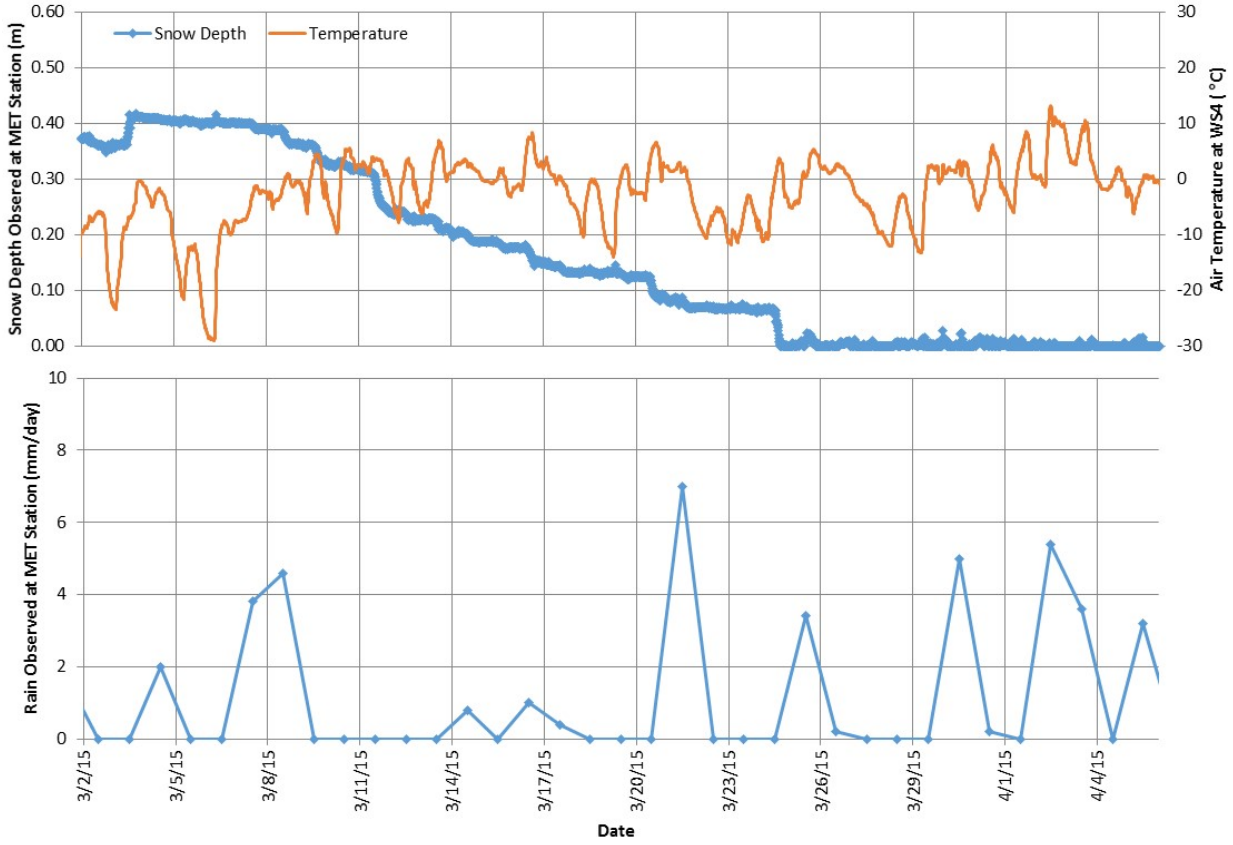

Figure 5.8. Snow depth, air temperature, and rainfall observed at the site during the Spring Melt Event.

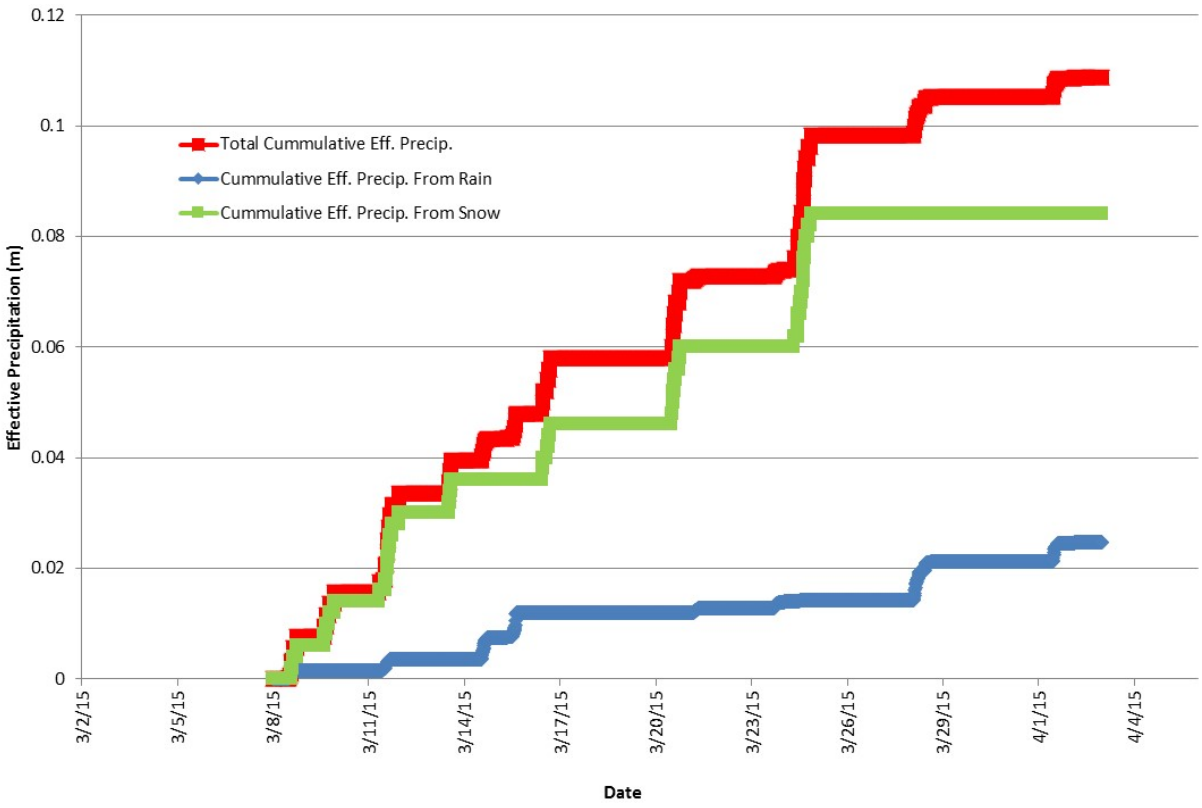

Figure 5.9. Cumulative water from precipitation and snowmelt (cumulative effective precipitation calculated by summing cumulative rainfall and snow melt) observed at the MET Station during Spring Melt Event.

5.2.1.3. Comparison of Hydrologic Events

The two hydrologic events included in the scope of this study have similarities and differences, which allows the results to be compared and contrasted in order to make observations about the effects of hydrologic event intensity and seasonality on recharge dynamics. The November Event and the Spring Melt Event are similar in the type and amount of water released at the ground surface during a hydrologic event and both have combined water inputs from both rain and snow melt. In the November Event and the Spring Melt Event, a cumulative amount of 80 and 110 mm of water (snow melt and rainfall), respectively were released. The events are different in their duration, existence of subsurface soil frost and the

influence of the adjacent stream, Alder Creek. The Spring Melt took place over 35 days, while the November Event took place over 1.8 days. In the case of the November Event, no soil frost was observed. In the Spring Melt Event, frost had penetrated to a depth of about 35 cm. Finally, the November Event showed coincident rises in Alder Creek and the closed depression, while the Spring Melt Event showed staggered surface water and groundwater hydrographs.

5.2.2. Groundwater and Surface Water Head Data

Detailed groundwater and surface water head observations were one of the primary datasets used to interpret and quantify recharge dynamics at the field site. Groundwater and surface water levels were monitored as described in Section 4.1.2. and Section 4.1.3.

5.2.2.1. Groundwater and Surface Water Head Data during the November Event

The combined snowmelt and rainfall observed during the November Event (80 mm in 1.8 days) caused the stage of Alder Creek to rise and overland flow to fill the closed depression. Groundwater levels then responded to changes in surface water levels as recharge occurred.

On November 22, surface water flowed across the field into the closed depression and filled the closed depression, and then water overflowed the edge of the closed depression and flowed into Alder Creek (Figure 5.10.). Overland flow persisted for approximately 23 hours and surface water persisted in the closed depression for approximately two days. Selected photos of the hydrologic events and surface water are shown in Appendix F.

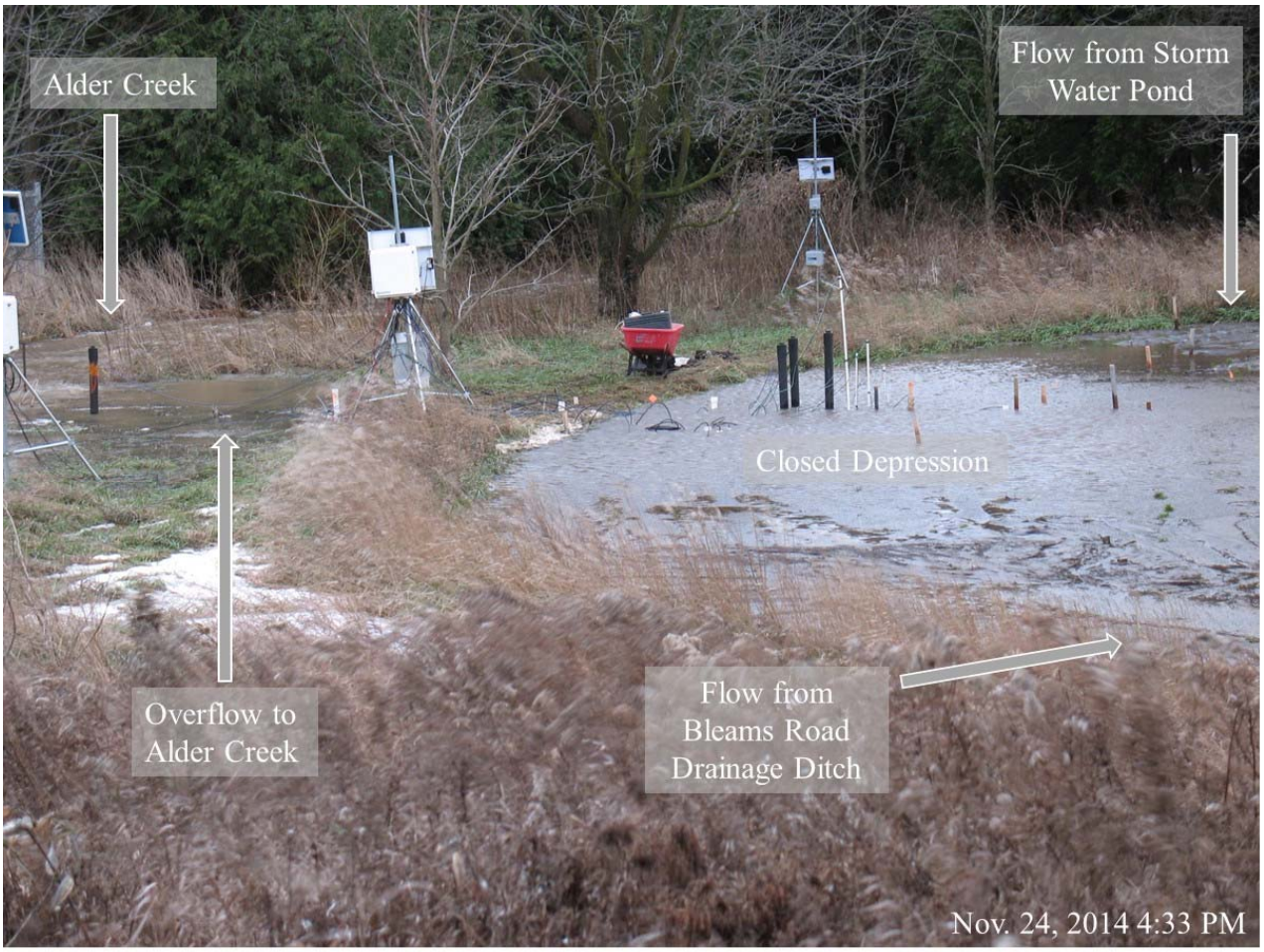

Figure 5.10. Ephemeral overland surface water flow at the site during the November Event as observed on November 24, 2014 (Refer to Section 3.5. and Figure 3.5. for plan view of surface water flow, sources, and discussion).

Water levels in the piezometers installed beneath the closed depression show a gentle rise (~10 cm) of the water table in response to the snow melt and rainfall between November 23rd and 24th (Figure 5.11.). On November 24th, the piezometers showed a much larger response to the climatic event. At their peak, observed groundwater heads indicate that the soil beneath the depression nearly reached the ground surface (Figure 5.11.). At this time, there was a vertical gradient in the system, indicating that water was flowing vertically downward beneath the closed depression and contributing to groundwater recharge (Figure 5.12.).

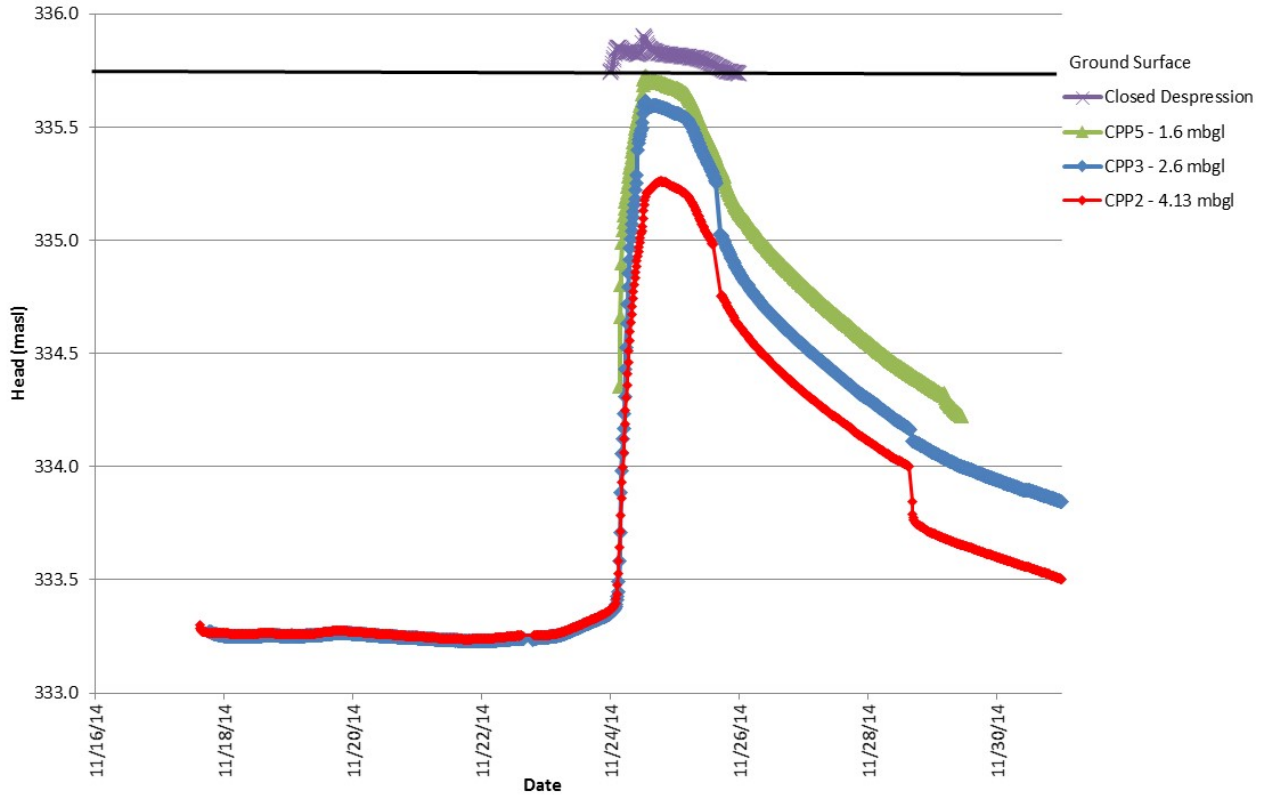

Figure 5.11. Groundwater heads observed beneath the closed depression during the November Event.

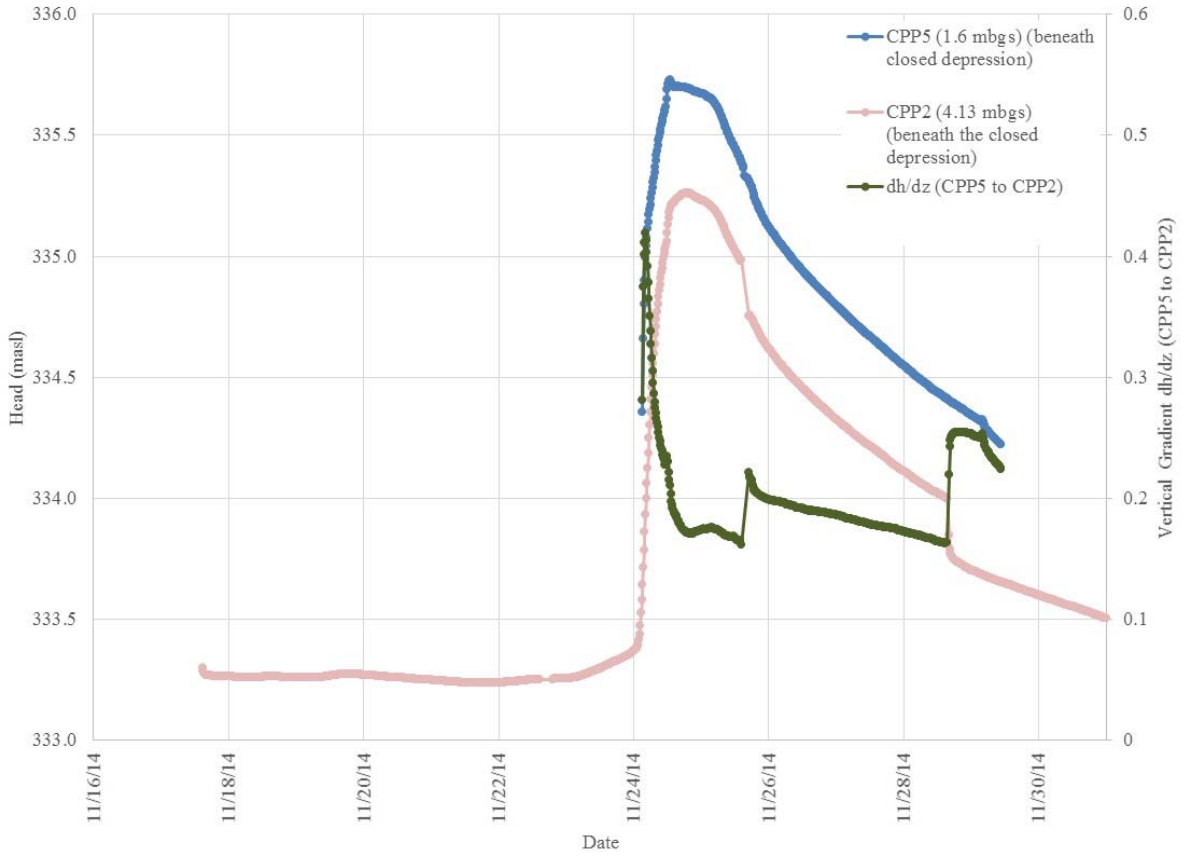

Figure 5.12. Hydraulic head and vertical hydraulic head gradient observed below the closed depression during the November Event.

The vertical gradients observed below the closed depression were consistently downward (positive in Figure 5.12.) during the course of the monitored event. The downward gradient was greatest initially as the surface water formed and caused flow downward into the subsurface. The gradient then gradually declined with the exception of two sudden steps when the slow recovering CPP2 was sampled (results of groundwater sampling are included in Appendix G).

In response to the snow melt and rainfall, the level of Alder Creek as measured with a pressure transducer located in the centre of the stream rose from 0.22 m before the event (November 19, 16:00) to 0.85 m at the peak (November 24, 14:00) (Figure 5.13.). Alder Creek remained within its banks throughout the November Event. The piezometer immediately adjacent to the stream, screened close two the water table, recorded a small increase in

groundwater head on November 22nd, similar to the observations of groundwater head beneath the closed depression. Then, following the intense rainfall on the 24th, Alder Creek rose and groundwater head adjacent to the Alder Creek increased rapidly to a level slightly above the creek bed. Throughout the hydrologic events there was a downward vertical gradient from the stream water level to the adjacent piezometer (CPP1 as shown in Figure 5.13), indicating that water flowed from Alder Creek into the aquifer. The combined data indicate that Alder Creek remained as a losing stream during the course of the November Event.

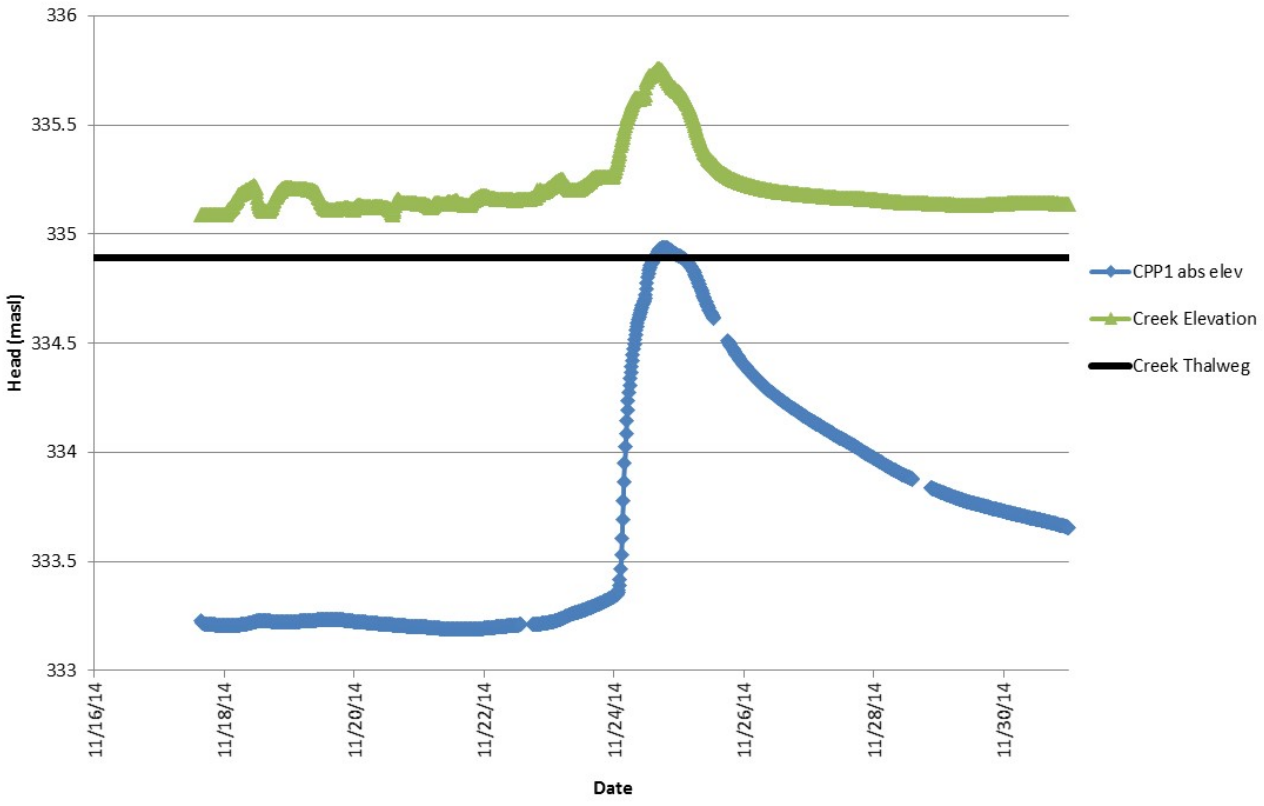

Figure 5.13. Water level in Alder Creek and groundwater head observed adjacent to Alder Creek during November Event.

The horizontal gradient between the instrument clusters adjacent to Alder Creek and below the closed depression was also calculated to analyze groundwater flow directions (Figure 5.14.). The gradient was calculated using to wells screened at the same depth below ground

surface (CPP1 adjacent to Alder Creek, and CPP2 below the closed depression). During the period prior to the start of the November Event the gradient showed groundwater was flowing from Alder Creek toward the closed depression. At the start of the event, the gradient briefly increased and then dropped rapidly to near a value near zero. The groundwater gradient showed that little or no lateral flow of groundwater occurred during the peak groundwater levels. The groundwater gradient then slowly increased towards its pre-November Event gradient (0.04), excluding two rapid steps in groundwater gradient at the times which CPP2 was sampled (November 25 and 28).

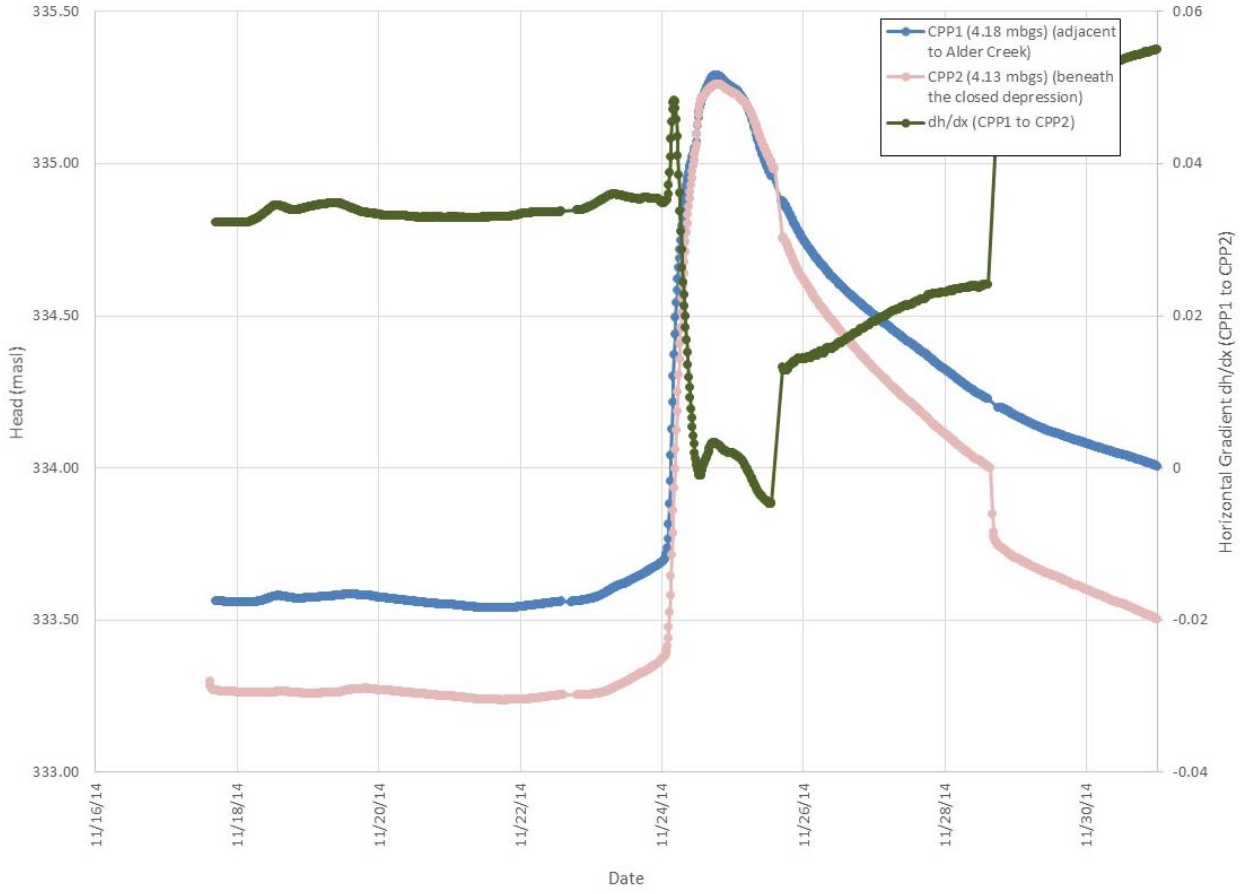

Figure 5.14. Horizontal gradient observed in the shallow aquifer during the November Event.

Groundwater head was also monitored at a background location ~18 m from the edge of the closed depression (CPP6 as shown in Figure 5.15.). Data from piezometer CPP6 showed

little or no response to the initial snow melt on November 22nd. On November 24th a rise of 0.35 m was observed. CPP6 showed a smaller, slightly delayed, and more gradual rise in comparison to the hydrographs of piezometers beneath the closed depression, as shown in Figure 5.15. The data illustrate the variable nature of the recharge rate and timing associated with the different topographic locations within the study site. These data also illustrate that the focussed recharge beneath the closed depression generates a local groundwater mount that may radiate outward influencing hydraulic head in the adjacent subsurface materials.

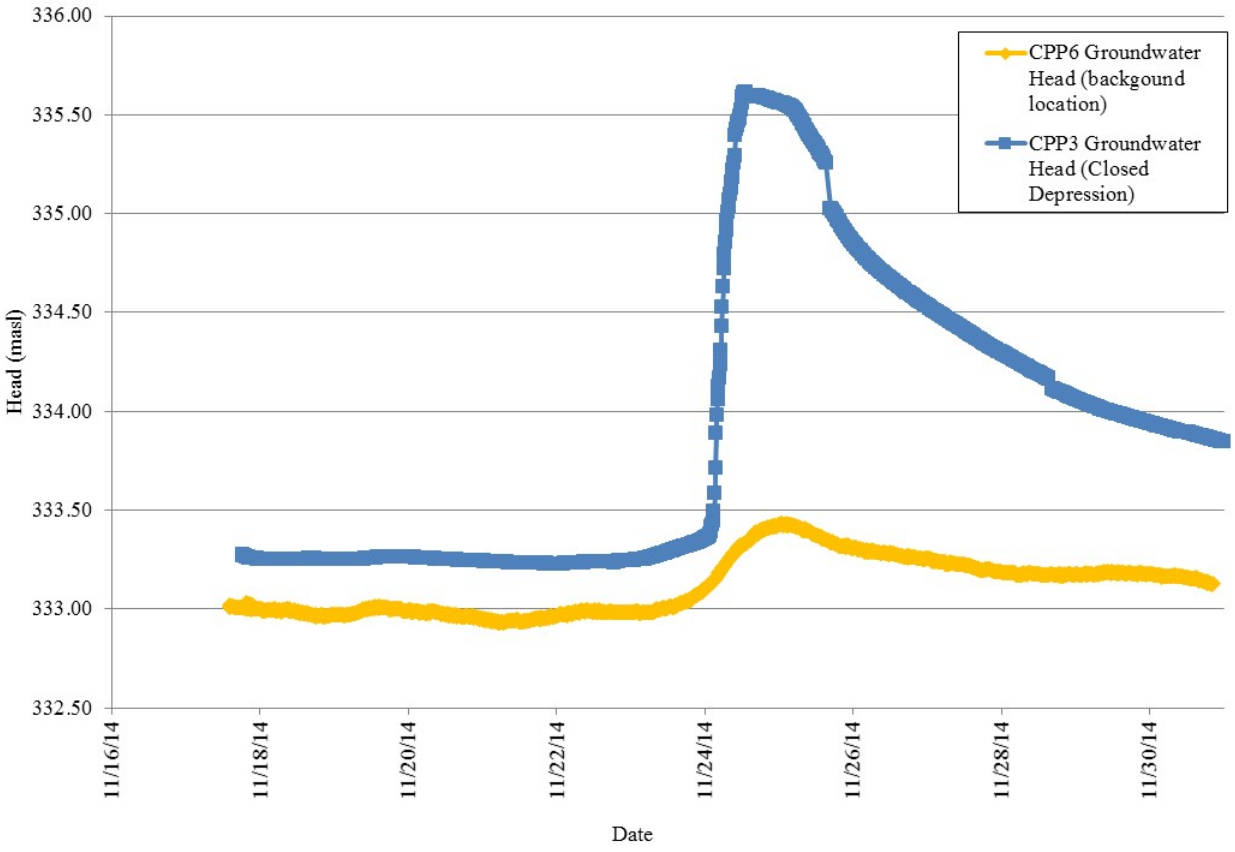

Figure 5.15. Groundwater heads observed beneath the depression (CPP3) and at the background instrument cluster (CPP6) during the November Event.

5.2.2.2. Groundwater and Surface Water Head Data during the Spring Melt Event

Transient changes in groundwater levels, surface water levels and hydraulic gradients appear to relate to gradually increasing air temperatures and rainfall during the Spring Melt Event, which released a combined 110 mm of water (as shown in Figure 5.9.). Surface water features and the groundwater system reacted in a highly transient fashion to snow melt and rain fall. The stage of Alder Creek changed rapidly in response to changing meteorological conditions. The hydrograph of Alder Creek shows an increase in stage each time warm weather increased the rate of snow melt in Alder Creek's catchment (March 11 to 13, 14, 16 to 17, and 21, 2015) (Figure 5.16).

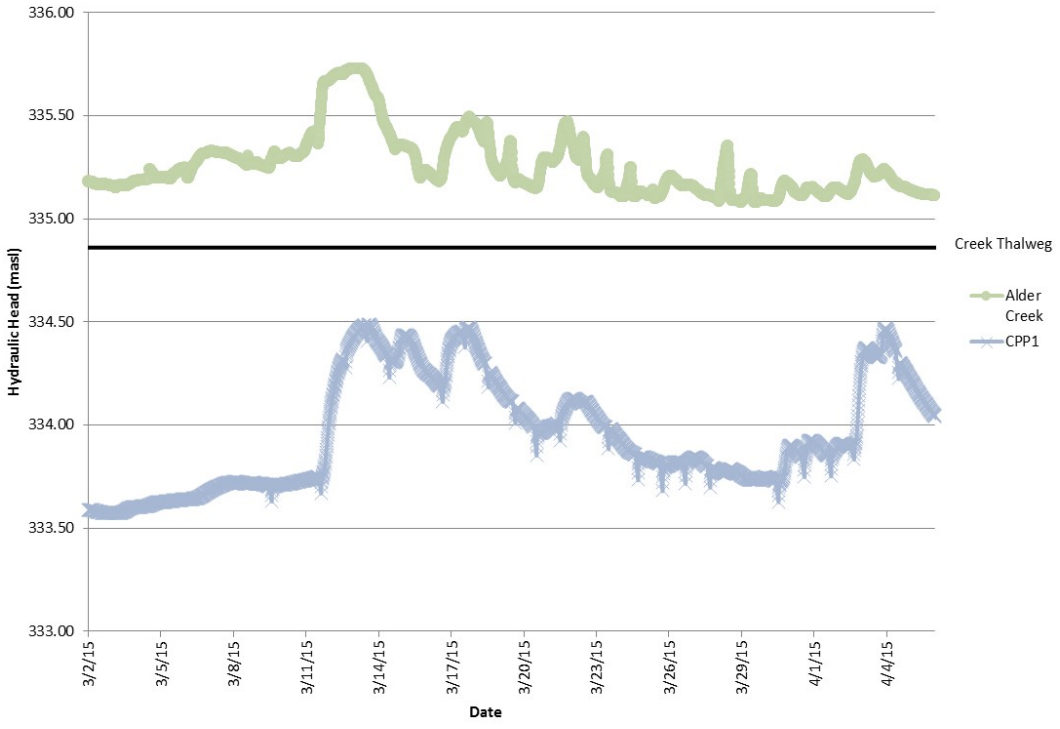

Figure 5.16. Alder Creek level and groundwater head observed adjacent to Alder Creek (CPP1) during the Spring Melt Event.

On the site, there are several possible sources of recharge: depression focussed recharge beneath the closed depression (DFR), diffuse areal recharge occurring broadly across the ground surface (DAR), and infiltration of surface water beneath Alder Creek. Hydraulic head data collected from the various groundwater monitoring wells installed within the field study site was evaluated to assess the nature of these combined recharge processes. Prior to the start of the melt event, there was a strong downward hydraulic head gradient from Alder Creek to the subsurface (Figure 5.13). As the melt event began, the hydraulic head hydrograph in the well adjacent to Alder Creek (CPP1) shows a rapid response to changes in the stage of Alder Creek (Figure 5.16.). Following the rise in temperatures, Alder Creek's stage rose by 0.41 m. The groundwater head observed adjacent to Alder Creek rose by 0.72 m, 3.5 hours after the beginning of the steep rise in the stage of Alder Creek.

During the Spring Melt Event, groundwater levels beneath the closed depression responded to changes in the surface water conditions in Alder Creek and in the closed depression (Figure 5.17.). Selected photos of the snow melt and the formation of surface water in the closed depression are included in Appendix F. Rapid snow melt occurred on March 11th and 12th, 2015, causing a rise in the stream stage of Alder Creek. On the March 12th, surface water formed under the sheet of ice in the closed depression. Similar to the November Event, groundwater levels increased rapidly following precipitation and the melting of the snow pack. The four groundwater head increases between March 11th and March 22nd occurred rapidly following the increases in stage of Alder Creek. As water levels in Alder Creek began to drop following the snow melt event, groundwater levels observed beneath the closed depression then receded gradually. However, ponded surface water remained in the closed depression for several more days (Figure 5.17.). Between March 30th and April 2nd, 2015, groundwater levels beneath the closed depression increased in a series of small magnitude peaks. Then on April 2nd and 3rd, 2015, a large groundwater level increase was observed at the time the surface water in the closed depression infiltrated and disappeared (Figure 5.17.). Throughout the Spring Melt a vertically downward hydraulic gradient was observed by the array of piezometers beneath the closed depression (Figure 5.18.). The hydrographs of the four piezometers (CPP2, CPP3, CPP4, and CPP5) in the array within the closed depression followed each other closely throughout the Spring Melt.

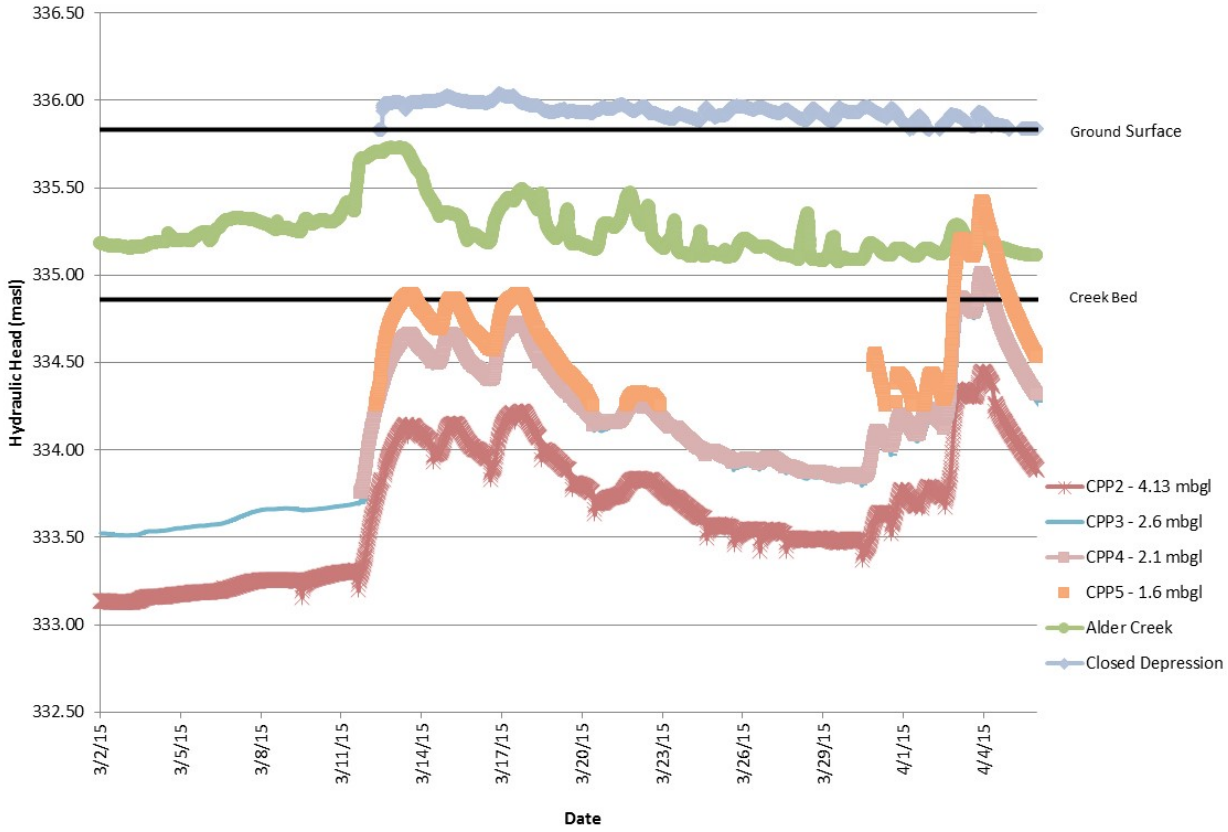

Figure 5.17. Surface water levels in Alder Creek and the closed depression and groundwater head observed beneath the closed depression (CPP2 to CPP5) during the Spring Melt Event.

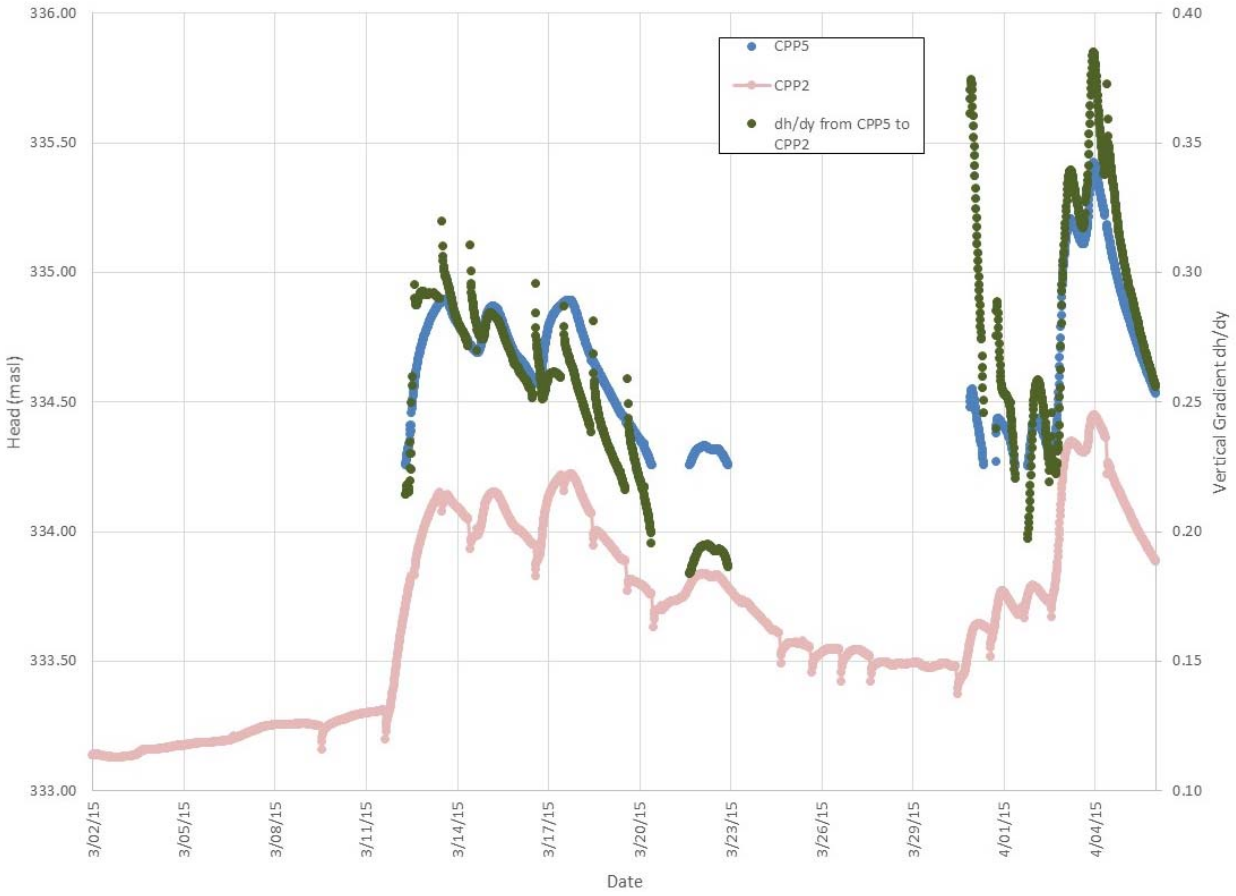

Figure 5.18. Vertical gradient observed beneath the closed depression during the Spring Melt Event.

During the Spring Melt Event, the horizontal gradients in the shallow aquifer were measured between the piezometers adjacent to Alder Creek and the array of piezometers beneath the closed depression, as shown on Figure 5.19.

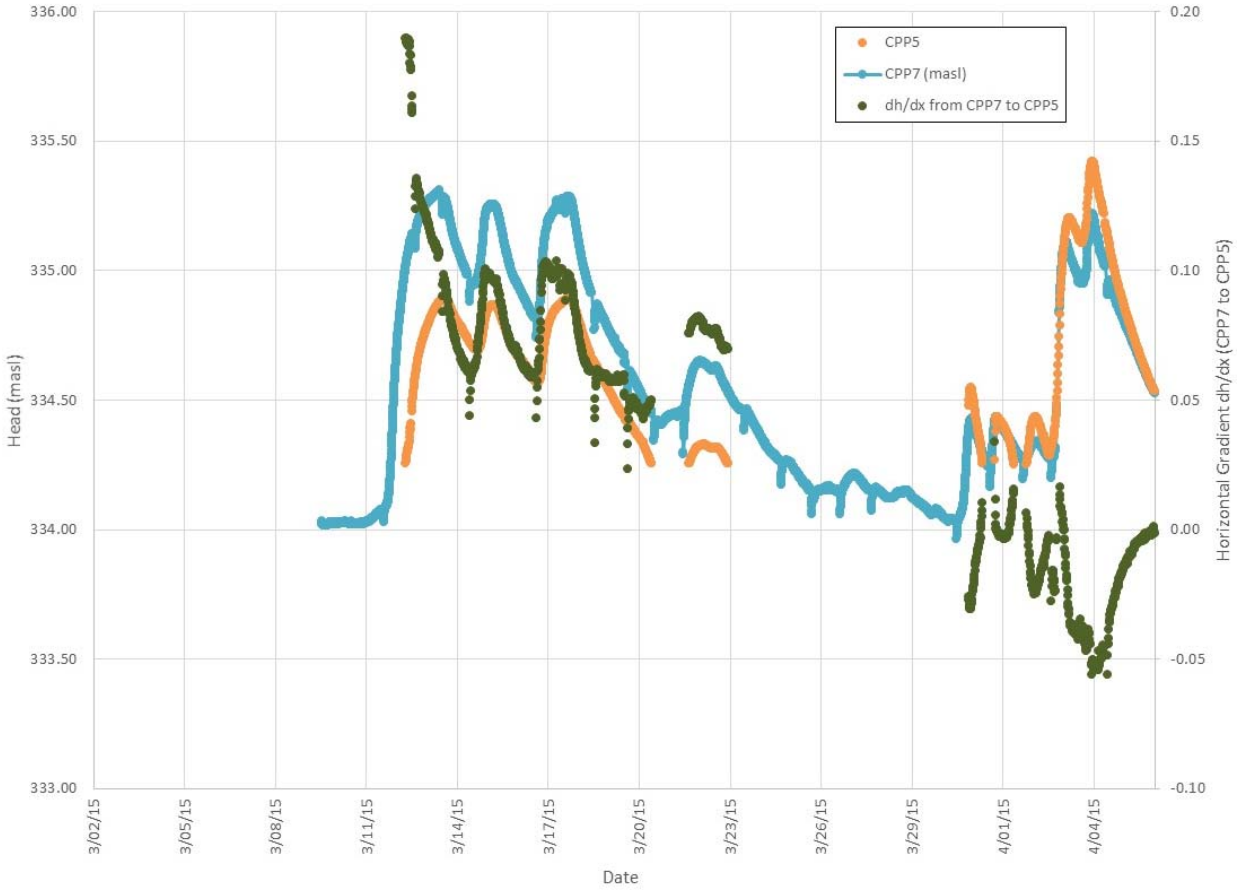

Figure 5.19. Horizontal gradient observed in the shallow aquifer during the Spring Melt Event (where a positive gradient causes flow from the piezometer adjacent to Alder Creek toward the closed depression).

In the hydrographs, and more noticeably in the groundwater gradient plots, there are small sudden drops in the water levels which were the result of the groundwater sampling, as discussed in detail in Section 5.2.6.

5.2.3. Temperature Data

Groundwater, surface water and air temperature datasets were collected during the study period to provide supporting data for recharge quantification and another means for observing recharge dynamics. Temperature observations were made as described in Sections 4.2.2., 4.2.3., and 4.2.6. For reference, the location of the temperature monitoring instrument clusters is shown in Figure 4.2. Additionally, soil temperature data were also collected during the course of the Spring Event.

5.2.3.1. Temperature Data during the November Event

During the November Event air temperatures rose leading to the melting of the snow pack and the warming of surface water features. Surface water and groundwater temperatures were observed during the November Event as summarized in this section. Groundwater and surface water temperature instrumentation was completed on November 17, 2014, so some initial temperature equalization occurred shortly after temperature installation.

Before the event, Alder Creek remained at a temperature slightly above 0°C while air temperatures were below zero freezing temperatures (Figure 5.20.). Then on the afternoon of November 23, 2014, Alder Creek's temperature began to increase and remained between 1°C and 8°C for several days. The piezometer adjacent to the Alder Creek (CPP1) shows a gradual decline in shallow groundwater temperature then a sudden drop from 10.0°C to 9.7°C over 16 hours on November 24, 2014, simultaneous with the rise in observed groundwater head. The groundwater temperature remained at this lower level with a gentle downward trend over the course of the measurement period.

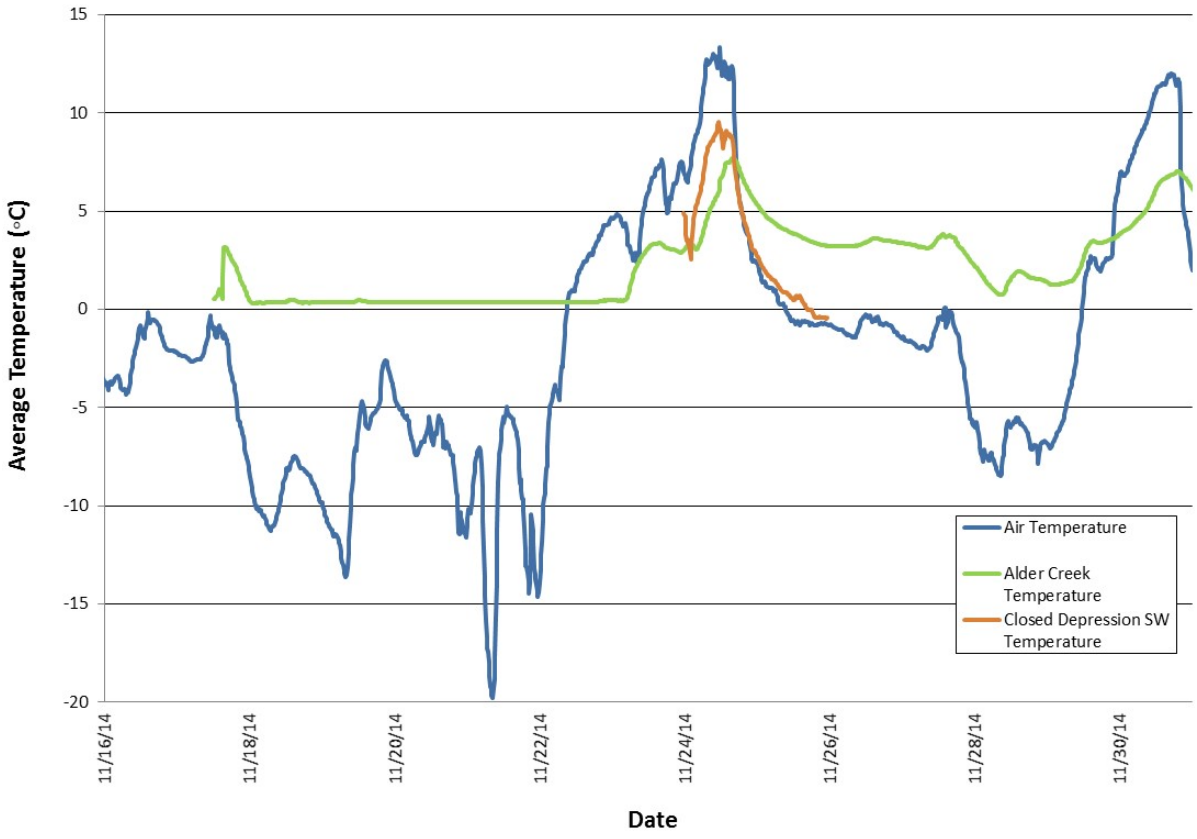

Figure 5.20. Air, surface water, and groundwater temperature observed at the Alder Creek instrument cluster during the November Event.

Groundwater temperature followed a similar trend beneath the closed depression (Figure 5.21). During the initial period of sub-zero air temperatures, the array of piezometers (CPP2 (deepest) to CPP5 (shallowest)) beneath the closed depression show a slow seasonal decline in shallow subsurface temperature. The shallowest piezometer showed a sudden drop from 10.0°C to 8.6°C in 7 hours on November 24, simultaneous with the rise in observed groundwater head. Then the groundwater temperature observed in CPP5 continued to follow a similar cooling trend as seen prior to the event, but at a lower temperature. The deepest piezometer (CPP2) showed a gradual cooling trend throughout the November Event, with little response to the event. The piezometers screened between CPP5 and CPP2 showed muted versions of the observed temperature closer to the surface.

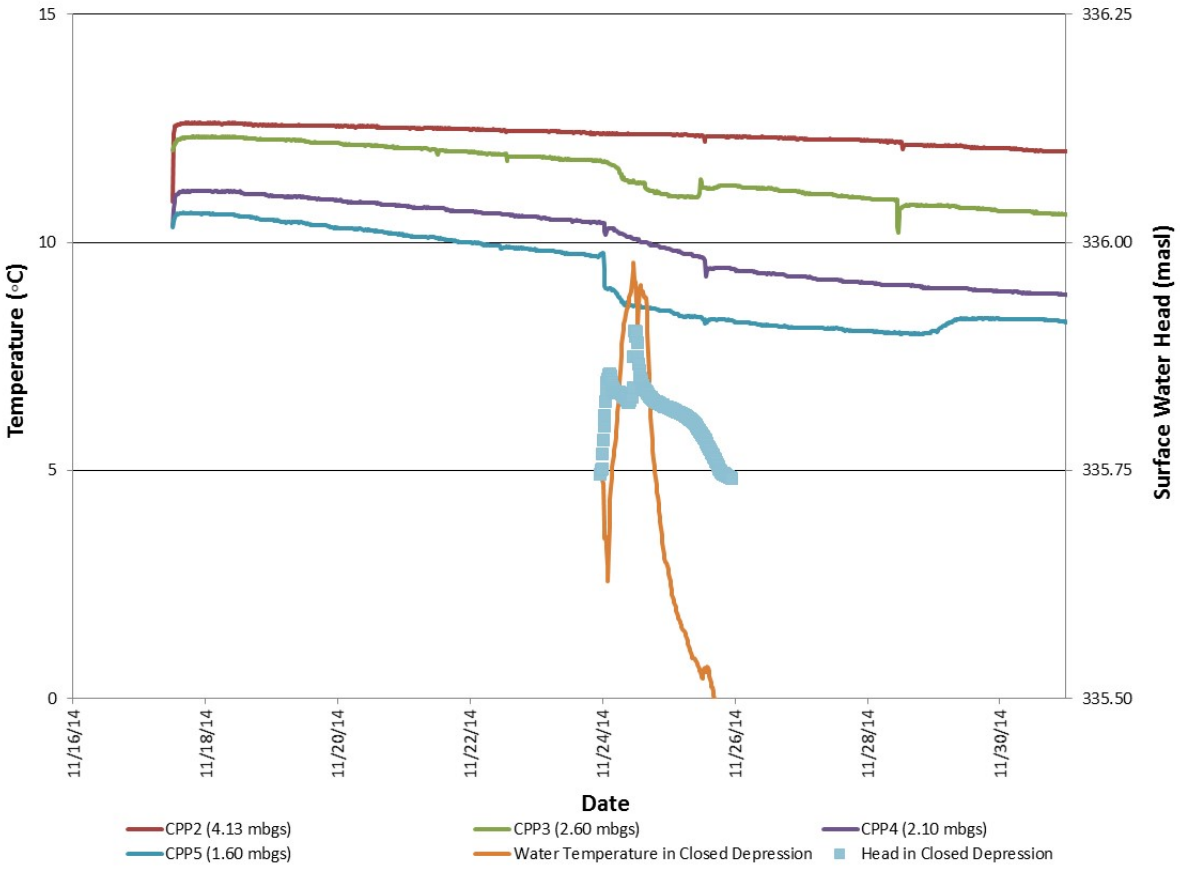

Figure 5.21. Surface water and groundwater temperature and surface water depth observed within and beneath the closed depression instrument cluster during the November Event.

The November Event occurred while equipment installations were taking place. As a result, the soil temperature arrays were not available during the event, as they were in the Spring Event.

5.2.3.2. Temperature Data during the Spring Event

During the course of the winter of 2014 – 2015, temperatures at the Site were below freezing for 117 days, including a record low temperature for the area. The freezing

temperatures caused the development of a frost zone in the shallow soils over the course of the winter, as observed by arrays of temperature probes at the background instrument cluster and beneath the closed depression. This section describes, first the surface water temperature, air temperature, the soil temperature data observed at the background location, and then beneath the closed depression during the course of the Spring Melt Event.

During the Spring Melt Event, air temperatures began to exceed zero regularly on March 7, 2015. Snow melt and rainfall caused the formation of surface water, as described in Section 5.2.1.2. Air temperature and surface water temperature observations are summarized in Figure 5.22.

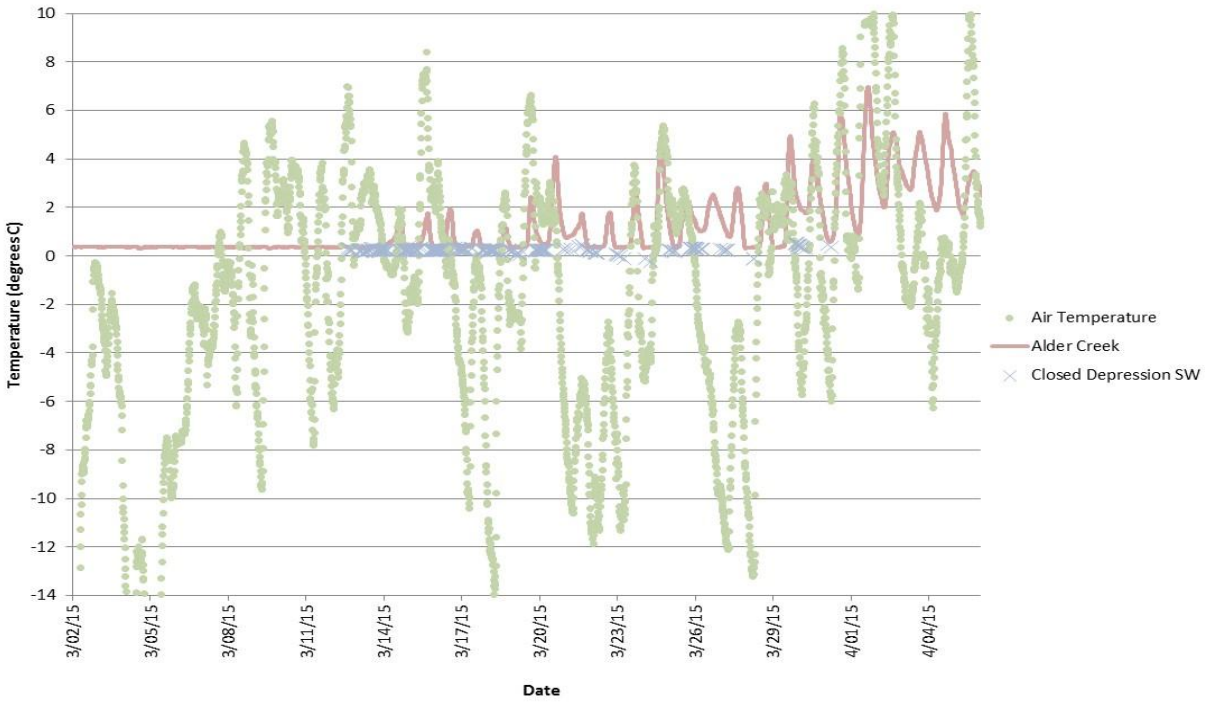

Figure 5.22. Air temperature (observed at the MET Station) and surface water temperature during the Spring Melt Event.

Air temperature during the Spring Melt Event showed diurnal fluctuations. Prior to March 14, Alder Creek was largely ice covered and remained near zero degrees. Following March 14, Alder Creek's temperature varied diurnally. Surface water in the closed depression

remained consistently zero degrees during the Spring Melt Event, likely due to the snow and ice which persisted in the closed depression.

At the background location, the soil temperature profile showed the development of the frost zone throughout the winter months, then the response of the subsurface temperatures to the Spring Melt Event (Figure 5.23).

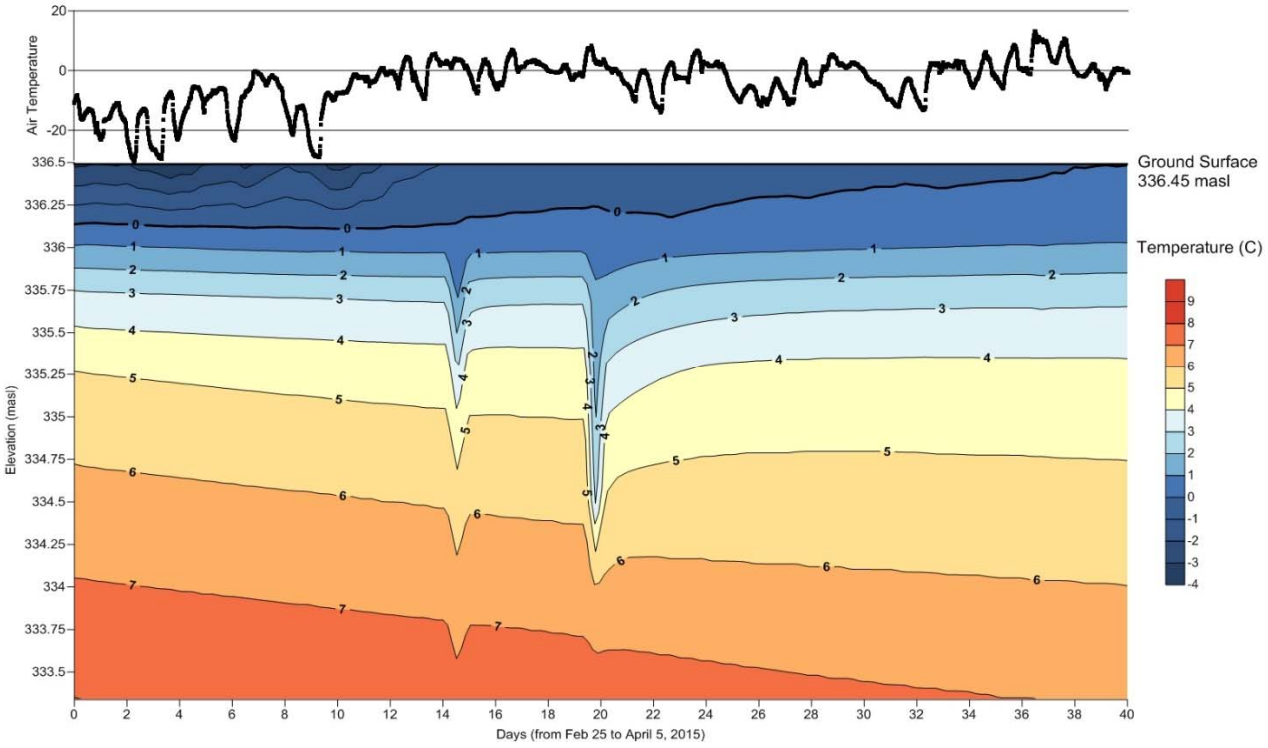

Figure 5.23. Soil temperature and air temperature observed during the Spring Melt at the Background Location between February 25 and April 5, 2015. The 0°C contour line is interpreted to be the base of the frost zone. (Groundwater head was typically observed at a elevation of ~ 333.3 masl.)

At the background location outside of the depression area, the sub-zero air temperatures led to the development of a frost zone starting at the ground surface and propagating downward into the ground. At its peak the frost zone reached a depth of 35 cm, measured at the background

location on March 11, 2015 (Figure 5.23.). Prior to the start of the Spring Melt, which is interpreted to have begun on March 7th, the water table was at ~ 333.3 masl, and the groundwater temperature was ~ 7°C. A slow downward cooling trend is apparent throughout the soil profile. During the Spring Melt Event, two isolated temperature anomalies occurred on the March 11 and March 16, 2015 (day 14 and 19). During these events, the temperatures throughout the soil profile dropped suddenly, then gradually recovered over the following days to pre-event temperatures. Both temperature events resulted in a significant decrease in subsurface temperatures to depths of up to 3 m below ground surface. It is anticipated that these rapid temperature fluctuations may have resulted from the rapid infiltration of cold, melted surface waters that may have briefly accumulated around the thermistor clusters resulting in temporary temperature drops along the vertical profiles. During and following the end of the Spring Melt Event, shallow subsurface temperatures gradually increased in response to seasonal temperature increases and the frost zone thawed on April 3 at the background location (Day 38) (Figure 5.23).

The temperature arrays beneath the closed depression also showed a maximum frost zone depth of 35 cm on March 7) (day 10 on Figure 5.24). Until the tenth day in Figure 5.24., the gradual downward trend in freezing temperatures into the shallow subsurface continued. Prior to the start of the Spring Melt, the water table was at ~ 333.5 masl, and the groundwater temperature was ~ 4°C. On March 12 (day 15), while the frost zone was ~22 cm thick, temperatures throughout most of the soil profile dropped rapidly and then followed a slow cooling trend until approximately March 22 (day 25). This change in subsurface temperatures occurred throughout the soil profile coincident with the increase in groundwater levels (Figure 5.24). The combined drop in soil water temperatures and rapid rise in the groundwater level beneath the depression may indicate the influence of recharging cold surface water. As was observed at the background site, a temporary drop in temperatures throughout much of the soil profile occurred on March 25 (day 28). There was no obvious correlation with changes in the groundwater levels during this brief event and the temperature profiles returned back to the pre-event levels and trends within a day suggesting a potential localized infiltration of cold surface water within the vicinity of the soil temperature cluster. On April 3 (day 37), soil temperatures again showed a rapid and significant decline from the top of the profile to bottom of the array, coincident with a large increase in groundwater level and the coincident disappearance of surface

water from within the closed depression. This combination of observations may again suggest the rapid infiltration of cold surface water from the pond within the depression area.

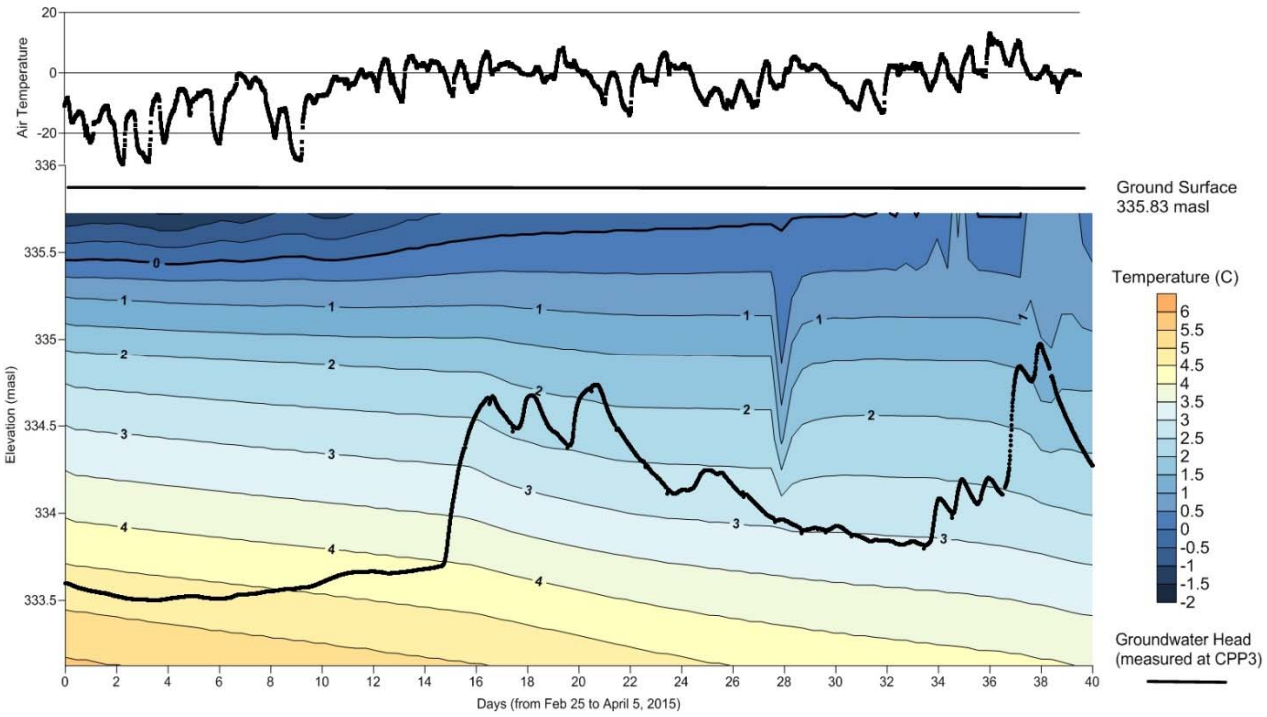

Figure 5.24. Soil temperature, air temperature, and groundwater level beneath the closed depression (well CPP3) observed during the Spring Melt beneath the closed depression. The 0°C contour line is interpreted to be the base of the frost zone.

5.2.4. Soil Moisture Data

Soil moisture observations provide useful insight into recharge and water movement in the unsaturated zone within the subsurface. The neutron probe provided instantaneous vertically dense soil moisture profiles, which were augmented by arrays of TDR probes to collect shallow depth, time dense, observations of soil moisture. Soil moisture observations were made at the

three instrument cluster locations: adjacent to Alder Creek, beneath the closed depression, and at the background location.

5.2.4.1. Soil Moisture Data during the November Event

During the November Event, the combined snow melt and rainfall on November 22nd resulted in an increase in the soil moisture as observed at the three TDR arrays (shown in Figure 5.25 to Figure 5.27) and two neutron access tubes (shown in Figure 5.28. and Figure 5.29.). No surface water was observed in the closed depression during the period. As detailed in Section 4.1., during the November Event, neutron access tubes and TDR arrays were installed adjacent to Alder Creek and in the closed depression. During the November Event, there were no soil moisture equipment was installed at the background location. Soil moisture increased gradually in all three TDR arrays with the trends appearing to be more rapid and irregular in the shallowest probes (15 cmbgs) and progressively smoother with increasing depth. The similar overall temporal trends appear similar at the three TDR arrays. Soil moisture values gradually increased from pre-event levels on November 22. On November 23rd, shortly after the intense rainfall, soil moisture increased rapidly to a its maximum value. The soil water remained at these elevated values for approximately 1 – 2 days and then progressively drained over the remaining monitoring time period. The magnitude of increase in soil water content appeared to be the highest beneath the closed depression (Figure 5.27).

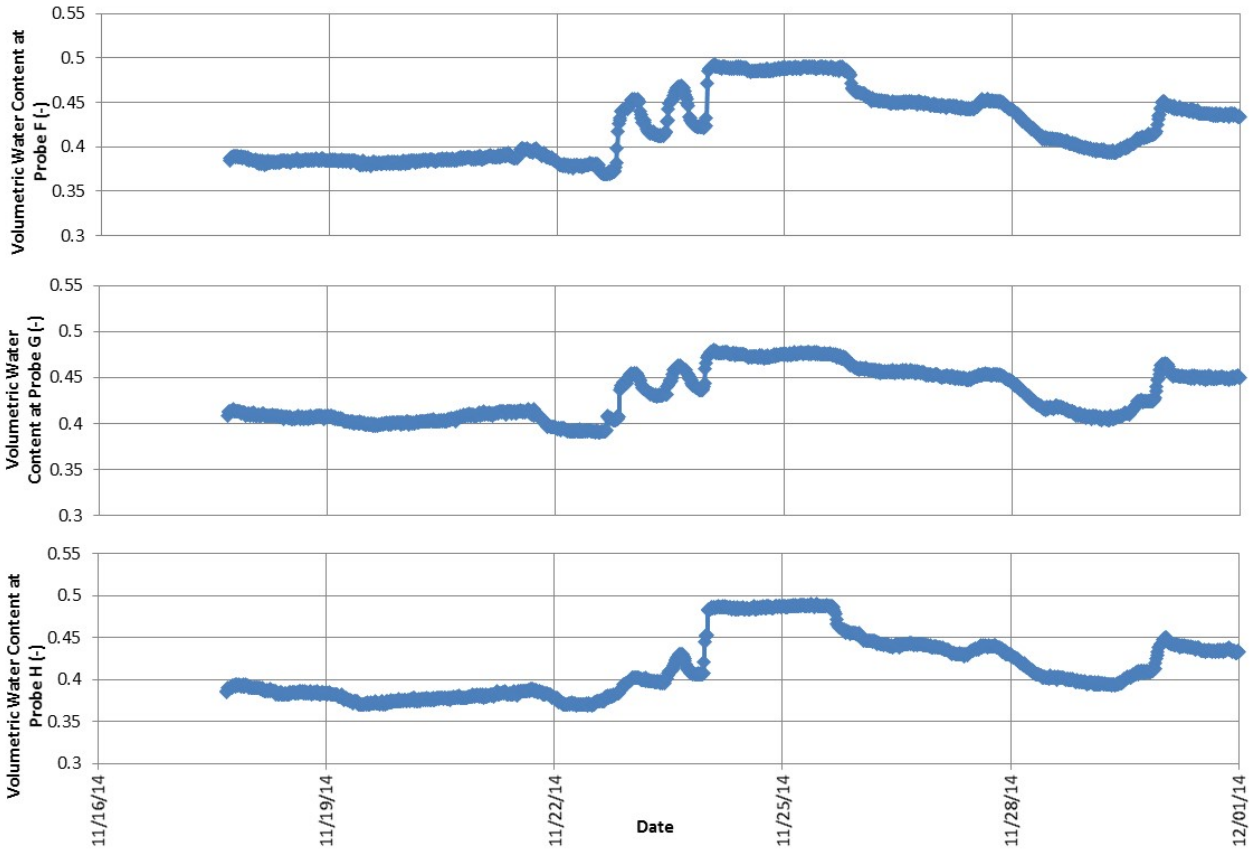

Figure 5.25. Soil moisture observed beneath the closed depression during the November Event using TDR. (Where the centroid of probe F is at a depth of 0.15 mbgs, probe G is at a depth of 0.45 mbgs, and probe H is at a depth of 0.76 mbgs.)

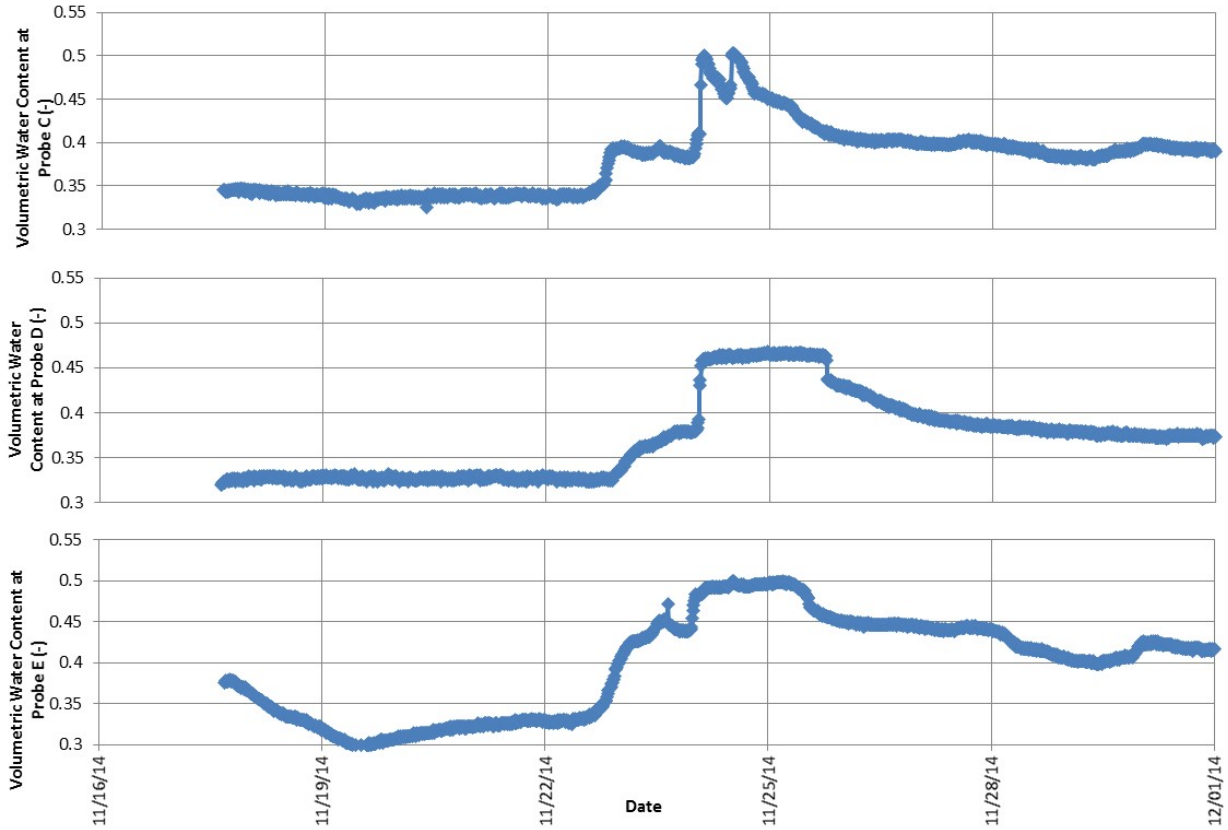

Figure 5.26. Soil moisture observed beneath the edge of the closed depression during the November Event using TDR. (Where the centroid of probe C is at a depth of 0.15 mbgs, probe D is at a depth of 0.46 mbgs, and probe E is at a depth of 1.35 mbgs.)

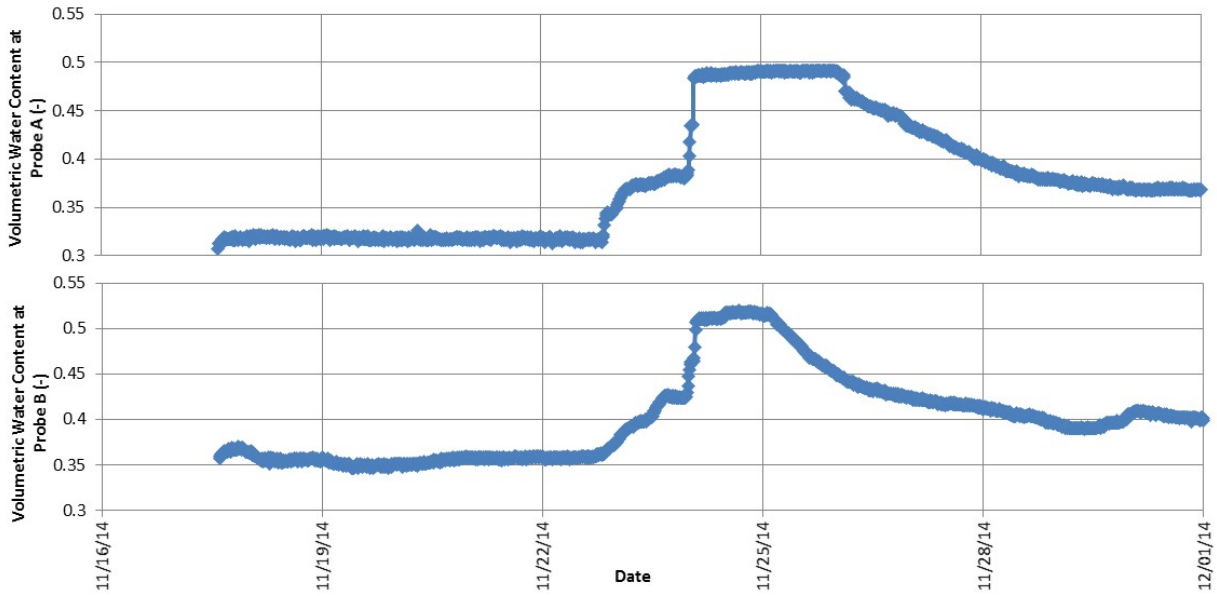

Figure 5.27. Soil moisture observed between Alder Creek and the closed depression during the November Event using TDR. (Where the centroid of probe A is at a depth of 0.15 mbgs and probe B is at a depth of 0.46 mbgs.)

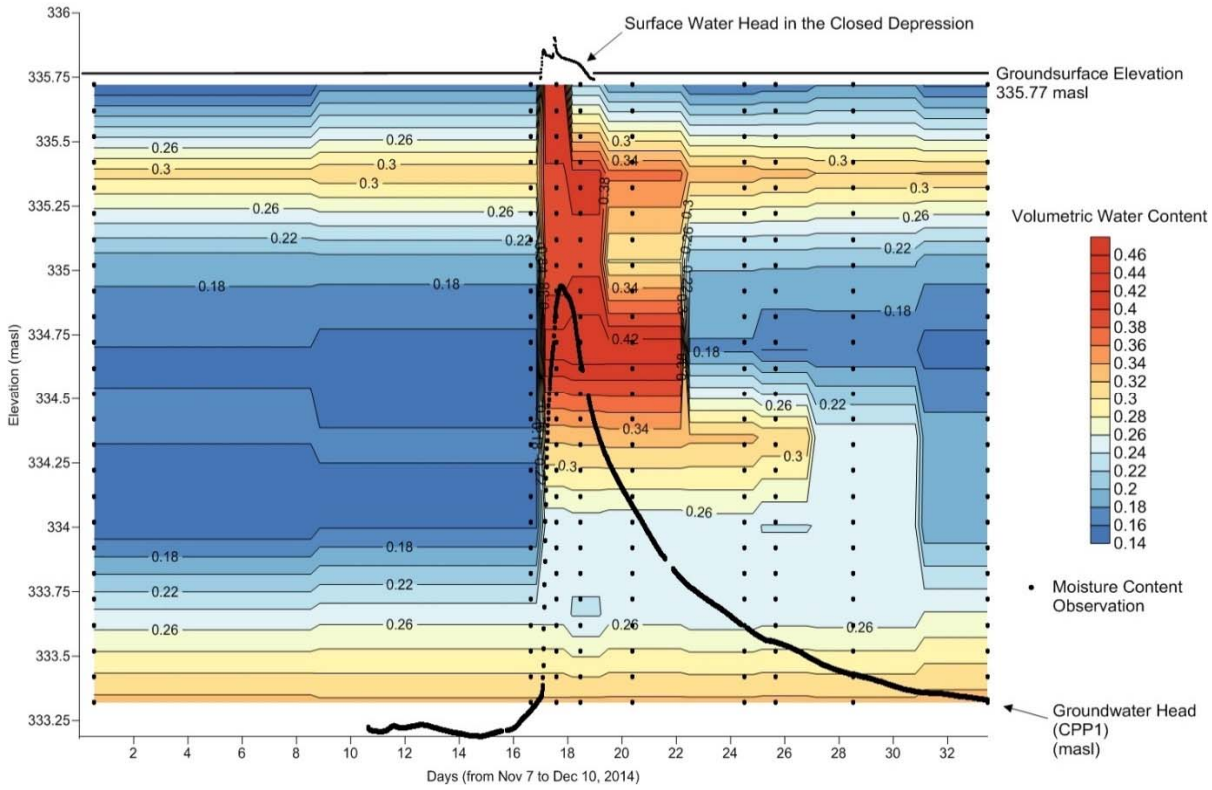

Figure 5.28. Soil moisture (CPAT1) measured with the neutron probe, groundwater hydraulic head (CPP1), and surface water level observed adjacent to Alder Creek during the November Event.

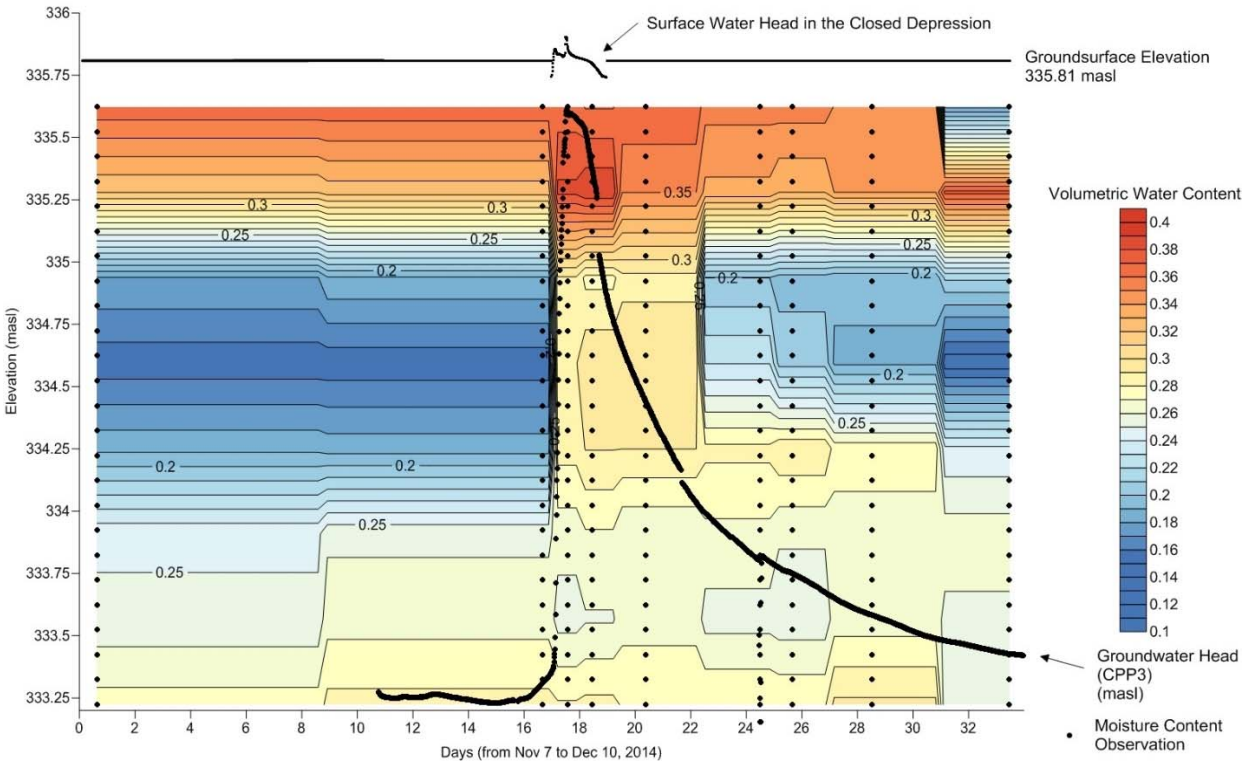

Figure 5.29. Soil moisture (CPAT2) measured with the neutron probe, hydraulic head (CPP3), and surface water level observed beneath the closed depression during the November Event.

During the intense rainfall on November 24th, surface water flowed over the agricultural field and into the closed depression. The observations made using the TDR probes showed that the shallow soil moisture rapidly reached its maximum value (believed to be near field saturation) while surface water was present in the closed depression (Figure 5.25.). During this time period, the closed depression overflowed and surface water flowed over the TDR array installed adjacent to the depression and the TDR array near Alder Creek (Figure 5.26.). Soil water contents approaching full saturation levels appear to have also been reached at this location.

In addition to continuous shallow soil moisture observations, nine vertically dense soil moisture profiles were collected in the two neutron probe tubes, one adjacent to Alder Creek (Figure 5.28.) and one beneath the closed depression (Figure 5.29.). In addition to continuous shallow soil moisture observations made with the TDR probes, nine vertically dense soil

moisture profiles were collected in each of the two neutron probe tubes, one adjacent to Alder Creek (Figure 5.28.) and one beneath the closed depression (Figure 5.29.). The moisture content profile beneath the closed depression and adjacent to Alder Creek showed an initially drained condition with high moisture contents (>25%) in the vicinity of the water table. High moisture content was also initially observed in the top 0.5 m of the profile beneath the closed depression where the fine grained soils are rich in organic material. The moisture profile adjacent to Alder Creek showed higher soil moisture at a depth of 40 cm, which is the base of the silty topsoil layer above a coarse gravel and cobbles unit. This local zone of higher soil water content may be the result of the finer grained near surface soils overlying the well-drained coarser underlying sediment, resulting in a significant contrast in hydraulic conductivity, and perhaps a condition referred to as a capillary barrier effect (as discussed in Section 2.3.1.). A capillary barrier could be taking place at the interface between the fine grained shallow soils and the cobbly streambed, causing soil moisture to accumulate above the interface.

Both moisture content profiles responded rapidly to the ponding of surface water in the closed depression and the rise in Alder Creek's stage, which happened after the start of the meteorological event on day 16. The surface water head and the groundwater head hydrographs, plotted on Figure 5.28 and Figure 5.29 responded immediately following the start of the event (day 16) and the transient soil moisture content profiles closely followed the temporal trends of the groundwater hydrograph. Soil moisture content and groundwater head remained high for the following measurement on day 17. After the precipitation event was over (day 17), both the groundwater head and the soil moisture content gradually declined toward the pre-event condition at both locations. The soil moisture profile illustrated drainage starting at the top of the profile and following the groundwater head decline toward the initial, pre-event water table position. The combined observations suggest significant groundwater recharge occurred throughout the site during this significant snow melt and precipitation event.

5.2.4.2. Soil Moisture Data during the Spring Melt Event

Soil moisture was monitored during the Spring Melt Event to provide a supporting dataset to quantify recharge and to observe recharge dynamics. Soil moisture measurements were collected in the shallow subsurface using three TDR arrays (Figure 5.30. to Figure 5.32., two beneath the closed depression and one adjacent to Alder Creek) and three neutron probe access tubes (Figure 5.33. to Figure 5.35.), one beneath the closed depression, one adjacent to Alder Creek, and one at the background location).

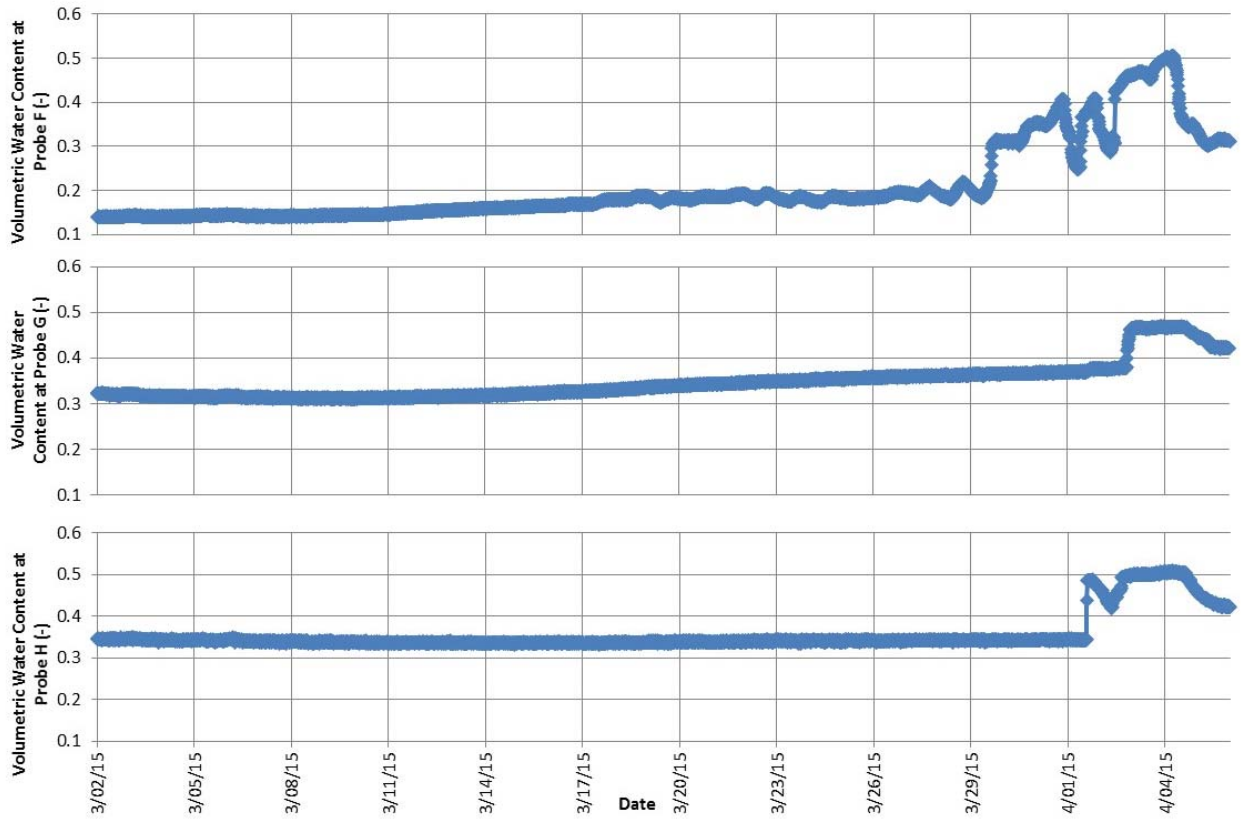

Figure 5.30. Soil moisture beneath the closed depression during the Spring Melt Event using TDR. (Where the centroid of probe F is at a depth of 0.15 mbgs, probe G is at a depth of 0.45 mbgs, and probe H is at a depth of 0.76 mbgs.)

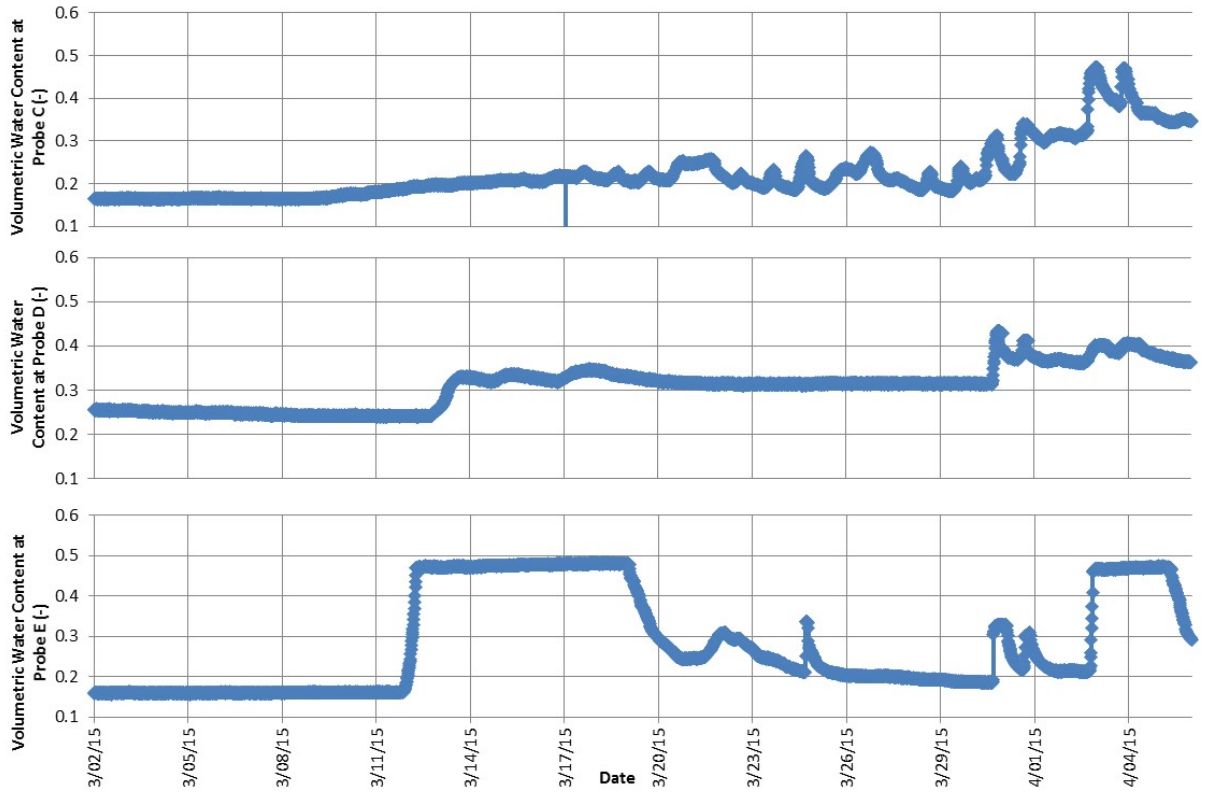

Figure 5.31. Soil moisture beneath the edge of the closed depression during the Spring Melt Event using TDR. (Where the centroid of probe C is at a depth of 0.15 mbgs, probe D is at a depth of 0.46 mbgs, and probe E is at a depth of 1.35 mbgs.)

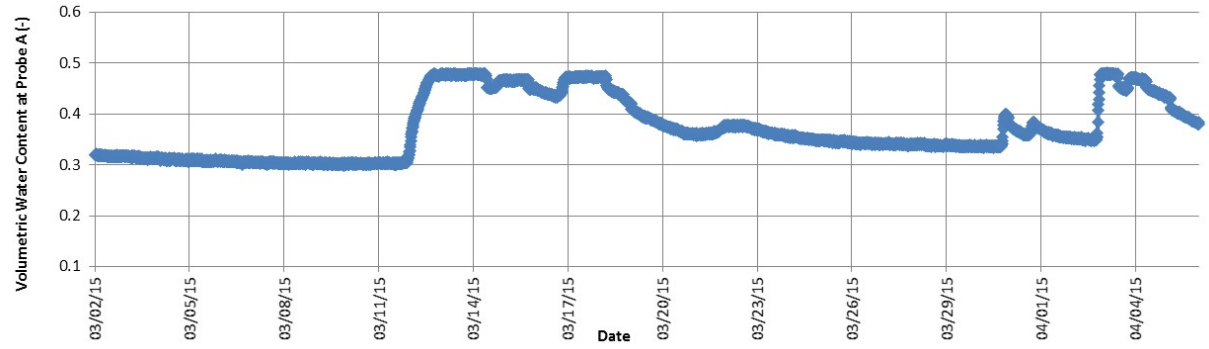

Figure 5.32. Soil moisture adjacent to Alder Creek during the Spring Melt Event using TDR. (Where the centroid of probe A is at a depth of 0.15 mbgs.)

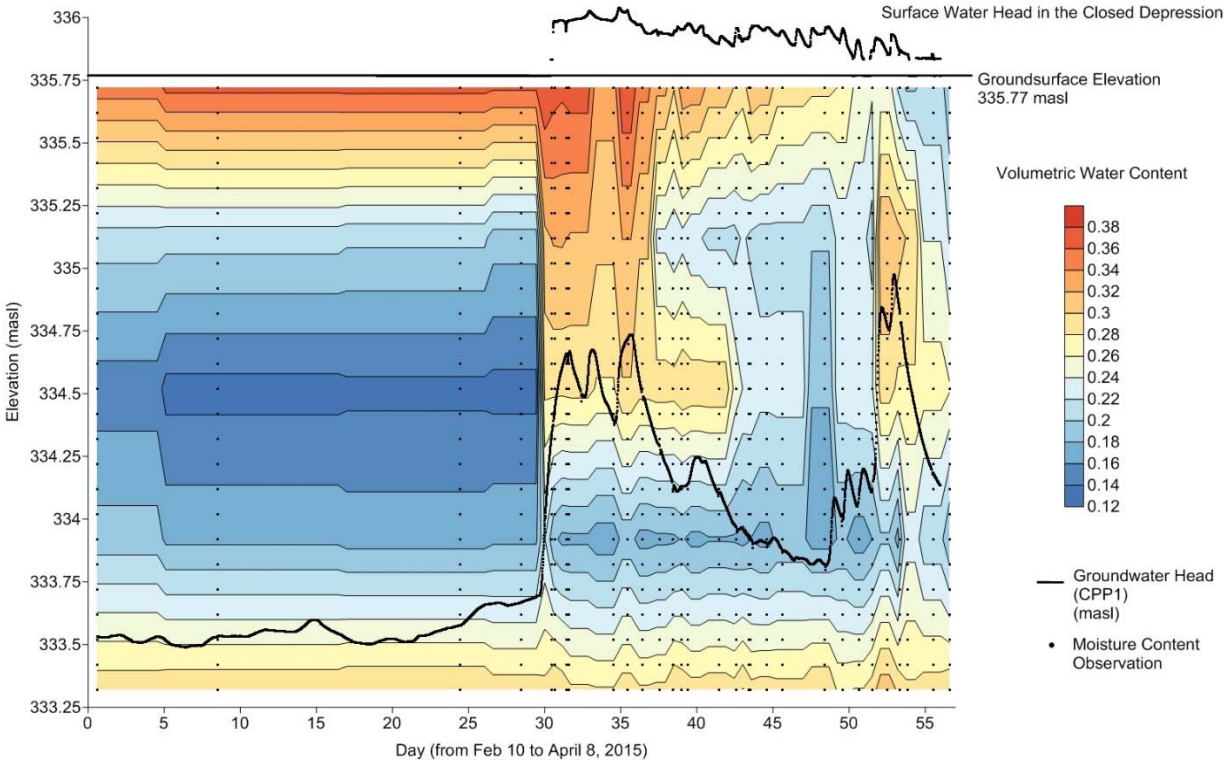

Figure 5.33. Soil moisture (CPAT1) measured with the neutron probe and groundwater head (CPP1) observed adjacent to Alder Creek and surface water level observed in the closed depression during the Spring Melt Event.

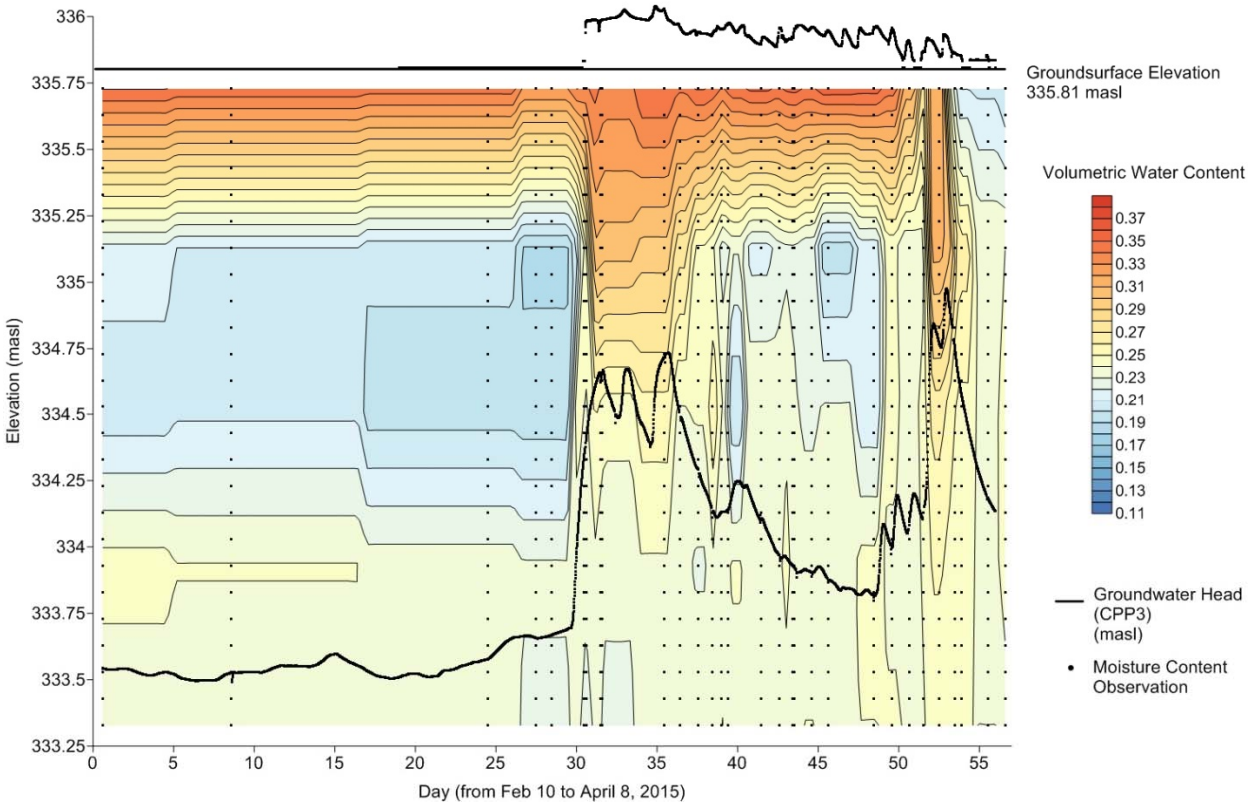

Figure 5.34. Soil moisture (CPAT2) measured with the neutron probe, groundwater head (CPP3), and surface water level observed beneath the closed depression during the Spring Melt Event.

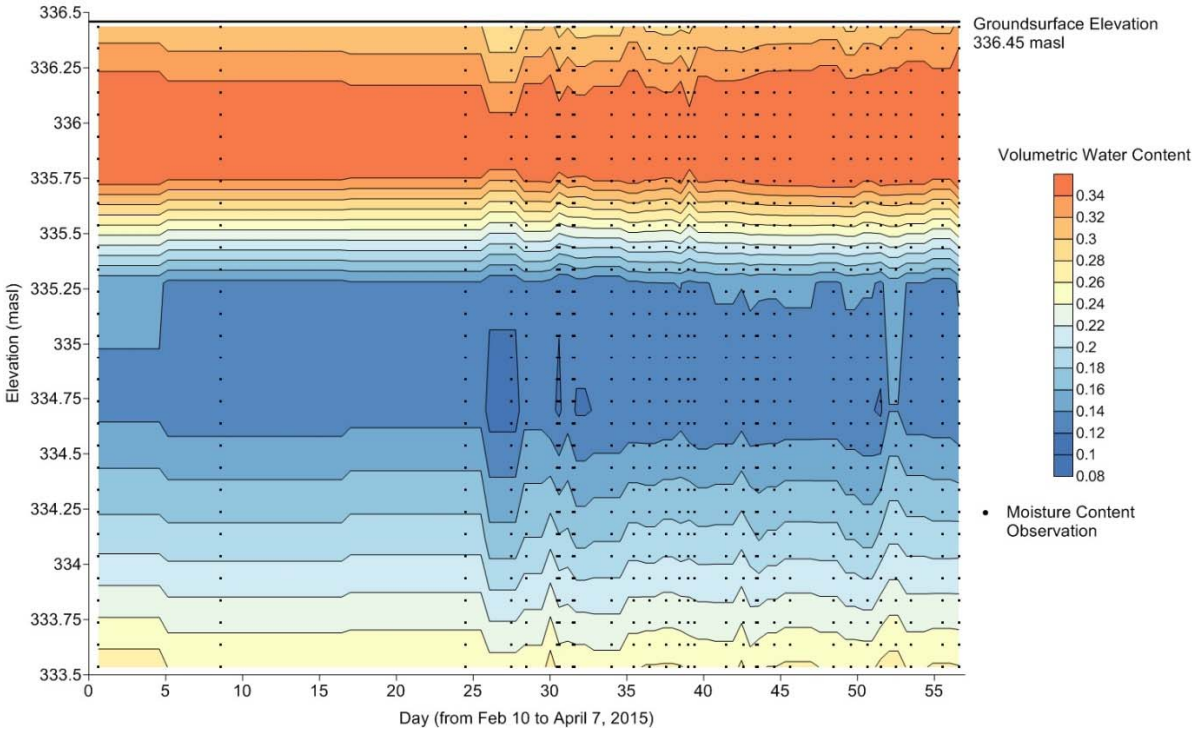

Figure 5.35. Soil moisture (CPAT3) measured with the neutron probe observed at the Background Location during the Spring Melt Event. (The water table near this location, at CPP8, is typically around 333.1 masl.)

The data sets collected with both the TDR (Figure 5.30. to Figure 5.32.) and neutron probe (Figure 5.33. to Figure 5.35.) will be discussed together, by instrument cluster, in this section to illustrate the nature of the transient soil moisture content distributions observed during the Spring Melt Event. Prior to the start of the event, the soil moisture content profiles observed with the neutron probe at each of the monitoring locations were temporally stable with a zone of higher soil moisture in the shallow organic topsoil and decreasing through the middle part of the monitored section. In the lower monitoring depths, closer to the water table, the soil moisture again rose through the capillary fringe (Figure 5.33., Figure 5.34., and Figure 5.35.). This was the case up until March 11 (day 30), when the Spring Melt Event started. The observations of soil moisture during and after the event will be discussed by instrument cluster in this section.

At the instrument cluster in the closed depression, soil moisture was observed by a neutron access tube (Figure 5.34.) and two TDR arrays, one located near the center of the closed depression, and one at the edge of the closed depression nearest to Alder Creek (Figure 5.30. and Figure 5.31.). Between March 11 and March 30, only the deepest of the six TDR probes beneath the closed depression reached saturated soil moisture content (Figure 5.31.). Shallower probes showed gradual small magnitude soil moisture changes during this time period. The observations of the neutron probe are consistent with the TDR probes. Soil moisture below 0.8 mbgs increased at the same time the groundwater head increased between day 30 (March 12) and day 36 (March 18). Between day 37 (March 19) and day 52 (April 3), when Alder Creek receded to a more typical level, soil moisture contents declined steadily throughout the profile following the lowering of the water table level. On day 53 (April 4), when the frost zone thawed (Figure 5.24.), the surface water disappeared in the closed depression and the groundwater levels and moisture content beneath the depression and adjacent Alder Creek increased throughout the profile (Figure 5.34.). Also on day 53, the highest soil moisture contents were observed beneath the closed depression, between 0.3 mbgs and 1.5 mbgs and the arrays of TDR probes beneath and adjacent to the closed depression (Figure 5.30. and Figure 5.31.). Following the sudden increase in soil moisture on day 53 (April 4), soil moisture declined following the trend of the groundwater head observed beneath the depression.

Soil moisture was monitored at the Alder Creek instrument cluster using a TDR probe (Figure 5.32.) and a neutron access tube (Figure 5.33.). The shallow TDR probe adjacent to Alder Creek (Figure 5.32.) showed a rise in soil moisture on March 13 (day 30) near the start of the hydrologic event, which was marked by Alder Creek's stage rising, and the formation of surface water in the closed depression (Figure 5.16.). Shortly after that, groundwater levels observed adjacent to Alder Creek also rose sharply. Notably, the three peak hydrograph observed in data collected from Alder Creek and the adjacent piezometers between April 11th and 23rd, (Figure 5.16.) is also observed in the shallow TDR adjacent to Alder Creek (Figure 5.32.). The neutron access tube observations were consistent with the TDR observations (Figure 5.33.). At the start of the Spring Melt Event, March 11 (day 30), the soil moisture increased rapidly to a near saturated condition throughout the profile, in response to Alder Creek exceeding its banks, similar to the groundwater hydrographs (Figure 5.17.). Then, after Alder Creek level fell to be within its banks, soil moisture began to recede, with saturated soil moisture levels

following the receding ground water head closely. A second sudden rise in soil moisture occurred at the same time (day 53, April 4) the surface water disappeared in the closed depression, groundwater head rose beneath the closed depression, and adjacent to Alder Creek. The second increase in soil moisture content was also observed by the TDR probe adjacent to Alder Creek (Figure 5.32.). After the second rise in soil moisture, soil moisture gradually declined along the same trend as the groundwater head, in the same way as it did after the first rise in soil moisture.

Soil moisture observations were also made at the background location using a neutron probe (Figure 5.35.). The profile at that location shows an initial condition with higher water content at the bottom of the array, slightly above the water table, lower soil moisture between 2.7 mbgs and 0.9 mbgs, increasing soil moisture between 0.9 mbgs and the ground surface, similar to the initial condition at the other two instrument clusters. During and after the Spring Melt Event, there was little change observed throughout the soil moisture profile and groundwater levels did not reach the bottom of the neutron access tube during the event.

5.2.5. Water Quality Results

Water samples were collected during the hydrologic events from the surface water sources and shallow groundwater monitoring wells. Samples were analyzed for ten ions and two isotopes typically found in surface water and groundwater. The water quality data are contained in Appendix G. Water quality samples were not collected to at great enough frequency to show significant trends in response to the hydrologic events.

In addition to ionic and isotopic samples collected during the Spring Melt Event, microbial samples were collected from the surface water features including Alder Creek, the pond within the closed depression and the storm water retention pond near the site. (as summarized in Table 5.7.). The objective of the microbial analysis was to determine if the surface water sources contained microbial indicator species, which would suggest a potential source of contamination to nearby receptors such as a public supply well.

Table 5.7. Surface Water Microbial Indicator Species

			Location		
Parameter	Units	PWQO (2)	Stormwater Pond	Alder Creek	SW in closed depression
Fecal coliform	CFU/100mL	100 (4)	8	190	350
Heterotrophic plate count	CFU/mL	NA (3)	570	1900	>5700
Total Coliforms	CFU/100mL	1000 (4)	260	NDOGT (1)	17000
Escherichia coli	CFU/100mL	100	8	NDOGT (1)	300

Notes:
(1) NDOGT- No data due to overgrowth for target organisms
(2) Provincial water quality objective (PWQO). (MOECC, 2018)
(3) NA = Not Applicable
(4) Historical MOECC objective per PWQO 1994
(5) Grey shading indicates an exceedance of PWQO
(6) Samples collected on April 2, 2015.

Microbial sample results exceeded PWQO in Alder Creek and in the closed depression. Samples from the storm water pond were below the PWQO standards.

The results of these microbial water quality samples show the risk posed by transient surface water features to surficial aquifers. If rapid recharge of water containing microbial indicator species occurred through a closed topographic feature (as discussed in Section 5.3.) near a supply well during a hydrologic event, then it would pose a risk of microbial contamination, reaching the public supply well. This risk will be considered within the context of the transient infiltration processes observed during the Spring Melt Event.

5.2.6. Soil Sample Observations

During the Spring Melt Event, it was unclear why groundwater head was receding while surface water persisted in the closed depression for 20 days (Figure 5.17.). To observe if the shallow soil structure was affecting infiltration, a soil sample of the top 15 cm of soil in the

closed depression was retrieved on April 1, 2015, immediately adjacent to the surface water in the south-east corner of the closed depression. In that sample ice was observed in the pore spaces from a depth of 3 cm to 4 cm below ground surface. This observation may suggest that infiltration was limited by the presence of ice in the shallow soil's pore spaces.

5.3. Conceptual Model of Event Based Groundwater Recharge Dynamics

During the hydrologic events, an extensive dataset (presented in Section 5.2.) was collected and can be used to construct a conceptual model of the mechanisms by which recharge took place. This section develops conceptual models for how recharge occurred during the November Event and during the Spring Melt Event, makes observations of recharge dynamics, and contrasts recharge mechanisms between the two events. These interpretations will be used to support the quantification of recharge attributed to specific sources and mechanisms in Section 5.3.

5.3.1. Conceptual Model of the November Event Groundwater Recharge Dynamics

The combined field data sets collected during the November Event and presented earlier were considered in proposing a conceptual model of groundwater recharge dynamics, which includes several different recharge mechanisms. Firstly, based on the field data, increased water levels in Alder Creek caused flow from the creek to temporarily infiltrate at a high rate into the adjacent subsurface through the stream bank and channel sediments. The second significant recharge mechanism was DFR, which occurred when surface waters filled the closed depression, infiltrated, and reached the water table. It is also possible that diffuse areal recharge (DAR) may have occurred at the ground surface where precipitation and snow melt infiltrated directly. Recharge from Alder Creek and DFR recharge occurred rapidly and simultaneously in response to the start of the November Event. Both sources simultaneously contributed similar rates of

recharge. Recharge was caused by primarily vertical flow, with limited horizontal groundwater flow during the recharge event. The combined interpretation of the groundwater and surface water head, temperature, moisture content, and water quality data sets are considered below to support the proposed conceptual model of recharge.

Because recharge from both the closed depression and Alder Creek caused groundwater levels to increase in close proximity to one another (~8 m apart), it is not obvious which surface water feature caused recharge and subsequent groundwater level increases. The datasets in Section 5.2. were examined to support the delineation of recharge sources. First, groundwater head and gradients were examined (Section 5.2.2.1.). To understand the source of groundwater head increases, the horizontal gradient between two shallow piezometers is plotted in Figure 5.14. The typical gradient before the November Event causes flow from Alder Creek toward the closed depression. This can be attributed to surface water losses from Alder Creek when Alder Creek is at typical stages. At the start of the hydrologic event, horizontal hydraulic head gradient declines sharply to near zero and remained near zero while there was surface water in the closed depression and Alder Creek's stage remained high (Figure 5.13.). Groundwater recharge was caused by dominantly vertical flow (~ 10 times greater vertical gradient than the magnitude of the horizontal gradient, as shown by Figure 5.12. and Figure 5.14.).

The groundwater and surface water head data also show that the peak of the hydrograph nearly reaches the ground surface as observed by piezometer CPP3 (2.6 mbgs shown in Figure 5.11.). Each piezometer screened higher shows a peak head closer to the ground surface than that of the piezometers screened below it. The saturated state of the soil profile was also observed by soil moisture content data (Figure 5.25., Figure 5.26., and Figure 5.29.), so it is a reasonable inference that the soils below the closed depression reached saturation while surface water filled the closed depression.

Temperature data (Figure 5.20. and Figure 5.21.) also supports that recharge took place due to vertical flow from surface water in the closed depression and in Alder Creek. At the start of the November Event, Alder Creek's stage rose and surface water formed in the closed depression. The temperature of Alder Creek and the surface water in the closed depression were colder than the shallow groundwater temperatures. Shallow groundwater temperatures beneath the closed depression and adjacent to Alder Creek dropped sharply. This is consistent with cold

water infiltrating from surface water sources. However, the data does not help to delineate the source of groundwater recharge, as both Alder Creek and surface water in the closed depression were colder than groundwater temperatures.

The moisture content observed during the November Event supports the interpretation of which mechanisms caused groundwater recharge. Shallow soil moisture observations made using TDR (Figure 5.25. to Figure 5.27.) showed that soil moisture rose during snow melt then increased sharply to a near saturated value when surface water formed in the closed depression. Vertical moisture content profiles (Figure 5.28. and Figure 5.29.) observed adjacent to Alder Creek and beneath the closed depression showed that at both locations soil moisture contents reached saturation at the peak surface water levels. The saturated moisture content beneath the closed depression persisted while surface water was present. This supports the conclusions that DFR occurred beneath the closed depression. Because the closed depression overflowed over the ground surface (and along the ground surface at the neutron access tube adjacent to Alder Creek), the soil moisture observations adjacent to Alder Creek reflect direct infiltration at the ground surface instead of Alder Creek losses. This means that soil moisture observations are consistent with recharge occurring as a result of vertical flow from Alder Creek, however it could also be the result of direct infiltration at the ground surface.

Based on these supporting data sets, in particular the head gradient data and soil moisture content data, recharge occurred rapidly and simultaneously from the closed depression and Alder Creek. By comparison to the dynamic observations of DFR and Alder Creek losses, DAR was not observed in the datasets, as it was overwhelmed by the more dynamic recharge sources.

5.3.2. Conceptual Model of the Spring Melt Event Groundwater Recharge Dynamics

During the Spring Melt Event, the presence of freezing and thawing conditions in the shallow subsurface and the presence of multiple recharge sources affected the distribution of recharge in space and time. Surface water collected in the closed depression and Alder Creek's stage increased simultaneously in response to the hydrologic event (as described in Section

5.2.1.2.) (Figure 5.16.). Similar to the November Event, multiple possible sources of recharge could contribute simultaneously to an increase in observed groundwater levels. This considerably complicates the isolation of an individual source of recharge. To quantify recharge during this event all available data sets were analyzed in an effort to separate the influences of Alder Creek and DFR.

The conceptual model of the recharge dynamics is that groundwater recharge occurred sequentially, first being dominated by Alder Creek exceeding its banks during the Spring Melt (between March 11th and 20th), and subsequently by surface water infiltrating beneath the closed depression (between March 30th and April 3rd). This is likely because the Spring Melt took place when the (approximately 35cm thick) frost zone beneath the closed depression restricted infiltration of the ponded surface water and delayed infiltration until the frost had sufficiently thawed, at which point the surface water in the depression could freely infiltrate. It is anticipated that no frost existed beneath Alder Creek. During the Spring Melt surface water formed on March 12, 2015, and flowed into the closed depression (Figure 5.17.). The temperature of the surface water was approximately 0˚C and it infiltrated into the sub-zero frost zone environment at ground surface. It is hypothesized that after infiltrating into the shallow frost zone, the water re-froze. This formed a continuous, near impervious ice layer beneath the closed depression, effectively sealing the closed depression. The presence of ice in the shallow soil pore spaces was observed in a shallow soil core. It is further anticipated that until the frost zone thawed, little or no DFR took place. Between March 12, and March 30, 2015, recharge was dominated by losses from Alder Creek, which caused groundwater mounds and subsequent lateral flow. Between March 30 and April 2, 2015, a series of small rises in the groundwater levels and fluctuations in soil moisture were observed, which would be consistent with transient bursts of infiltration as the ice layer began to thaw. On April 2nd and 3rd, surface water collected within the closed depression infiltrated rapidly and groundwater levels beneath the closed depression increased, at which point it is believed that the near surface frost zone had thawed sufficiently to permit the surface water to infiltrate. The presence of Alder Creek contributions to recharge and DFR overwhelmed any DAR which took place at the site during the Spring Melt Event.

The conceptual model of sequential recharge described above is supported by field evidence collected during the course of the Spring Melt Event:

1. Observation of ice saturated pore spaces in the frost zone,
2. Surface water head, groundwater head, and gradients,
3. Continuous observation of volumetric water content in the shallow subsurface; and
4. Soil temperature in the vadose zone and shallow groundwater.

The first data supporting the interpretation of the recharge processes is the soil sample retrieved during the Spring Melt Event described in Section 5.2.6. It showed that ice had filled the pore spaces inside the frost zone. It is theorized that the formation of ice within the shallow frost zone occurred throughout the closed depression and formed a nearly impervious ice layer.

The second set of observations supporting a sequential model of infiltration during the Spring Melt Event are the heads and gradients in the surface water and groundwater. At the start of the Spring Melt Event, Alder Creek rose rapidly to its highest stage during the study. Alder Creek remained at a high stage, above its banks, for 44 hours (Figure 5.16.). Alder Creek then receded within its banks, followed by three smaller peaks in the stream hydrograph. At the crests of the Alder Creek hydrograph the shallow groundwater piezometer hydrographs closely mimicked the Alder Creek hydrograph with four peaks. Between March 30th and April 4th, 2015, shallow groundwater levels underwent a series of water level increases, while Alder Creek's stage remained constant. At the same time as the later rises in groundwater levels, between March 30th and April 4th, the surface water in the depression decreased and disappeared. This similarity between the surface water and groundwater hydrographs supports attributing early recharge to Alder Creek overtopping its banks and later recharge to the closed depression.

The horizontal and vertical gradients in hydraulic head also support this interpretation, as shown in Figure 5.18. and Figure 5.19. The horizontal gradient between Alder Creek (observed at CPP7) and the closed depression (observed at CPP5) showed that during typical conditions, prior to the Spring Melt, the groundwater heads close to Alder Creek are higher than those under the closed depression. This is likely caused by some continuous recharge from Alder Creek during low flow conditions. During the first portion of the Spring Melt Event, the horizontal gradient between the creek and the surface depression increases, causing greater groundwater flow from beneath Alder Creek toward the closed depression. This is believed to have been caused by the significant increase in water levels within Alder Creek temporarily resulting in

enhanced infiltration. During the final stage of the Spring Melt Event, the horizontal gradient reversed causing flow from the closed depression toward Alder Creek. This suggests that recharge first took place at Alder Creek, then at the closed depression.

The third dataset supporting the proposed conceptual model of recharge dynamics is the transient soil moisture content information collected with TDR (Figure 5.30. and Figure 5.31.) and neutron probe (Figure 5.33. and Figure 5.34.). During the first series of recharge events (between March 11th and 21st) no increase in moisture content was observed beneath the closed depression despite rises in groundwater level beneath the closed depression and surface water forming in the closed depression above the TDR array. If surface water infiltration had been taking place beneath the closed depression, an increase in moisture content would have been observed (Figure 5.33.). During the series of small groundwater head increases between March 30th and April 2nd, soil moisture varied spatially and temporally, as shown in Figure 5.30. and Figure 5.31., which is consistent with transient bursts of infiltration through the ice layer. Between April 2nd and 3rd, shallow soil moisture increased to the maximum observed values beneath the closed depression (Figure 5.30.) and increased throughout the soil profile beneath the closed depression (Figure 5.34.). These observations are also consistent with the interpretation that the ice layer thawed and surface water in the closed depression infiltrated rapidly.

The final dataset supporting the conceptual model of transient recharge is the soil temperature as observed by the soil thermistor arrays (Section 5.2.3.2.). The soil temperature observed beneath the closed depression is shown in Figure 5.24. On March 11th (day 9) when the Spring Melt Event began, Alder Creek rose rapidly, exceeded its banks contributing to groundwater recharge and shallow groundwater levels. At its peak Alder Creek water level did not reach the closed depression, so the recharge sources can be considered separate. Changes in the temperature profile are initially detected during the first groundwater level crest on March 19th (day 17), when subsurface temperatures below the water table were observed (Figure 5.24.). There is no evidence of temperature change between the top of the water table and ground surface. If cold surface water had infiltrated from the closed depression, temperatures within the vadose zone would have been affected as well as the temperatures below the water table. This suggests that cooler water arriving below the closed depression was the result of horizontal flow rather than vertical. The next notable feature shown in the temperature data occurred on March

30th, 2015, (day 28) when there is a sudden decrease in subsurface temperature ground surface to 1.6 mbgs (Figure 5.24.). This coincided with a small rise in shallow groundwater head below the closed depression. The temperature throughout the profile then recovered to near identical values shortly after the initial cooling. This can be explained by a small amount of water caused by a transient macropore flow in the frost zone allowing some surface water to infiltrate rapidly before it refroze. The last notable feature in the temperature data occurs during the end of the event (day 38) during the final rises in groundwater levels. During this time temperatures throughout the soil profile were affected (Figure 5.24.). Above 0.5 mbgs temperatures increased from near zero to 0.5°C as the ice layer thawed and surface water warmed the shallow subsurface. Below 0.5 mbgs, soil temperatures decreased as near zero surface water flowed down through the soil sequence.

In addition to the development of a conceptual model of recharge, this study provides the opportunity to observe recharge dynamics and contrast the unfrozen soils in November Event and the frozen surficial soils during the Spring Melt Event. Observed recharge dynamics included: the formation of an ice layer, the formation of transient macropore structures, and resealing the structures in the ice layer.

The differences between the two events showed that it is possible for an ice layer to form in the frost zone and the affects of the ice layer on recharge. The ice layer prevented recharge from taking place immediately when surface water flowed into the closed depression, because the ice layer was continuous and impervious. The integrity of the layer of ice in the subsurface is demonstrated by the data on Figure 5.17. The figure shows that surface water persisted for 18 days in the depression without infiltrating and making a significant contribution to recharge. If the layer of ice had formed discontinuously or had leaked significantly, the surface water would have infiltrated and contributed rapidly to groundwater recharge as it did in the November Event. The delay caused the recharge sources in the Spring Melt Event to be sequential, while the recharge sources during the November Event contributed simultaneously.

Although the bulk behavior of the ice layer appeared to be nearly impervious during the Spring Melt Event, some discontinuous leaks in the ice layer were observed during the test. The transient flow through the ice was observed several times. The TDR array located below the closed depression (Figure 5.30.) showed significant variations in moisture content immediately

before the ice layer thawed. These variations indicate that some water was flowing in the vadose zone below the ice layer, in sufficient quantity to increase groundwater levels (Figure 5.17.). On other occasions, the data are best explained by small burst which affects localized soil temperature or soil moisture. On March 25 (day 28) in Figure 5.24., a temporary temperature cold temperature spike was observed below the closed depression, as the result of a transient leak in the ice layer (as detailed in Section 5.2.4.2.). Daniel and Staricka (2000) observed a number of mechanisms by which frost could lead to the presence of transient macropore features in the soil, including the partial collapse of frozen soil structures (as discussed in Section 2.3.2.). In both cases the movement of water in the vadose zone was transient, which is believed to be the result of the temporary formation and subsequent refreezing of leaks in the ice layer. These occurrences would be difficult to observe or predict without detailed site scale observation. These observations provide a site scale demonstration of the complexity of recharge dynamics in cold climates.

Based on the conceptual model of recharge dynamics, both Alder Creek and DFR occurring through the closed depression are potential pathways for microbes or other contaminants in the surface water to enter the shallow aquifer system. To demonstrate this risk, water quality samples were collected during the Spring Melt and analyzed for microbial indicator species (as described in Section 5.2.5.). Both Alder Creek and the transient surface water in the closed depression were contained significant quantities of microbial indicator species, and potentially dangerous microbes. When rapid recharge of potentially microbe laden transient surface water occurs through a closed depression near the supply well during the hydrologic events, it creates a potential transient water quality threat to the nearby public supply well. Similarly, recharge from Alder Creek to the shallow aquifer creates a potential contamination threat that is exacerbated during high flow conditions.

5.4. Recharge Quantification

Recharge is a challenging process to quantify as discussed in Section 2.4. A number of approaches have been developed in scientific literature to quantify recharge based on varying types of data and the dynamics of the recharge process taking place.

One of the most common methods described in the scientific literature is the Water Table Fluctuation Method (WTF) (Section 2.4.1.) (Healy and Cook, 2002). The data that are required to utilize this method (noted below) were collected at the field site during the two hydrologic event periods that were monitored as part of the current research. The WTF method assumes that:

(1) the aquifer is unconfined,

(2) a rise in groundwater head levels is associated with a recharge event and single recharge mechanism,

(3) recharge is near instantaneous (and that groundwater flow is limited),

(4) the selected wells are representative of head in the aquifer of interest, and

(5) specific yield is constant.

In this application, the aquifer is considered to be unconfined (Assumption 1). In general, increases in groundwater head in response to hydrologic events observed in this study are rapid, so it is reasonable to assume that recharge is the result of rapid vertical flow, resulting in a fluctuation in the water table elevation. However, any horizontal flow resulting from recharge occurring beneath a focused feature such as the depression or stream would reduce the observed water table fluctuation, and therefore the quantity of recharge estimated by the WTF method, and would reduce the validity of Assumptions 2 and 3 noted above. Also, Assumption 2 of the WTF method requires that no other recharge phenomenon or source affects the groundwater head in the aquifer during a given event. If the groundwater head data were interpreted without using supporting datasets, a rise in the water table could incorrectly be assessed as resulting from local recharge (illustrated in an example below). These assumptions are evaluated in more detail for the November Event in Section 5.4.1. and for the Spring Melt Event in Section 5.4.2. Assumption 3, that the recharge takes place nearly instantly, neglects time lag of flow through the vadose zone and does not account for a continuous inflow of

recharge water even after the water table rise reaches its maximum magnitude. As such the total recharge magnitude could be underestimated. Assumption 4 requires that piezometers are representative of aquifer of interest, which is satisfied by designing the instruments in clusters so that observations can be attributed to a specified aquifer and recharge phenomena. Finally, the WTF method assumes that the specific yield of the aquifer is constant with respect to time (i.e. there is no entrapped air) (Assumption 5). This assumption is difficult to evaluate and is rarely completely correct, since air is entrapped in different amounts each time the water level fluctuates and therefore specific yield varies. If specific yield is simply assumed to be equal to a typical literature value, there would be significant uncertainty in evaluating Assumption 5. However, for purposes of this study, the method for evaluating this assumption and quantifying specific yield is discussed in Section 4.1.9. and Section 5.1.3.2, to reduce uncertainty in estimating specific yield. After considering the difficulty in evaluating the assumptions and the limitations of the data collection methods, the WTF method provides a useful estimate of recharge, although it's accuracy is limited. In some cases, the accuracy of the WTF is reduced by limited data to confirm assumptions and potential violations of those assumptions, such as horizontal flow, unsaturated transient flow, and sources of head variations in the aquifer other than the identified recharge source.

A case that illustrates the difficulty of evaluating Assumption (2) is the application of the WTF method at the background location (CPP6) during the November Event, as shown in Figure 5.36.

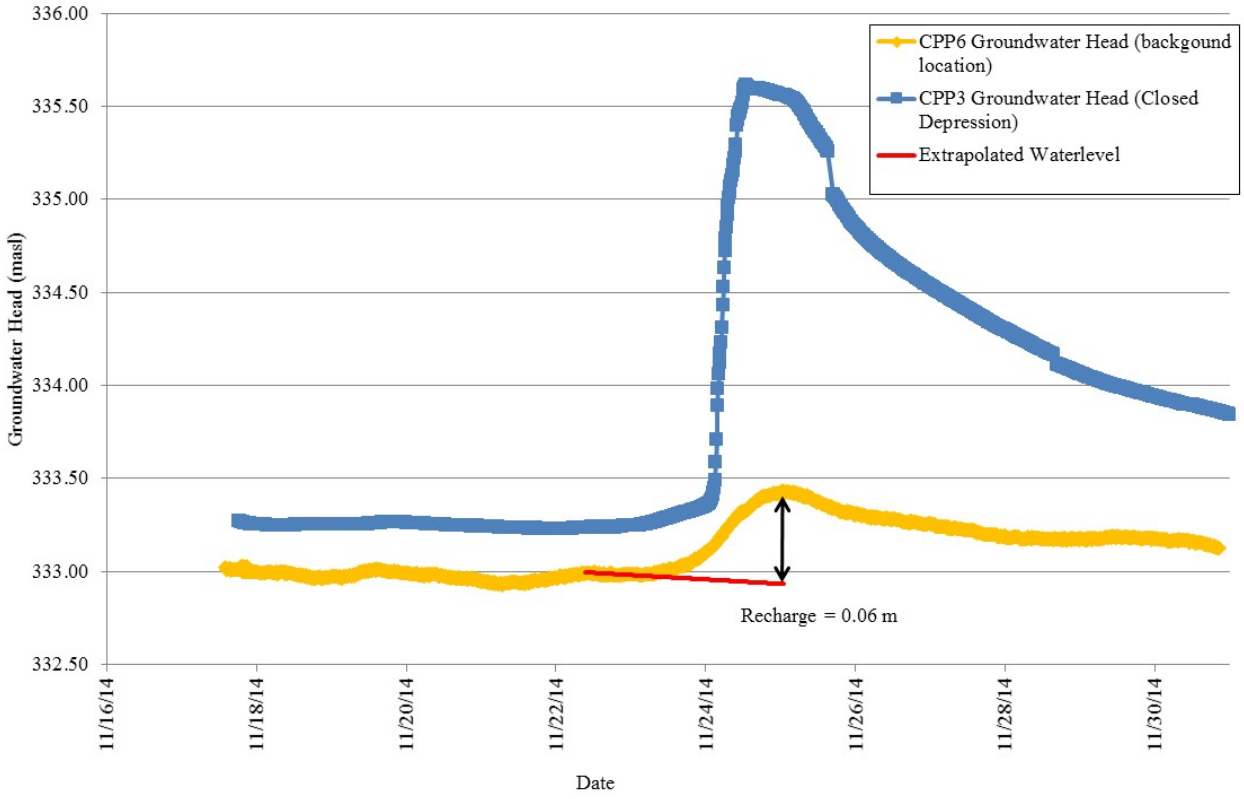

Figure 5.36. WTF method during the November Event at the background location (CPP6).

This would lead to an estimate of 0.06 m of recharge. The amount of cumulative effective precipitation released by the November Event amounted to approximately 0.1 m, so it was clear that the initial recharge estimate at the background location (CPP6) is unlikely to arrive that rapidly beneath 3 m of unsaturated soil and in such a large fraction of CEP. Instead it is likely that the peak in the hydrograph is explained by the rapid increase of groundwater head observed in the closed depression, which subsequently increases in groundwater head to travel laterally through the aquifer and caused the first peak in the hydrograph. A similar mistake is possible whenever the WTF method is applied without the use of supporting data sets to evaluate the validity of assumption 2.

During each event at which recharge was quantified supported by complimentary datasets to identify the source of the recharge and gain insight into the mechanisms by which it occurred

(assumption 2). The use of complimentary data sets to develop a conceptual model of recharge dynamics are developed in Section 5.3.

5.4.1. Recharge Quantification during the November Event

Based on the conceptual model of the recharge processes (explained in Section 5.3.1.), the WTF method can be applied to the hydrographs of piezometers adjacent to Alder Creek and beneath the closed depression to roughly quantify recharge during the November Event. The groundwater hydrograph shows a sharp rise suitable for analysis using the WTF method (Assumption 3 in Section 5.4.). For the conceptual model of recharge developed to represent the November Event (developed in Section 5.3.1.) two observations were made that affect the application of the WTF method to the November Event: the simultaneous recharge from Alder Creek and DFR, and the saturated soil profile beneath the closed depression.

As discussed in Section 5.3.1., groundwater flow was primarily vertical, as shown by strong downward gradients and small horizontal gradients (Figure 5.12. and Figure 5.14.). Although the lack of a horizontal gradient indicates that little horizontal flow took place between the closed depression and Alder Creek, the two simultaneous sources of increased head in the aquifer cause two superimposed head increases in the aquifer. The effect of the two sources increasing head in an aquifer is similar to the effect of two simultaneously operating injection wells, as described by Fetter (2001). In that case, the head increases in the aquifer are cumulative; the effect of each source is additive at each point in the aquifer (Fetter, 2001). The WTF method can be applied simultaneously to both the closed depression and Alder Creek to estimate groundwater recharge, because the recharge is occurring due to vertical groundwater flow (Assumption 2 and 3) and the other assumptions of the WTF method are satisfied, however this will be an overestimate due to the superimposed head increases.

Secondly, the WTF method does not account for a saturated soil profile, which occurred during the peak of the November Event, as shown by groundwater head and soil moisture measurements. As discussed in Section 5.3.1., the soils beneath the closed depression reached

saturation during the November Event. To account for the additional recharge after the soil profile had reached saturation, an additional term for saturated vertical groundwater flow is added to the WTF method calculation of recharge (Fetter, 2001). While vertical flow does take place throughout the November Event, the vertical flow contribution to recharge is dominated by flow at saturated conditions, and the unsaturated vertical flow component is considered to be negligible. This simplification is justified by the short duration of water level rise (while unsaturated vertical flow could take place) and the lower unsaturated hydraulic conductivity of the soils. Saturated conditions persisted for the majority of the recharge event and vertical flow to the aquifer can be estimated using the saturated hydraulic conductivity (Section 5.1.3.1.5.) and the gradient observed between the surface water and a piezometer near the typical water table depth (CPP3).

The WTF method modified to include a saturated vertical flow term is applied in Figure 5.37. resulting in an estimated 0.27 m of DFR through the closed depression during the 72-hour event. The complimentary datasets suggest that the soil profile adjacent to Alder Creek did not reach saturation for an extended period, so no modification to the WTF method to include a saturated Darcy flux is required. Figure 5.38. shows the application of the WTF method to the groundwater hydrograph adjacent to Alder Creek. The resulting estimated recharge based on the WTF method is 0.31 m. These are overestimates of groundwater recharge due to the superposition of head increases in the aquifer caused by simultaneous recharge from multiple sources.

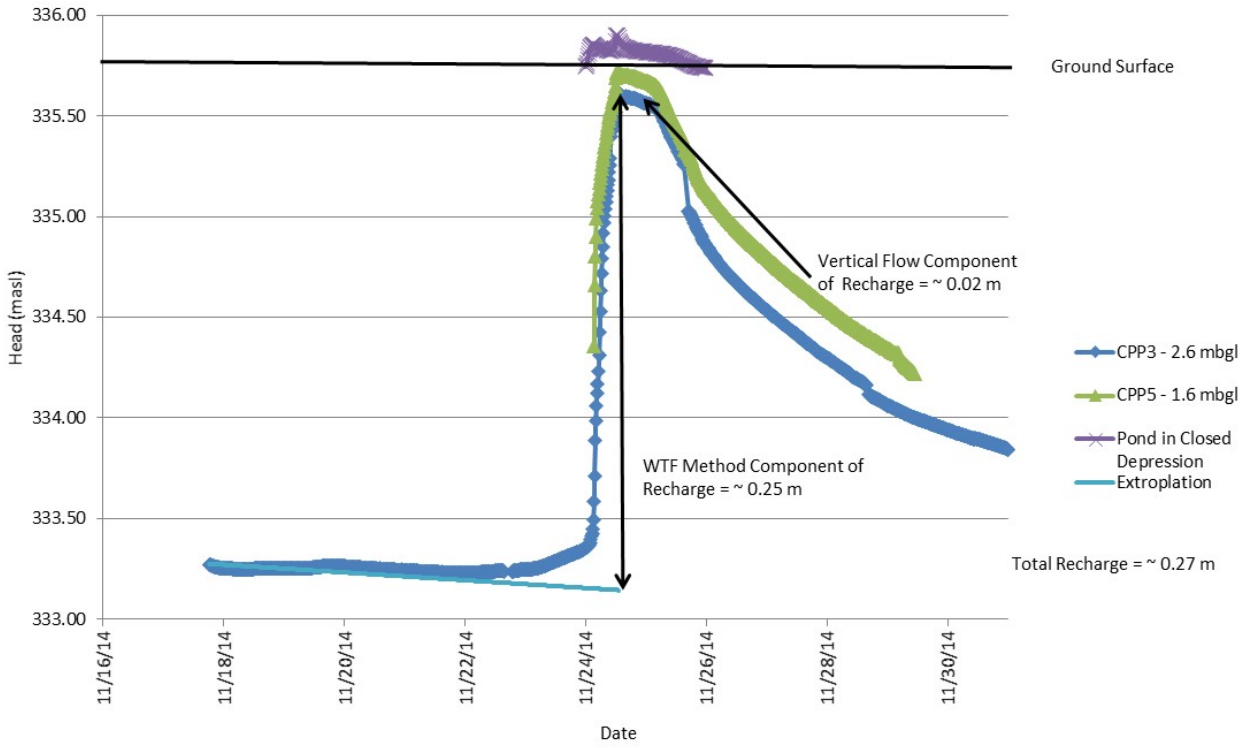

Figure 5.37. WTF method analysis applied to beneath the closed depression (CPP3) during the November Event. (Note: recharge is overestimated by the WTF method in this case, due to multiple simultaneous recharge sources.)

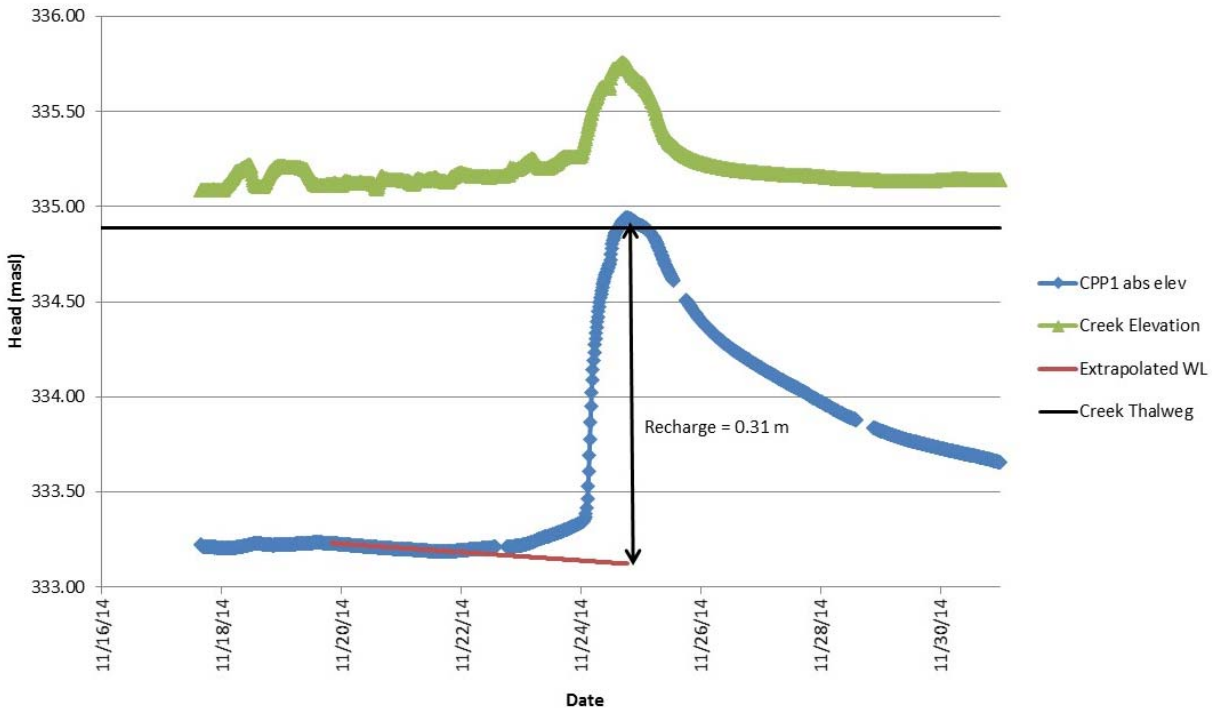

Figure 5.38. WTF method analysis applied adjacent to Alder Creek (CPP1) during the November Event. (Note: recharge is overestimated by the WTF method in this case, due to multiple simultaneous recharge sources.)

5.4.2. Recharge Quantification during the Spring Melt Event

Based on the conceptual model of recharge dynamics during the Spring Melt Event (Section 5.3.2.), recharge occurred sequentially from Alder Creek (from March 11th to March 22nd) then from the closed depression (March 30th to April 4th). Based on this interpretation, the WTF method can be applied to shallow piezometers near Alder Creek to quantify from March 11th to March 22nd, and applied to shallow piezometers beneath the closed depression from March 30th to April 4th. The WTF method is applied to shallow piezometers adjacent to Alder Creek and beneath the closed depression, in Figure 5.39. and Figure 5.40, respectively.

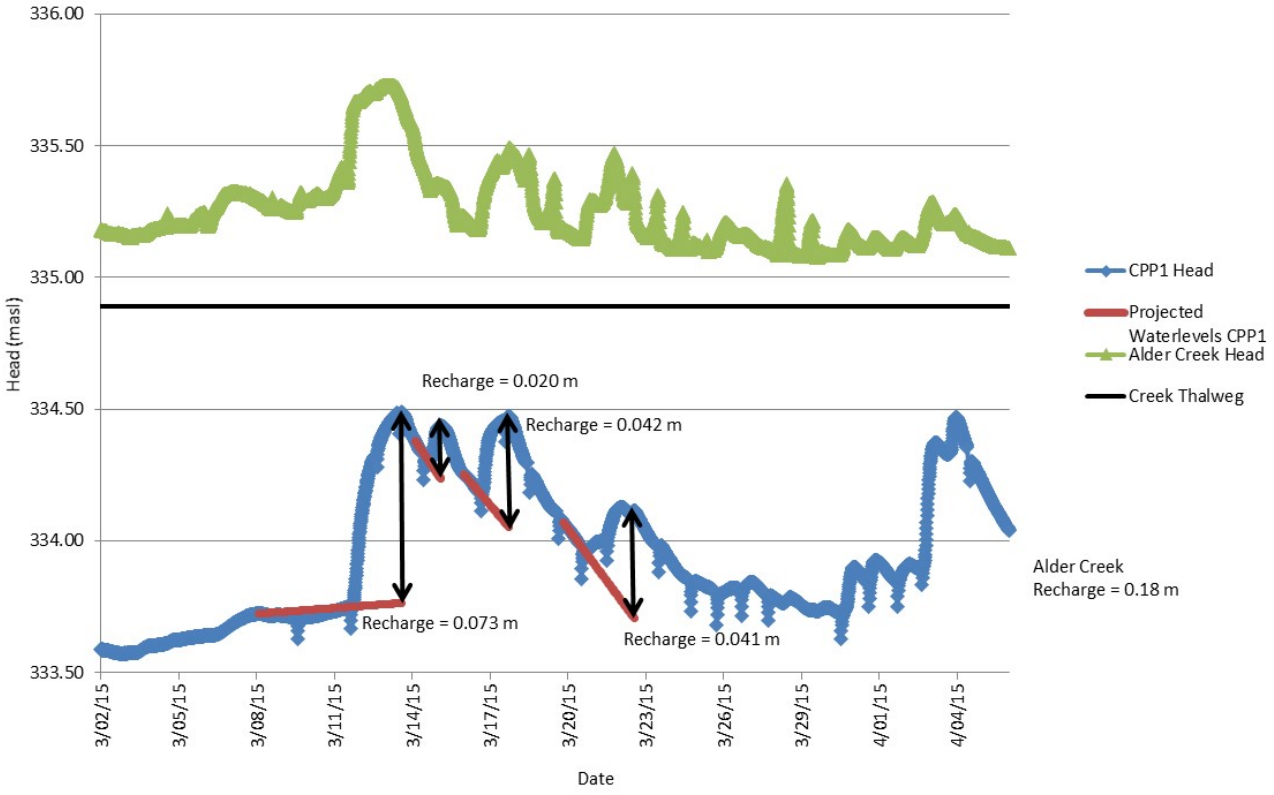

Figure 5.39. WTF method analysis applied to CPP1 (adjacent to Alder Creek) during the Spring Melt Event.

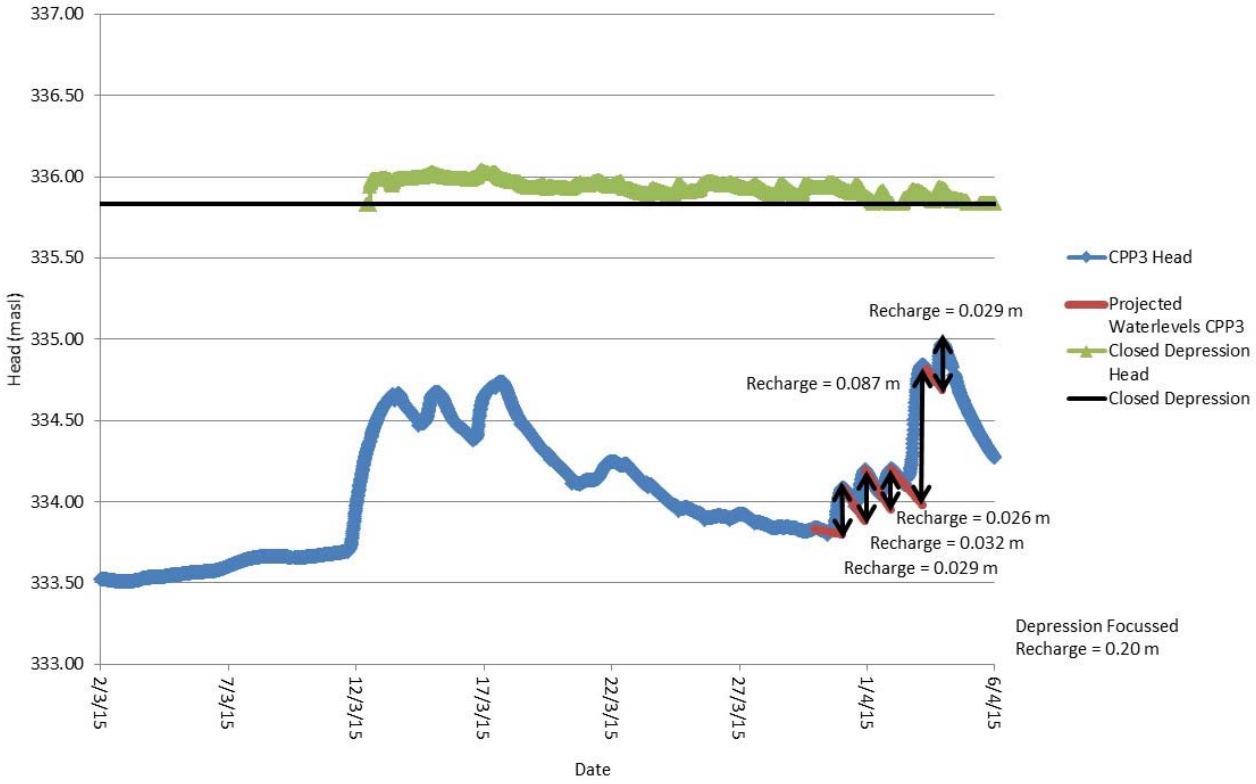

Figure 5.40. WTF method applied to CPP3 (below the closed depression) during the Spring Melt Event.

The results of the WTF method applied to CPP1 near Alder Creek showed that approximately 0.18 m of recharge was contributed by Alder Creek to the shallow aquifer (Figure 5.39.). Similarly, Figure 5.40. shows that approximately 0.20 m of recharge was contributed by the closed depression to the shallow aquifer. Over the duration of the recharge events the recharge occurred in nine distinct peaks.

5.4.3. Recharge Observation Summary

This study observed recharge during two events to quantify the magnitude of the contributions of sources of recharge. The recharge events and the quantification of the recharge sources are summarized in Table 5.8.

Table 5.8. Summary of Recharge Observations

Event	Duration (days)	CEP[1] (m)	Alder Creek Recharge (m)	Closed Depression Recharge (m)
November Event	1.8	~0.08	0.27[2]	0.31[2]
Spring Melt Event	35	~0.11	0.18	0.20

Notes:
(1) CEP is Cumulative Effective Precipitation defined as the sum of rainfall and snow melt.
(2) Recharge is overestimated by the WTF method in this case, due to multiple simultaneous recharge sources.

The events offer an opportunity to compare the effects of seasonality, event duration, and recharge mechanisms between a late fall and a spring event. A detailed discussion of the effects of seasonality can be found in Section 5.3. The duration differed significantly between the two events. The Spring Melt Event took place over 35 days, while the November Event occurred in only 1.8 days. Unlike the November Event, the Spring Melt Event occurred in 9 distinct groundwater hydrograph peaks (while the November Event occurred in a single peak). Despite slightly more CEP available during the Spring Melt Event, the Spring Melt Event showed somewhat less Alder Creek contributions to recharge and less DFR than the November Event because of the different recharge dynamics.

Although Alder Creek is a much larger feature, and therefore could potentially contribute a much larger volume than the closed depression, it is noteworthy that the closed depression caused a similar amount of one dimensional recharge to Alder Creek. Although the area of the

closed depression is relatively small (approximately 100 m^2), the closed depression is caused by a small topographic feature, which is common throughout the watershed. The cumulative effect of the features may be significant in a hummocky watershed.

The recharge observed in this chapter occurred rapidly and in significant quantity from a transient surface water feature in a closed depression adjacent to a public supply well. Further the observation of microbial indicator species in the closed depression (as discussed in Section 5.2.5.) demonstrates a potential pathway for microbial contamination of the aquifer and subsequent contamination of the public supply well.

6. Conclusions

This study observed and quantified recharge from a transient surface water feature in a closed depression in hummocky terrain and a losing stream at various stages. The hypotheses of this study are: that transient surface water features in closed depressions can contribute to rapid recharge, and that seasonal dynamics affect the mechanisms and timing of recharge.

To address the first hypothesis: an area where transient surface water frequently forms was instrumented with adequate detail to reliably quantify recharge. In order to observe the seasonal dynamics of recharge, a late fall rain and melt event (when recharge occurred through unfrozen soils), and a spring melt event (when there was a frost zone) were observed during the study period.

The rain and snow melt event in November, called the November Event, showed that in the absence of frost, intense rainfall caused rapid snow melt (combined ~80 mm of water), and overland flow into closed depressions. During the 1.8 day event, depression focused recharge occurred rapidly, contributed to overall recharge, and immediately posed a risk to shallow groundwater supplies. Under unfrozen conditions the site scale observations showed that recharge from Alder Creek and the closed depression occurred simultaneously and rapidly, based on the observations of hydraulic head, soil moisture, and temperature. Due to the effect of the two simultaneous sources of recharge, the groundwater head increases are superimposed on each

other and cause the WTF method to potentially overestimate the recharge during this event. The magnitude of recharge estimated adjacent to Alder Creek and beneath the closed depression, was 0.27 m and 0.31 m, respectively.

The second recharge event included in the scope of the study is the Spring Melt Event in 2015. Similar to the November Event, rainfall and snow melt contributed to the precipitation available at the ground surface, in this case ~110 mm of precipitation, and surface water formed and flowed into the closed depression. The Spring Melt occurred over 35 days and caused recharge to take place beneath the closed depression and Alder Creek. Similar to the November Event, recharge occurred rapidly through the unfrozen soils around Alder Creek. 0.18 m of recharge were observed adjacent to Alder Creek. By contrast to the November Event, near zero-degree water infiltrated into the 35 cm thick frost zone and froze forming a near impervious ice layer. This layer persisted and delayed DFR for 20 days after the start of the Spring Melt Event; effectively causing recharge source to occur in sequence. When the ice layer thawed, the surface water infiltrated, and contributed 0.20 m of recharge. In addition to the effect of delaying recharge, the study provided opportunity to observe recharge dynamics. While DFR did not occur in large enough amounts during the first period of the Spring Melt Event to increase groundwater levels beneath the closed depression, some short-term fluctuations in soil temperature and soil moisture show that short term bursts of water occurred through the ice layer, then the bursts resealed as ice reformed in the pore spaces.

The observations made during this study have implications for watershed scale recharge calculations and shallow groundwater supply vulnerability. The significant amount of recharge which took place in a small closed depression (~100 m^2) within a small catchment (~12 acres), indicates that in a hummocky watershed, depression focused recharge may be a significant source at a watershed scale. The study also has clear implications for groundwater vulnerability. The presence of a public supply well 40 m from the closed depression screened in the shallow aquifer, the observation of rapid recharge in the closed depression, and presence of microbial indicator species in the surface water, show a clear source and pathway for microbial contamination of the supply well.

6.1. Recommendations

Based on the data collected, observations made, and the limitations of methods the following recommendations should be considered for further study:

- A complete evaluation of the risk of pathogens to the public supply well from the transient surface water and DFR feature should be undertaken. This could be approached by detailed numerical modelling or performing a pumping test during a hydrological event. A numerical model could be parameterized using the data collected in this study and the pump test performed by Hillier (2014). The model could be used to simulate a hydrologic event, such as a spring melt event, while the supply well was being pumped to simulate the threat posed by the event. Alternatively, a field study could operate the supply well during a hydrologic event and observe pathogens in the water supply and shallow groundwater flow paths to observe the contamination of the shallow and the transport mechanism. A conservative solute tracer would be helpful in this field study in tracking the flow path of water infiltrating in the closed depression. This case study may show the need for groundwater vulnerability evaluations to consider transient surface water features.
- To improve recharge quantification, and therefore the clarity of the implications of this research, a three dimensional, variably saturated, groundwater flow and temperature transport model could be constructed to provide more rigorous and accurate estimate of recharge. Notably to simulate the Spring Melt Event the model will need to accommodate the variable permeability of the shallow soil layer which became saturated with ice.
- To build on the understanding of seasonal and annual variations in recharge quantity and rate, the Site should be monitored for additional years, with detailed observations around recharge events. This would provide useful insight into the variability of recharge distribution and quantity, and therefore quantity and quality of water contributed to the shallow aquifer.

- Additional detail in the monitoring network and additional years of monitoring would also provide greater insight into recharge mechanisms, specifically, the formation of the ice layer, how Alder Creek contributes to groundwater recharge, and the interaction of simultaneous recharge source. This would serve to clarify whether the formation of an impervious ice layer, described in Sections 5.3.2., is a near annual occurrence or if it is an uncommon event. Perhaps with additional observations of the ice layer its formation and thawing could be predicted based on temperature, precipitation, and solar radiation. To better characterize the dynamics of a losing stream at high stage, observations could be improved using additional arrays of vertically nested piezometers adjacent to Alder Creek. This site showed the real-world complexity of simultaneous and adjacent recharge sources. To better observe the interaction of recharge dynamics from Alder Creek and the closed depression, additional vertical arrays of piezometers between Alder Creek and the closed depression could be installed.
- In order to evaluate recharge on a watershed scale, similar site scale observations could be made in different typical recharge features, vegetation zones, and catchment sizes. By mapping the recharge features and types and using the detailed observations it may be possible to estimate recharge distributions throughout the watershed.
- Finally, to provide a case study of the how lateral flow from a localized recharge feature can affect the results of the WTF method, an additional recharge event should be observed using additional piezometers between the recharge sources and the background location. The water level change at the background location can then be clearly shown to be the result of lateral flow, and therefore provide an example of a potential error in the application of the WTF method; overestimating recharge due to horizontal flow in the aquifer (as discussed in Section 5.4.1.).

References

Appelo, C. A. J., and Postma, D. 2005. Geochemistry Groundwater and Pollution 2nd Edition. A.A. Balkema Publishers. Amsterdam, the Netherlands.

Bajc, A.F., Russell, H.A.J., and Sharpe, D.R. 2014. A three-dimensional hydrostratigraphic model of the Waterloo Moraine area, southern Ontario, Canada. Canadian Water Resources Journal, 39 (2), pp. 95-119.

Bekeris, L. 2007. Field-Scale Evaluation of Enhanced Agricultural Management Practices Using a Novel Unsaturated Zone Nitrate Mass Load Approach. M.Sc. thesis, Department of Earth and Environmental Science, The University of Waterloo, Waterloo, On.

Bouwer, H., and R. C. Rice (1976), A slug test for determining hydraulic conductivity of unconfined aquifers with completely or partially penetrating wells, Water Resource Research, 12(3), 423–428, doi:10.1029/WR012i003p00423.

Buckingham, E. 1907. Studies on the movement of soil moisture. Bull. 38. USDA, Bureau of Soils, Washington D.C

Cey, E.E., Rudolph, D.L., and Passmore, J. 2009. Influence of macroporosity on preferential solute and colloid transport in unsaturated field soils. Journal of Contaminant Hydrology, 107 (1-2), pp. 45-57.

Christian-Smith, J., Levy, M.C., Gleick, P.H. 2015. Maladaptation to drought: a case report from California, USA. Sustainability Science, 10 (3), pp. 491-501.

Daniel, J.A., and Staricka, J.A. 2000. Frozen soil impact on ground water-surface water interaction. Journal of the American Water Resources Association, 36 (1), pp. 151-160.

Devlin, J.F., 2015. HydrogeoSieveXL: an Excel-based tool to estimate hydraulic conductivity from grain-size analysis. Hydrogeology Journal Official Journal of the International Association of Hydrogeologists ISSN 1431-2174.

Environment Canada. (2016). Climate Archives. Retrieved July 20, 2016, from http://climate.weather.gc.ca/

Finch, J. W. 1998. Estimating direct groundwater recharge using a simple water balance model – sensitivity to land surface parameters. Journal of Hydrology, 211:112-125.

Freeze, R. A., and Cherry, J. A. 1979. Groundwater. Prentice-Hall, Englewood Cliffs, N.J.

Hayashi, M., and Farrow, C.R. 2014. Watershed-scale response of groundwater recharge to inter-annual and inter-decadal variability in precipitation (Alberta, Canada). Hydrogeology Journal, 22 (8), pp. 1825-1839.

Hayashi, M., and Van Der Kamp, G. 2000. Simple equations to represent the volume-area-depth relations of shallow wetlands in small topographic depressions. Journal of Hydrology, 237 (1-2), pp. 74-85.

Hayashi, M., Van Der Kamp, G., and Schmidt, R. 2003. Focused infiltration of snowmelt water in partially frozen soil under small depressions. Journal of Hydrology, 270 (3-4), pp. 214-229.

Healy, R. W. 2010. Estimating Groundwater Recharge. Cambridge University Press the Edinburgh Building, Cambridge, U.K.

Healy, R.W. and Cook, P.G. 2002. Using groundwater levels to estimate recharge. Hydrogeology Journal, 10 (1), pp. 91-109.

Hillier, C. E. 2014. Establishing Metrics to Quantify the Vulnerability of Municipal Supply Wells to Contaminants from Surface Water Sources. M.Sc. thesis, Department of Earth and Environmental Science, The University of Waterloo, Waterloo, On.

Huang, M., Barbour, L.S., Elshorbagy, A., Zettl, J.D., and Si, B.C. 2011. Infiltration and drainage processes in multi-layered coarse soils. Canadian Journal of Soil Science, 91 (2), pp. 169-183.

Hvorslev, M. J., 1951. Time lag and soil permeability in ground-water observations, Bulletin 36, US Army Corps of Engineers, Waterways Experiment Station, Vicksburg, Mississippi, 55 pp.

Ma, K-C, Tan, Y-C, Chen, C-H, 2011, The influence of water retention curve hysteresis on the stability of unsaturated soil slopes, Hydrological Processes, 25 (23), pp. 3563-3574.

Meinzer, O. E. 1923. The occurrence of groundwater in the United States with a discussion of principles. US Geologic Survey Water-Supply Paper 489.

Minke, A.G., Westbrook, C.J., and Van Der Kamp, G. 2010. Simplified volume-area-depth method for estimating water storage of prairie potholes. Wetlands, 30 (3), pp. 541-551.

Ministry of the Environment. 2018. Water Management: Policies, Guidelines, Provincial Water Quality Objectives. Retrieved April 5, 2018, from https://www.ontario.ca/page/water-management-policies-guidelines-provincial-water-quality-objectives

Missori, M. 2015. Study of hydrogeologic characterization of a glaciofluvial aquifer of Ontario (CANADA): A comparison of field and laboratory methods to estimate hydraulic conductivity in heterogeneous porous media. M.Sc., Faculty of Mathematical, Physical and Natural Sciences University of Rome

O'Connor, D. R. 2002. Report of the Walkerton Enquiry: The Events of May 2000 and Related Issues. Toronto, ON: Queen's Printer.

Province of Ontario. 2004. Watershed-based source protection planning: A threats assessment framework. Technical Experts Committee Report to the Minister of the Environment. Toronto, ON: Queen's Printer.

Reynolds, W. D. and Elrick, D. E. 1986. A method for simultaneous in situ measurement in the vadose zone of field saturated hydraulic conductivity, sorptivity, and the conductivity-pressure head relationship. Ground Water Monitoring & Remediation, March 1986, Vol. 6(1), pp. 84-95

Richards, L.A. 1931. Capillary conduction of liquids through porous mediums. Physics 1 (5): 318–333.

Risser, D.W., Gburek, W.J., and Folmar, G.J. 2009. Comparison of recharge estimates at a small watershed in east-central Pennsylvania, USA. Hydrogeology Journal, 17 (2): pp. 287-298.

Scanlon, B. R. 2010. Chemical tracer methods. In Estimating Groundwater Recharge. Edited by R. W. Healy. Cambridge University Press the Edinburgh Building, Cambridge, U.K.

Scanlon, B.R., Healy, R.W., and Cook, P.G. 2002. Choosing appropriate techniques for quantifying groundwater recharge. Hydrogeology Journal, 10 (1), pp. 18-39

Schaap, M.G., and Leij, F.J. 2000. Improved prediction of unsaturated hydraulic conductivity with the Mualem-van Genuchten, Soil Science Society of America Journal, 64 (3), pp. 843-851.

Schaap, M.G., Leij, F.J., and van Genuchten, M. Th. 2001. Rosetta: a computer program for estimating soil hydraulic parameters with hierarchical pedotransfer functions. Journal of Hydrology, 251:163-176.

Sousa, M.R., Frind, E.O., and Rudolph, D.L. 2013. An integrated approach for addressing uncertainty in the delineation of groundwater management areas. Journal of Contaminant Hydrology, 148, pp. 12-24.

Van Dijk, T. 2005. Depression-focused recharge and the impacts of land use on the hydrology of small depressions in Calgary, Alberta. M.Sc. thesis, Department of Geology and Geophysics, The University of Calgary, AL.

van Genuchten, M.Th. 1980. CLOSED-FORM EQUATION FOR PREDICTING THE HYDRAULIC CONDUCTIVITY OF UNSATURATED SOILS. Soil Science Society of America Journal, 44 (5), pp. 892-898.

Wiebe, A.J., Conant, B., Jr., Rudolph, D.L., and Korkka-Niemi, K. 2015. An approach to improve direct runoff estimates and reduce uncertainty in the calculated groundwater component in water balances of large lakes. Journal of Hydrology, 531, pp. 655-670.